Characterisation of an inbred mouse strain with a deletion of the α-synuclein locus

A thesis presented for the degree of
Doctor of Philosophy,
University of London

Christian G. Specht M.Sc., Dipl.-Biochem.

Wellcome Laboratory for Molecular Pharmacology
Department of Pharmacology
University College London

January 2002

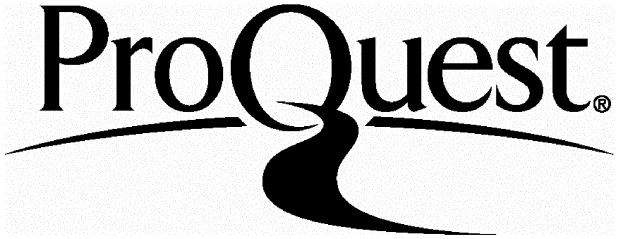

for Nadine

Abstract

mRNA expression profiling was performed on a knock-in mouse model with a mutation in the NMDA receptor subunit NR1 (N598R) that affects the receptors' function as coincidence detector. This approach was aimed at identifying downstream effects produced by the Ca^{2+} influx through NMDA receptors at the level of gene expression.

cDNA array technology revealed striking differences only in the mRNA expression level of α-synuclein, a protein that has been implicated in the pathophysiology of a range of neurodegenerative diseases. However, this was not caused by the NR1 mutation, but by a chromosomal deletion of the α-synuclein gene locus in the C57BL/6J inbred mice that were used for backcrossing the mutant strain. The deletion was shown to be present only in a subpopulation of C57BL/6J mice, now referred to as C57BL/6JOlaHsd-Del(6)*Snca*1Slab. In addition to α-synuclein, other genes may be affected by the deletion that is estimated to be 120-500 kb in size.

α-synuclein-deficient animals appear phenotypically normal. They show no compensatory upregulation of other members of the synuclein family, namely β-synuclein and γ-synuclein. Similarly, the expression of synphilin-1, a known interacting partner of α-synuclein was unaffected. The C57BL/6JOlaHsd-Del(6)*Snca*1Slab mouse model should help in the understanding of the physiological function of α-synuclein and its involvement in synucleinopathies. Also, the findings exemplify unexpected complications that may arise during the study of transgenic models or inbred strains.

A Sindbis virus system was developed for the expression of fluorescent α-synuclein fusion proteins in neurons. A range of recombinant virion preparations was tested in plaque assays and the expression of the recombinant proteins was characterised. Initial analysis of the expression of α-synuclein-eGFP in organotypic hippocampal neurons suggested that the protein accumulated in presynaptic locations. This approach could be used for the study of the subcellular localisation and of protein interactions of α-synuclein.

Acknowledgements

There are many people I want to thank for making my time in London an enjoyable experience. I am particularly grateful to Ralf Schoepfer for his supervision. Steve Davies, Tony Dickenson, and Martin Raff have also contributed lots of useful help and advice.

Above all, I would like to thank my former and current colleagues for their friendship and support throughout the last three years. Especially, I am very thankful to Philip Chen who helped me with the mice, Cezar Tigaret who helped establish the viral system, York Rudhard for his advice on the yeast work, Georg Rast for some of his hippocampal slice cultures, and Marco Peters for the screening of a YAC library. Raffaella Bosurgi, Tony Langford, and Mohammed Nassar have also helped me in many day-to-day situations. Besides, I should mention that this thesis would be even more confusing, had it not been for the proofreading, which some of the above mentioned have had to go through.

I would like to thank Steve Davies and Rushee Singh Jolly for interesting discussions and some unpublished data (EM / immunohistochemistry) and Diane Griffin and Michel Goedert for the supply of antibodies. The Biological Services Unit (UCL) has helped maintaining the mouse colony, and Matthias Kneussel and Klaus Rajewski have provided the mutant mouse models used in this study.

I am extremely thankful to the Wellcome Trust for the generous support, which allowed me to carry out this project.

I want to thank especially my London friends, Kate, Marguerite, Alastair, Ollie, Rony, Aden, and Simon. Also, lots of thanks to my friends elsewhere. Many of them are probably as glad as I am that this thesis is finally submitted. Most of all, I thank Nadine for encouraging me continuously during the last years, and particularly weeks.

Contents

Abstract 3

Acknowledgements 4

Contents 5

Figures 8

Abbreviations 9

Nomenclature 10

Bioinformatics 10

CHAPTER 1 INTRODUCTION 11

1.1 α-synuclein 11
1.1.1 General overview 11
1.1.2 The synuclein protein family 11
1.1.3 Structure of the synucleins 12
1.1.4 Expression patterns of the synucleins 15
1.1.5 Synucleins in neurodegeneration 18
1.1.6 Animal models of altered α-synuclein expression 20
1.1.7 Possible functions of α-synuclein 22

1.2 Sindbis virus 25
1.2.1 The Sindbis virus life cycle 25
1.2.2 Sindbis viral expression systems 27

1.3 The NMDA receptor 29
1.3.1 General overview 29
1.3.2 Structure of NMDA receptors 31
1.3.3 Expression patterns of NMDA receptor subunits 31
1.3.4 Electrophysiological properties of NMDA receptors 32
1.3.5 Downstream signalling of the NMDA receptor activation 33
1.3.6 Long term potentiation 33
1.3.7 The NR1 N598R mutant mouse model 34

1.4 Aim of the project 37
1.4.1 Downstream effects to the NMDA receptor activation 37
1.4.2 Viral expression system of α-synuclein 37

CHAPTER 2 MATERIALS AND METHODS 38

2.1 Materials 38
2.1.1 Chemicals 38
2.1.2 Standard buffers and solutions 38

2.2 Standard molecular biology techniques **39**
2.2.1 Bacterial cultures 39
2.2.2 Small-scale preparation of plasmid DNA 39
2.2.3 Large-scale preparation of plasmid DNA 39
2.2.4 Polymerase chain reaction 40
2.2.5 Determination of the concentration of nucleic acids 40
2.2.6 Restriction digestion of DNA 40
2.2.7 Agarose gel electrophoresis of DNA 41
2.2.8 Polyacrylamide gel electrophoresis of DNA 41
2.2.9 Gel extraction of DNA fragments 41
2.2.10 Phenol / chloroform extraction of DNA 42
2.2.11 Ethanol precipitation of DNA 42
2.2.12 Ligation of DNA fragments 42
2.2.13 Preparation of frozen electrocompetent *E.coli* 42
2.2.14 Transformation of competent *E.coli* 43
2.2.15 DNA Sequencing 43

2.3 Genomic DNA techniques **45**
2.3.1 Wildtype mouse strains / mutant mouse models 45
2.3.2 Preparation of genomic DNA from mouse tail 45
2.3.3 Genomic PCR 46
2.3.4 Yeast cultures 47
2.3.5 Small-scale purification of yeast genomic DNA 47
2.3.6 Pulsed field gel electrophoresis 48
2.3.7 Southern blotting and cDNA probes 49

2.4 RNA techniques **49**
2.4.1 General considerations 49
2.4.2 Preparation of total RNA 49
2.4.3 Preparation of polyA$^+$-RNA 50
2.4.4 cDNA array experiments 51
2.4.5 Agarose gel electrophoresis of RNA 51
2.4.6 Northern blotting 52
2.4.7 Generation of radiolabelled cDNA probes 52
2.4.8 Templates for radiolabelled cDNA probes 53
2.4.9 Reverse transcriptase PCR 54

2.5 Techniques for protein analysis **54**
2.5.1 SDS-PAGE 54
2.5.2 Coomassie blue / silver staining 55
2.5.3 Western blotting 55
2.5.4 Antibodies 56

2.6 Sindbis viral expression system **56**
2.6.1 Culturing of BHK cells 56
2.6.2 cRNA synthesis 57
2.6.3 Transfection of BHK cells / virion preparation 58
2.6.4 Plaque assay 58
2.6.5 Immunohistochemistry 58
2.6.6 Metabolic labelling 59
2.6.7 Organotypic hippocampal slice cultures 60
2.6.8 Morphology of organotypic slice cultures 60
2.6.9 Preparation of antibody-coupled Protein G-Sepharose beads 61
2.6.10 Immunoprecipitation 61
2.6.11 Confocal microscopy 62

CHAPTER 3 RESULTS 63

3.1 Overview 63

3.2 Screening for downstream effects of the NMDA receptor activation 64
3.2.1 Identification of α-synuclein by mRNA profiling in the $NR1^{R/+}$ mouse model 64
3.2.2 Inconsistent expression of α-synuclein mRNA in $NR1^{R/+}$ mutant mice 67

3.3 The strain BL6JHUK carries a chromosomal deletion of α-synuclein 69
3.3.1 α-synuclein expression levels in different mouse strains 69
3.3.2 Deletion of the α-synuclein gene locus in BL6JHUK animals 71
3.3.3 Initial characterisation of the chromosomal *Snca* deletion 73
3.3.4 Mapping of the *Snca* deletion using YAC clones 75
3.3.5 Recent mapping data of the *Snca* deletion 76
3.3.6 Expression of β-synuclein is unaffected by the α-synuclein deletion 78
3.3.7 Expression of γ-synuclein is unaffected by the α-synuclein deletion 78
3.3.8 Synphilin-1 expression is unaffected by the α-synuclein deletion 80
3.3.9 Adult $NR1^{Rneo/+}$ mouse model 82
3.3.10 Survival of $NR1^{Rneo/+}$ animals 84

3.4 Sindbis viral expression system 85
3.4.1 Cloning of SV contructs for the expression of α-synuclein fusion proteins 85
3.4.2 Preparation of recombinant Sindbis virions 86
3.4.3 Plaque assay of recombinant Sindbis virions 88
3.4.4 Biochemical analysis of expressed α-synuclein fusion proteins in BHK cells 91
3.4.5 Morphology of cultured organotypic hippocampal slices 94
3.4.6 Immunoprecipitation of α-synuclein-eGFP expressed in slice cultures 94
3.4.7 Expression of α-synuclein-eGFP fusion protein in organotypic slice cultures 96

CHAPTER 4 DISCUSSION 100

4.1 Identification of a mouse strain with a deletion of the α-synuclein gene locus 100
4.1.1 Deletion of the α-synuclein gene locus in C57BL/6J inbred mice 100
4.1.2 Size of the *Snca* deletion in a C57BL/6J substrain 101
4.1.3 Nomenclature of the *Snca* deletion in a C57BL/6J substrain 103
4.1.4 Frequencies of chromosomal deletions 103
4.1.5 Lack of an obvious phenotype in animals with the *Snca* deletion 104
4.1.6 Potential compensatory effects in animals with the *Snca* deletion 105
4.1.7 Potential downstream effects in animals with the *Snca* deletion 106
4.1.8 Future work – deletion of the *Snca* locus in a C57BL/6J substrain 108

4.2 Screening for downstream effects to the NMDA receptor activation 109
4.2.1 mRNA profiling in an NR1 mutant mouse model 109
4.2.2 Survival of $NR1^{Rneo/+}$ animals 110
4.2.3 Future work – NR1 mutant mouse model 110

4.3 Sindbis viral expression of α-synuclein fusion proteins 112
4.3.1 Preparation and analysis of recombinant Sindbis virions 112
4.3.2 Biochemical analysis of expressed α-synuclein fusion proteins 113
4.3.3 Expression of α-synuclein-eGFP fusion protein in hippocampal cultures 115
4.3.4 Future work – viral expression of α-synuclein 117

Conclusions 117

References 118

Appendix 130

Figures

Fig.1	Alignment of the synuclein family of proteins	14
Fig.2	Presynaptic localisation of α-synuclein	17
Fig.3	Life cycle of the Sindbis virus	26
Fig.4	Schematic representation of the NMDA receptor function	30
Fig.5	The NR1 N598R mutant mouse model	36
Fig.6	Identification of α-synuclein in the $NR1^{R/+}$ mouse model using cDNA array technology	66
Fig.7	Inconsistent expression of α-synuclein in $NR1^{R/+}$ mutant mice	68
Fig.8	α-synuclein expression levels in different mouse strains	70
Fig.9	Deletion of the *Snca* locus in BL6JHUK animals	72
Fig.10	Characterisation of the *Snca* chromosomal deletion in the BL6JHUK strain	74
Fig.11	Mapping of the *Snca* locus in the BL6JHUK strain	77
Fig.12	Developmental expression of β- and γ-synuclein in different mouse strains	79
Fig.13	Developmental expression of synphilin-1 in different mouse strains	81
Fig.14	Studies on the adult $NR1^{Rneo/+}$ mouse model	83
Fig.15	Sindbis viral constructs for the expression of α-synuclein fusion proteins	87
Fig.16	Plaque assay of recombinant Sindbis virions	90
Fig.17	Biochemical analysis of expressed α-synuclein fusion proteins in BHK cells	92
Fig.18	Morphology of cultured organotypic hippocampal slices	95
Fig.19	Immunoprecipitation of α-synuclein fusion proteins expressed in hippocampal cultures	97
Fig.20	Expression of α-synuclein-eGFP fusion protein in hippocampal cultures	99

Abbreviations

Aβ	β-amyloid protein
AD	Alzheimer's disease
βAPP	β-amyloid precursor protein
BHK	baby hamster kidney
bp	base pairs
CA	cornu ammonis
CD	circular dichroism
CDS	coding sequence
CNS	central nervous system
DG	dentate gyrus
DRG	dorsal root ganglion
DIV	day *in vitro*
E	embryonic day
eGFP	enhanced green fluorescent protein
EM	electron microscopy
EST	expressed sequence tag
g	standard acceleration of gravity
GFP	green fluorescent protein
HAc	acetic acid
IU	infectious unit
KAc	potassium acetate
kb	kilobase pairs
LB	Lewy bodies
LTP	long term potentiation
MCS	multiple cloning site
NaAc	sodium acetate
NAC	non-Aβ component of AD amyloid
NMDA	N-methyl-D-aspartate
NR	NMDA receptor subunit
P	postnatal day
PD	Parkinson's disease
PFU	plaque-forming unit
PS	packaging signal
P_{SG}	subgenomic promoter
RFP	red fluorescent protein
SN	substantia nigra
Snca	α-synuclein gene locus
SV	Sindbis virus
TH	tyrosine hydroxylase
UTR	untranslated sequence
YAC	yeast artificial chromosome

Nomenclature

C57BL/6J inbred mouse populations:

BL6Jax	C57BL/6J DNA obtained from Jackson Laboratory
BL6JHUK	C57BL/6J mice from Harlan UK with a deletion of *Snca*

Mutant alleles of the NMDA receptor subunit NR1:

$NR1^{R/+}$	heterozygous animals carrying the NR1 N598R allele
$NR1^{Rneo/+}$	heterozygous animals carrying the NR1 N598Rneo allele

Fusion proteins expressed with a Sindbis virus system:

GS	eGFP-α-synuclein fusion protein
SG	α-synuclein-eGFP fusion protein
SR	α-synuclein-RFP fusion protein

Virion preparations for the expression of recombinant fusion proteins:

vGS(24), vGS(48)	virions for expression of GS fusion protein
vSG(24), vSG(48)	virions for expression of SG fusion protein
vSR(24), vSR(48)	virions for expression of SR fusion protein

Virions were harvested at 24 and 48 hours post-transfection (as indicated in brackets).

Bioinformatics

Genome Systems / Incyte Genomics	http://www.incyte.com/gem
Harlan UK	http://www.harlan.com/uk
ILAR	http://www4.nas.edu/cls/ilarhome.nsf
I.M.A.G.E. Consortium, HGMP	http://image.llnl.gov
Jackson Laboratory	http://www.jax.org
MGI Mouse Genome Informatics	http://www.informatics.jax.org
MGSC Ensembl database	http://mouse.ensembl.org
MRC HGMP Resource Centre	http://www.hgmp.mrc.ac.uk
NCBI	http://www.ncbi.nlm.nih.gov
Whitehead Institute / MIT	http://www-genome.wi.mit.edu

CHAPTER 1
Introduction

1.1 α-synuclein

1.1.1 General overview

Synuclein was first described as a protein enriched in the electric lobe of the pacific electric ray *Torpedo californica*. A mammalian homologue was cloned from a rat brain cDNA library and was referred to as synuclein (Maroteaux *et al.*, 1988). α-synuclein became the focus of intensive investigation when two missense mutations in the human gene were linked to rare inherited forms of Parkinson's disease (PD) (Polymeropoulos *et al.*, 1997; Kruger *et al.*, 1998). Subsequently, α-synuclein was shown to be a major component of Lewy bodies (LB) in PD (Spillantini *et al.*, 1997; Wakabayashi *et al.*, 1997) as well as in a range of other neurodegenerative diseases, classified as synucleinopathies (for review see Duda *et al.*, 2000; Goedert, 2001). Although synucleins and their involvement in neurodegenerative diseases have been intensively studied the physiological role of the proteins remains unknown.

1.1.2 The synuclein protein family

The synucleins form a closely related group of proteins, with its members α-, β-, and γ-synuclein (for review see Lavedan, 1998). Over the last decade synuclein cDNA sequences from a growing number of vertebrates have emerged. These include human α-synuclein (Ueda *et al.*, 1993), β-synuclein (Jakes *et al.*, 1994), γ-synuclein (Ji *et al.*, 1997), rat α-synuclein (Maroteaux *et al.*, 1988), β-synuclein (Tobe *et al.*, 1992), γ-synuclein (Akopian and Wood, 1995), and mouse α-synuclein (Hong *et al.*, 1998; Hsu *et al.*, 1998), β-synuclein (Sopher *et al.*, 2001), and γ-synuclein (Buchman *et al.*, 1998b). Also, the orthologue of α-synuclein in the zebra finch *Serinus canaria* (George *et al.*, 1995), bovine β-synuclein (Nakajo *et al.*, 1990; Nakajo *et al.*, 1993), and a synuclein from *Torpedo californica* (Maroteaux *et al.*, 1988) were cloned.

On the chromosomal level synucleins are encoded by individual genes. The human α-, β-, and γ-synuclein genes (*SNCA*, *SNCB*, and *SNCG*) map to the loci 4q21.3-22 (Campion *et al.*, 1995; Chen *et al.*, 1995; Shibasaki *et al.*, 1995; Spillantini *et al.*, 1995), 5q35 (Spillantini *et al.*, 1995; Lavedan *et al.*, 1998b), and 10q23.2-q23.3 (Lavedan *et al.*, 1998a; Ninkina *et al.*, 1998). The respective murine genes (*Snca*, *Sncb*, *Sncg*) are located on chromosome 6 (Touchman *et al.*, 2001), chromosome 13 (Sopher *et al.*, 2001), and chromosome 14 (Alimova-Kost *et al.*, 1999), respectively. The chromosomal organisation is well conserved between the synucleins. The coding sequences (CDS) are divided into five exons. The α- and β-synuclein genes contain an additional exon in the 5'-untranslated region (5'UTR). In the human α-synuclein gene (*SNCA*) this exon contains two alternative splice sites. Similarly, alternative splicing has been observed for exons 4 and 6 of *SNCA*, causing the expression of an mRNA transcript that lacks part of the C-terminal sequence in fetal and adult brain (Ueda *et al.*, 1994). However, the existence of the corresponding 112 amino acid residue protein has not yet been shown.

1.1.3 Structure of the synucleins

The length of the known primary protein sequences of the synucleins varies between 112 and 143 amino acid residues. Human and mouse α-synuclein contain 140 amino acid residues, with a high degree of sequence identity (95%). Likewise, the β-synuclein orthologues contain 134 and 133 residues in human and mouse, respectively, and share 96% identity. Human γ-synuclein (127 residues) is 87% identical with its mouse orthologue (123 residues). Between the homologues α-, β-, and γ-synuclein, sequence identities lie in the range of 50-60%. However, the sequences are more conserved in the N-terminal regions (Fig.1).

The N-terminal region of the synucleins forms a domain with a conserved periodicity of 11 residues. At the core of this repeat lies a motif of six residues, with the consensus sequence KTKEGV (Maroteaux *et al.*, 1988). The motif is repeated six times in α- and γ-synuclein, and five times in β-synuclein (Fig.1). Synuclein from *Torpedo californica* represents an exception with seven repeats. Proteins with such varying numbers of modular repeats have probably emerged by duplications of the module throughout evolution. The repeated motif in synuclein is homologous to the

Aplysia rho and the human ras protein (Maroteaux *et al.*, 1988). Both are small GTP-binding proteins that are believed to be involved in signalling cascades and the regulation of gene expression (for review see Takai *et al.*, 2001). A periodicity of 11 residues is found in the amphipathic α-helical lipid-binding domain of the apolipoproteins (for review see Segrest *et al.*, 1992). This led to the hypothesis that the N-terminal domain of the synucleins has a similar α-helical secondary structure that could promote lipid binding (George *et al.*, 1995). Indeed, α-synuclein can bind to lipid via its N-terminal domain (Jensen *et al.*, 1998; Perrin *et al.*, 2000). However, α-synuclein was found to assume a random structure in solution by circular dichroism (CD) (Weinreb *et al.*, 1996; Rochet *et al.*, 2000). These two findings could be reconciled when CD measurements showed that binding to synthetic membranes containing acidic phospholipids stabilises the α-helical structure of α-synuclein, increasing from 3% to 80% upon lipid binding (Davidson *et al.*, 1998).

Furthermore, α-synuclein has been found to adopt β-sheeted structures upon prolonged incubations. The conversion of the random coil to a β-sheeted conformation was not observed for β- and γ-synuclein (Serpell *et al.*, 2000). The conformational change of α-synuclein underlies the formation of elongated filaments that are visible by electron microscopy (Conway *et al.*, 1998; Giasson *et al.*, 1999). Such filaments are similar to those found in Lewy bodies (LB) and Lewy neurites in Parkinson's disease (PD). Indeed, purified LB filaments are strongly immunoreactive for α-synuclein (Spillantini *et al.*, 1998b). Thus, the β-sheeted conformation of α-synuclein appears to be involved in the neuropathology associated with the protein. A hydrophobic sequence in human α-synuclein (residues V71-V82; Fig.1) has been implicated in bringing about the β-sheeted conformation and the associated fibrillisation. Interestingly, β-synuclein has several mismatches in the respective sequence that could account for its reduced fibril formation (Giasson *et al.*, 2001b).

The C-terminus of the synucleins contains a number of acidic residues (Fig.1). Isoelectric focussing of rat β-synuclein indicates an isoelectric point (pI) of 4.5 (Cole and Hart, 2001). The C-terminal domain has been implicated in the interaction with other proteins, such as synphilin-1 (Kawamata *et al.*, 2001). Also, it contains a Ca^{2+} binding site within the last 24 residues of the α- and β-synuclein sequence (Nielsen *et al.*, 2001). Cysteine residues are absent from the primary sequence of human and rodent synucleins, excluding the formation of disulphide bonds.

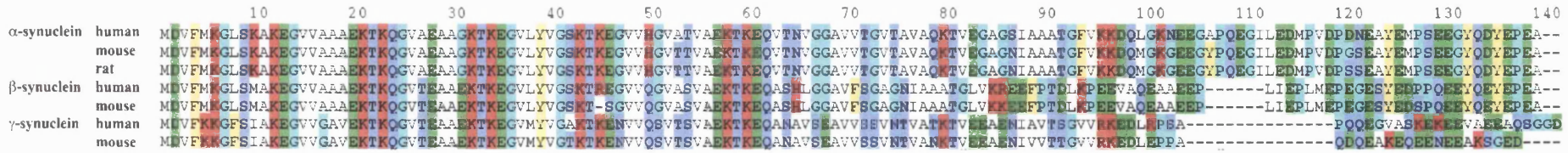

Figure 1. Alignment of the synuclein family of proteins

α-, β-, and γ-synucleins from different species are aligned using Jalview software (MRC HGMP Resource Centre; MAGI - Multiple Alignment General Interface). Amino acid residues are coloured according to their properties as aromatic (yellow), acidic (green), basic (red), hydrophilic (blue), and conformationally special (turquoise). The synucleins share common structural features such as a repeated motif throughout the N-terminal domain of the amino acid sequence and a C-terminal domain with acidic residues. Human and rodent α-synucleins contain 140 amino acid residues (human NM000345; mouse NM009221; rat NM019169). The β-synuclein sequences contain 134 and 133 residues (human NM003085; mouse NM033610), respectively, and the γ-synucleins 127 and 123 residues (human NM003087; mouse NM011430). Protein sequences were derived from the respective GenBank accession numbers (NCBI).

The calculated molecular weight of the synucleins lies in the range of 14 kDa. However, their apparent masses are closer to 19 kDa as judged by SDS-PAGE, with β-synuclein running slightly above, and γ-synuclein running below α-synuclein (Spillantini *et al.*, 1998b). An increased molecular weight was found for α- and β-synuclein, which could reflect posttranslational modifications (Jakes *et al.*, 1994). Indeed, several reports state the phosphorylation of synucleins (chapter 1.1.7), as well as O-glycosylation of rat β-synuclein (Cole and Hart, 2001). Synucleins are believed to form oligomers in solution. Size-exclusion chromatography of purified α- or β-synuclein suggests complexes of approximately 55 kDa (Nakajo *et al.*, 1990; Paik *et al.*, 1997). Also, α-synuclein can form homodimers, and heterodimers with β-synuclein (Jensen *et al.*, 1997).

1.1.4 Expression patterns of the synucleins

The three human synucleins share a similar overall tissue distribution. The human α-synuclein mRNA transcript is predominantly expressed in brain, and, to a lesser extent in most other tissues with the exception of liver (Ueda *et al.*, 1993). Within the brain, α-synuclein mRNA and protein expression occurs in the hippocampus, cortex, and cerebellum as early as four months from the start of human embryonic development (Bayer *et al.*, 1999a). In the human substantia nigra (SN), α-synuclein is initially expressed in week 15 of gestation, expression of β- and γ-synuclein is delayed to week 17 and 18, respectively (Galvin *et al.*, 2001). Human β-synuclein transcript is also highly expressed in brain, and weakly in skeletal muscle, but absent from most other tissues (Jakes *et al.*, 1994). Within the brain it is distributed predominantly in the thalamus, SN, hippocampus, and amygdala (Lavedan *et al.*, 1998b). Human γ-synuclein was identified by differential cDNA sequencing and was overexpressed in human breast cancer tissue. Its expression appears to parallel the progression of malignant tumors (Ji *et al.*, 1997). Also, α- and β-synucleins have been found to be expressed in a number of tumors (Bruening *et al.*, 2000). The γ-synuclein transcript is expressed in a similar pattern to α-synuclein, but is absent from liver and placental tissue (Ji *et al.*, 1997; Lavedan *et al.*, 1998a). In brain, γ-synuclein expression is widespread with highest transcript levels in the subthalamic nucleus and the SN (Lavedan *et al.*, 1998a).

The regional distribution of rodent synucleins parallels that in humans. Rat α-synuclein protein is mainly present in the hippocampus, cortex, and amygdala, but also in other areas of the brain (Iwai *et al.*, 1995; Petersen *et al.*, 1999). Mouse α-synuclein mRNA is expressed in most tissues, mainly in brain and spleen, with the exception of liver. Within the brain, expression levels are highest in the hippocampus and neocortex (Hong *et al.*, 1998). Mouse and rat β-synuclein protein is mainly present in brain including the cerebellum, and in spinal cord (Shibayama-Imazu *et al.*, 1993; Sopher *et al.*, 2001). Rat γ-synuclein was cloned from a dorsal root ganglia (DRG) library. The rodent γ-synucleins are predominantly expressed in the peripheral nervous system (Akopian and Wood, 1995; Buchman *et al.*, 1998b). Thus, the main differences in the tissue distribution appear to be the high expression of the rodent β-synucleins in spinal cord and cerebellum, compared to the human protein. Also, the rodent γ-synucleins are present in the cerebellum and the spinal cord, but much lower expression levels are detected in cortex compared to the human protein (Giasson *et al.*, 2001a).

The temporal expression profile of rodent synucleins is similar. Rat α-synuclein mRNA is expressed in brain throughout postnatal development, with a marked decrease after postnatal day P14. Rat α-synuclein protein is detected at P0 and expression increases to reach a plateau in adult animals (Petersen *et al.*, 1999). Similarly, rat β-synuclein protein expression starts around birth and reaches a plateau after three weeks (Shibayama-Imazu *et al.*, 1993). Mouse α-synuclein mRNA expression in brain is detected at embryonic day E12 and peaks at P7, whereas protein levels continue to rise until adulthood (Hong *et al.*, 1998; Hsu *et al.*, 1998). Mouse γ-synuclein is increasingly expressed in the peripheral nervous system from embryonic development to adulthood, and to a lesser amount in the cerebral cortex starting postnatally (Buchman *et al.*, 1998a; Buchman *et al.*, 1998b).

The name synuclein was originally chosen to illustrate the observed localisation of the protein in pre**syn**aptic nerve terminals and the **nucl**eus of neurons (Maroteaux *et al.*, 1988). However, nuclear localisation was not described in later studies. Subcellularly, both α- and β-synuclein from different species are located in presynaptic nerve terminals (Maroteaux *et al.*, 1988; Nakajo *et al.*, 1990; Jakes *et al.*, 1994; George *et al.*, 1995; Iwai *et al.*, 1995). Electron microscopy (EM) reveals that α-synuclein is located near the presynaptic vesicles (Fig.2). During brain development and in primary neurons *in vitro*, a redistribution of α-synuclein from the neuronal cell

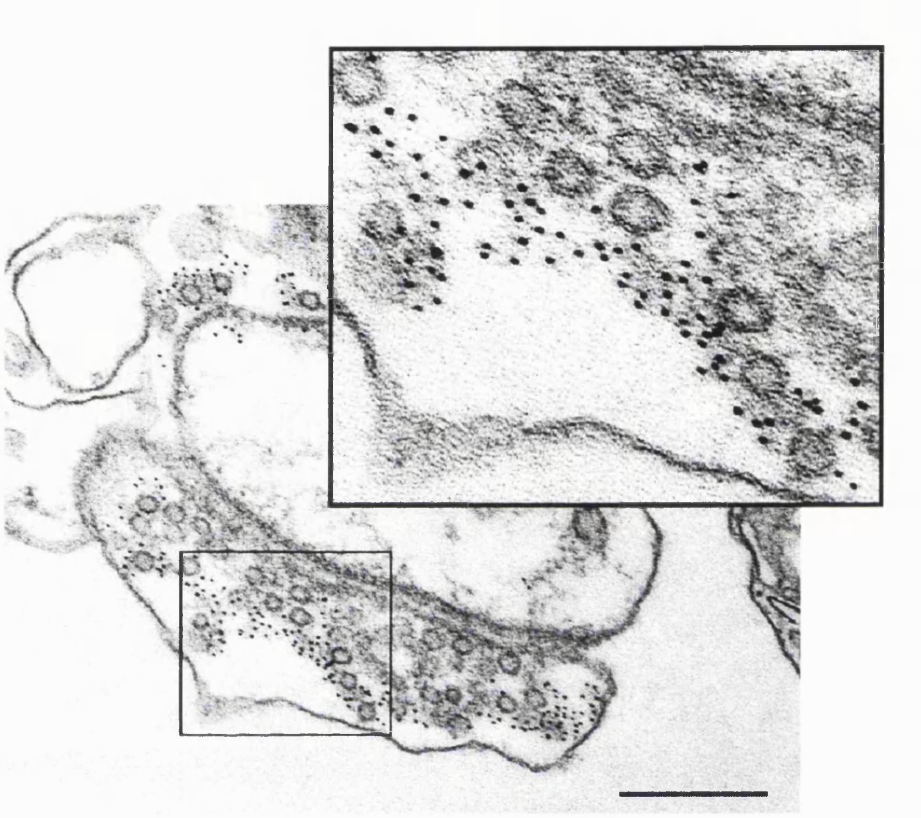

Figure 2. Presynaptic localisation of α-synuclein

Ultrastructural localisation of α-synuclein in the presynaptic nerve terminal (adapted from Clayton and George, 1999). Rat brain synaptosomes were prepared by hypotonic lysis, embedded in agarose, immunogold labelled with monoclonal anti-synuclein antibody, and processed for electron microscopy. Distinct pre- and postsynaptic compartments are visible, with an accumulation of synaptic vesicles on the presynaptic side and a prominent postsynaptic density. α-synuclein immunoreactivity is found predominantly in the presynaptic terminal, in close proximity to the synaptic vesicles. The scale bar represents 500 nm.

bodies to the presynaptic termini was observed (Withers *et al.*, 1997; Hsu *et al.*, 1998). The subcellular location of γ-synuclein in peripheral neurons are the cell bodies and axons (Buchman *et al.*, 1998a; Buchman *et al.*, 1998b). A similar perikaryal distribution was found for α- and β-synuclein in the DRG (Giasson *et al.*, 2001a).

1.1.5 Synucleins in neurodegeneration

Alzheimer's (AD) and Parkinson's disease (PD) are common progressive neurodegenerative diseases in humans that are characterised by the presence of abnormal protein deposits in the brain. In AD, neurofibrillary bundles composed of paired helical filaments (PHF) are present in the somata of neurons. The predominant component of these intracellular protein aggregates is the abnormally phosphorylated microtubuli-associated protein tau. The other molecular hallmark of AD is the presence of amyloid plaques, extracellular deposits composed of a heterogeneous core and surrounded by clusters of degenerated axons and dendrites. The core contains predominantly β-amyloid proteins (Aβ), proteolytic fragments (39-43 amino acid residues) of the precursor protein βAPP. A number of other proteins are also present in amyloid plaques, such as ubiquitin and apolipoprotein E.

The description of a 35 residue peptide as a component of amyloid plaques was the first indication that α-synuclein might be involved in neurodegenerative processes. The peptide was named NAC (non-Aβ component of AD amyloid) and its 140 residue precursor protein NACP (Ueda *et al.*, 1993), now known as human α-synuclein. The NAC peptide (α-synuclein residues E61-V95; Fig.1) encompasses the domain that is essential for the assembly of α-synuclein into β-sheeted filaments (Giasson *et al.*, 2001b). Also, α- and β-synuclein have been found to bind to Aβ1-40 (Jensen *et al.*, 1997). NAC peptide forms fibrils by nucleation-dependent polymerisation that seed and are seeded by Aβ. Interestingly, a homology was found between a sequence of the NAC (V66-G73), the C-terminus of Aβ (V36-T43), and scrapie prion protein PrP (V117-G124). PrP106-126 has also been shown to seed NAC fibrils (Han *et al.*, 1995). In contrast to these and other findings, two reports have questioned the presence of the NAC fragment in amyloid plaques (Bayer *et al.*, 1999b; Culvenor *et al.*, 1999). α-synuclein immunoreactivity was not observed in amyloid plaques, and only occasional staining for α-synuclein was detected in neurofibrillary bundles and in peripheral areas

of plaques. These findings might be explained by the presence of α-synuclein in Lewy bodies (LB), which are present in a LB variant of AD (LBVAD) (Spillantini *et al.*, 1998b; Wirths *et al.*, 2000).

Parkinson's disease (PD) is a progressive neurodegenerative disease that is characterised by the degeneration of dopaminergic neurons in the substantia nigra (SN). Pharmacological treatment is generally aimed at restoring dopamine levels in PD patients to reduce the symptoms. The neuropathological hallmarks of PD are Lewy bodies (LB) and Lewy neurites. LB are eosinophilic cytoplasmic inclusions that are particularly frequent in SN neurons of PD patients. They contain a range of proteins, including ubiquitin (Kuzuhara *et al.*, 1988), proteasome subunits (Ii *et al.*, 1997), ubiquitin C-terminal hydrolase-L1 (UCH-L1 or PGP 9.5) (Lowe *et al.*, 1990), parkin (Shimura *et al.*, 1999), synphilin-1 (Wakabayashi *et al.*, 2000), and α-synuclein (Spillantini *et al.*, 1997; Wakabayashi *et al.*, 1997). α-synuclein represents the major component of LB and Lewy neurites in PD, whereas β- and γ-synuclein immunoreactivity is not observed (Spillantini *et al.*, 1998b). This suggests that α-synuclein is specifically involved in the formation of these structures. Synphilin-1 is an interacting partner of α-synuclein (Engelender *et al.*, 1999). Other components of LB are part of the cellular protein degradation machinery, the ubiquitin / proteasome pathway (for review see Kornitzer and Ciechanover, 2000). Indeed, proteasome activity is impaired in the SN of PD patients (McNaught and Jenner, 2001). Also, proteasome inhibition *in vitro* can lead to the formation of ubiquitin inclusions that also contain α-synuclein, and to cell death (Rideout *et al.*, 2001). Proteasomal degradation of α-synuclein was not consistently reported (Bennett *et al.*, 1999; Ancolio *et al.*, 2000), but can occur in an ubiquitin-independent manner by the 20S proteasome (Tofaris *et al.*, 2001). These findings indicate that a deficiency of proteasome activity may be the underlying mechanism for the accumulation and possible neurotoxicity of α-synuclein.

On the ultrastructural level, LB are composed of α-synuclein fibrils (Spillantini *et al.*, 1998b). Synthetic filaments that are assembled from α-synuclein show a β-sheeted structure (Serpell *et al.*, 2000). Two missense mutations in the human α-synuclein gene were found in rare inherited forms of PD (Polymeropoulos *et al.*, 1997; Kruger *et al.*, 1998). These are point mutations within the N-terminal domain of α-synuclein, A53T and A30P (Fig.1). Both mutations have effects on the assembly and

the binding characteristics of α-synuclein. The formation of filaments is accelerated in mutant human A53T α-synuclein and to a lesser extent in A30P compared to the wildtype protein (Conway *et al.*, 1998; Narhi *et al.*, 1999; Serpell *et al.*, 2000). Also, the disruption of the α-helical domain by a proline residue in the A30P protein decreases the binding of α-synuclein to vesicles (Jensen *et al.*, 1998; Perrin *et al.*, 2000). Although it was reported that A30P has a slower fibrillisation rate compared to wildtype α-synuclein, its rate of oligomerisation is increased (Conway *et al.*, 2000). The protofibrils are stabilised by the formation of covalent adducts with the catecholamines dopamine and L-DOPA (Conway *et al.*, 2001). Protofibrils have a β-sheeted structure and strongly bind and temporarily permeabilise vesicles (Volles *et al.*, 2001). Therefore, the formation of protofibrils could be critical for the neurotoxicity of α-synucleins rather than their fibrillisation rates.

α-synuclein-positive neuronal inclusions are not only indicative of PD, but are also present in a range of other neurodegenerative diseases, classified as synucleinopathies (for review see Duda *et al.*, 2000; Goedert, 2001). These include dementia with LB (DLB), LB variant of AD (LBVAD), and multiple system atrophy (MSA), with cytoplasmic inclusions in oligodendroglial as well as in neuronal cells (Spillantini *et al.*, 1997; Arima *et al.*, 1998; Spillantini *et al.*, 1998a; Wakabayashi *et al.*, 1998; Wirths *et al.*, 2000). Also, an involvement of α-, β-, and γ-synuclein in presynaptic neurodegenerative processes was suggested by the finding of axon terminal lesions in hippocampal and other areas (Galvin *et al.*, 1999).

1.1.6 Animal models of altered α-synuclein expression

So far, a number of animal models have been developed for the study of α-synuclein (for review see Barbieri *et al.*, 2001). Overexpression of α-synuclein in *Drosophila* results in pathological and behavioural phenotypes similar to those found in PD. The expression of human α-synuclein as a transgene leads to the loss of dopaminergic neurons. Some neurons develop filamentous α-synuclein-positive inclusions with similarities to LB in PD. Aged transgenic flies display a marked deficit in a climbing test (Feany and Bender, 2000). This behavioural deficit can be restored by treatment with L-DOPA (Pendleton *et al.*, 2002). In mice, the neuronal expression of human α-synuclein causes the formation of nonfibrillar cytoplasmic inclusions with

α-synuclein immunoreactivity in the cortex, hippocampus, and SN. This is accompanied by a reduction in dopaminergic terminals and by motor impairments as assessed by rotorod training (Masliah *et al.*, 2000). However, the overexpression of human α-synuclein has little effect on the performance in the water maze paradigm (Masliah *et al.*, 2001). The coexpression of human α- and β-synuclein in doubly transgenic mice reduces the aggregation of α-synuclein and partially reverses the motor deficits observed in α-synuclein transgenic animals (Hashimoto *et al.*, 2001). This suggests an influence of β-synuclein on the folding of α-synuclein, and is consistent with the finding that the two proteins coprecipitate and can form heterodimers (Jensen *et al.*, 1997; Hashimoto *et al.*, 2001).

The expression of the human mutant A53T α-synuclein in mice leads to the formation of nonfibrillar cytoplasmic inclusions and to motor impairments (van der Putten *et al.*, 2000). Interestingly, alanine residue A53 in human wildtype α-synuclein is replaced by threonine in the rodent sequences. Further mismatches between human and rodent α-synucleins are present in the C-terminal domain (Fig.1). Mouse α-synuclein is more fibrillogenic than the human A53T and wildtype proteins and its fibrillisation can be inhibited by these (Rochet *et al.*, 2000). Thus, the overexpression of transgenic human α-synucleins on the background of the endogenous protein complicates the interpretation of murine α-synuclein models. This is in contrast to *Drosophila* that lacks endogenous α-synuclein. The expression of human A30P α-synuclein in transgenic mice causes an abnormal accumulation of the protein in neuronal cell bodies and neurites. However, fibril formation was not detected (Kahle *et al.*, 2000), in agreement with a slow rate of fibrillisation of human A30P α-synuclein (Conway *et al.*, 2000). Motor impairments or a decrease in dopaminergic neurons in the SN were not reported under the experimental conditions used in this study (Kahle *et al.*, 2000). Furthermore, the loss of dopaminergic neurons caused by 1-methyl-4-phenyl-1,2,3,6-tetrahydropyridine (MPTP) was not increased in transgenic A30P animals compared to wildtype littermates (Rathke-Hartlieb *et al.*, 2001). MPTP is a substance that produces PD-like symptoms in humans and mice. However, LB pathology is absent in this pharmacological PD model.

α-synuclein knockout mice have been generated to address the physiological function of the protein. Homozygous knockout mice are viable, fertile, and have an apparently normal brain morphology. The absence of α-synuclein had no effect on the

number and morphology of dopaminergic SN neurons. The synaptic plasticity in these mice was identical to wildtype animals as judged by measurements of hippocampal long term potentiation in the CA1 field. However, a minor increase in the recovery of the dopamine release by paired stimuli was observed in the nigrostriatal system. Also, the amphetamine-stimulated locomotion activity is reduced in knockout animals (Abeliovich *et al.*, 2000). A naturally occurring chromosomal deletion of the α-synuclein gene (*Snca*) was found in an inbred mouse strain (Specht and Schoepfer, 2001). The discovery and the study of this mouse model are described within the present thesis.

1.1.7 Possible functions of α-synuclein

Although the role of α-synuclein in the pathophysiology of a variety of diseases is well studied, its physiological function remains unclear. Possible functions of the synucleins in neurons can be inferred from their modular organisation, folding, assembly, and subcellular localisation. For example, it could be speculated that α- and β-synuclein may be involved in synaptic plasticity. Evidence for this concept comes from the finding that both proteins are expressed in brain regions involved in learning and memory processes, particularly the hippocampus (chapter 1.1.4). Subcellularly, α- and β-synuclein are located in presynaptic nerve terminals (Maroteaux *et al.*, 1988; Nakajo *et al.*, 1990) and show extensive colocalisation (Kahle *et al.*, 2000). α-synuclein binds to vesicles via its α-helical N-terminal domain (Jensen *et al.*, 1998; Perrin *et al.*, 2000). Also, α-synuclein appears to have an influence on the vesicle pool in the presynaptic terminal (Murphy *et al.*, 2000). Furthermore, it is present in the song control circuit during a period that is critical for song learning in zebra finch development (George *et al.*, 1995). The formation of homodimers by α-synuclein as well as heterodimers with β-synuclein (Jensen *et al.*, 1997) could reflect a physiological interaction that occurs at the presynaptic terminal. Taking into account the high degree of sequence identity between the N-termini of the two proteins, and to a lesser extent γ-synuclein, it could be assumed that they share similar functions (Fig.1). A functional compensation might explain the lack of an obvious phenotype in

α-synuclein-deficient animals (Abeliovich *et al.*, 2000; Specht and Schoepfer, 2001). This would be addressed by the generation of mice with deletions of both gene loci (*Snca* and *Sncb*).

A different approach to elucidate the function of α-synuclein is by identifying its protein interaction partners. It was shown that α- and β-synuclein are potent selective inhibitors of phospholipase D2 (PLD2) but have little effect on PLD1 activity (Jenco *et al.*, 1998). Unlike PLD1, PLD2 is localised at the cell membrane (Colley *et al.*, 1997). Phospholipases D produce phosphatidic acid (PA) by hydrolysis of phosphatidylcholine (PC). PA and its metabolites are mediators of a number of processes including the control of cell morphology and vesicular trafficking (for review see Liscovitch *et al.*, 2000).

Potential modulators of the synuclein function are protein kinases. Initial reports suggested a phosphorylation of rat β-synuclein on serine residue S118 (Nakajo *et al.*, 1993). The homologous residue S129 and to a lesser extent S87 represent phosphorylation sites in α-synuclein (Fig.1). Residue S129 in α-synuclein can be phosphorylated by the casein kinases CK-I and CK-II and by G protein-coupled receptor kinases (GRK) (Okochi *et al.*, 2000; Pronin *et al.*, 2000). GRK5-phosphorylation of α-synuclein decreases its lipid binding affinity and its inhibition of PLD2 (Pronin *et al.*, 2000). Phosphorylation of α-synuclein can also occur on the conserved C-terminal tyrosine residue Y125 by the action of c-src and fyn protein-tyrosine kinases (Ellis *et al.*, 2001; Nakamura *et al.*, 2001). Fyn has been implicated in synaptic plasticity through the finding, that *fyn*$^{-/-}$ knockout mice have a lower hippocampal long term potentiation (Grant *et al.*, 1992). However, the reduced performance in the water maze paradigm observed in this study was caused by swimming deficits rather than impaired spatial learning (Huerta *et al.*, 1996). A number of other behavioural phenotypes are associated with the deletion of the *fyn* gene (for review see Yagi, 1999). Also, fyn phosphorylates NR2 subunits of the NMDA receptor (Suzuki and Okumura-Noji, 1995), which is critically involved in many forms of long term potentiation (chapter 1.3).

Yeast-two-hybrid analysis with human cDNA fragments identified synphilin-1 as a specific interacting partner of α-synuclein. Its coexpression with the NAC region

of human α-synuclein led to eosinophilic inclusions in HEK cells. However, this was not observed when synphilin-1 was coexpressed with full-lengh α-synuclein (Engelender *et al.*, 1999). The interaction between the two proteins occurs via their C-termini (Kawamata *et al.*, 2001). Although little is known about the physiological relevance of its interaction with α-synuclein synphilin-1 has been implicated in the pathophysiology of synucleinopathies. Synphilin-1 is present in most LB in PD, but absent from α-synuclein-positive Lewy neurites (Wakabayashi *et al.*, 2000). Also, synphilin-1 is ubiquitinated by parkin (Chung *et al.*, 2001). The human synphilin-1 locus is mapped to chromosome 5q23.1-q23.3 (Engelender *et al.*, 2000), but unlike α-synuclein no mutations in the gene are known to be associated with PD (Bandopadhyay *et al.*, 2001; Farrer *et al.*, 2001).

Another binding partner of α-synuclein is the presynaptic dopamine transporter DAT, which mediates the uptake of released dopamine. The interaction of the two proteins accelerates dopamine uptake and thus implicates α-synuclein in the physiological and pathological function of the dopaminergic system (Lee *et al.*, 2001).

Further possible functions of α-synuclein have been postulated, including an involvement in signalling cascades as well as protein folding and degradation. For example, the homology between the proteins rho and ras and the N-terminal repeated consensus modules of α-synuclein (Maroteaux *et al.*, 1988) could imply a role in signalling pathways and gene expression (for review see Takai *et al.*, 2001). Similarly, α-synuclein coprecipitates with the transcription factor Elk-1, and binds to the MAP kinase ERK-2 (Iwata *et al.*, 2001). The inhibiting effect of synucleins on the aggregation of alcohol dehydrogenase and insulin suggests a chaperone-like activity (Souza *et al.*, 2000). Also, the N-terminus of α-synuclein has a homology with the 14-3-3 chaperones, and α-synuclein coprecipitates with 14-3-3b (Ostrerova *et al.*, 1999). However, the binding of α-synuclein to the inducer of apoptosis BAD that was observed in this study could not be confirmed (Nagano *et al.*, 2001). A number of the proteins that are present in LB are involved in protein degradation pathways (chapter 1.1.5). It could thus be speculated that this is also the case for α-synuclein. In a yeast-two-hybrid screen, α-synuclein was shown to interact with Tat binding protein 1 (TBP1), which is part of the regulatory complex of the 26S proteasome (Ghee *et al.*, 2000).

1.2 Sindbis virus

1.2.1 The Sindbis virus life cycle

The Sindbis virus (SV) belongs to the alphavirus family. These are small RNA viruses that are transmitted to mammals and birds by mosquitoes (for review see Griffin, 1998; Flint *et al.*, 2000). Sindbis virions are enveloped particles containing a positive-stranded (+) RNA genome. SV can infect a variety of mammalian cell lines. However, SV infection is predominantly neurotropic and can cause encephalomyelitis in young mice. Infected neurons undergo apoptotic cell death in neonatal mice, but in adult mouse brain SV establishes a persistent noncytopathic infection.

The Sindbis virion binds to the cell surface predominantly via the structural protein E2 and is internalised by receptor-mediated endocytosis. The 11.7 kb RNA genome is released into the cytoplasm upon acidification of the vesicle. The 5'-region of the genome is then translated to form the nonstructural proteins. The active replicase nsP1234 is formed through maturation processes from its precursor protein P1234 and acts as RNA-dependent RNA polymerase. It transcribes the full-length (+) RNA genome into the (-) RNA strand and vice versa, causing an amplification of the full-length viral genome. The replicase also amplifies the subgenomic (+) RNA species from the (-) strand, which is under control of the subgenomic promoter (P_{SG}). The subgenomic (+) RNA corresponds to the 3'-region of the full-length genome, and its translation results in the expression of the structural proteins that are necessary for packaging the viral genomic RNA into capsids and virions. Initially, the structural proteins are translated as a precursor protein capsid-PE2-6K-E1. Proteolytic cleavage releases the capsid protein. The protein PE2-6K-E1 enters the secretory pathway via the endoplasmic reticulum (ER) and the Golgi system. It undergoes maturation steps that lead to the cell surface expression of the glycoproteins E1 and E2. The capsid protein assembles with (+)-stranded genomic RNA to form T=4 icosahedral capsids. Packaging of the genome is brought about by a packaging signal (PS) in the genomic RNA sequence. Capsids migrate to the cell membrane, where they assemble with the glycoproteins, and are then released from the cell as virions (Fig.3). The T=4

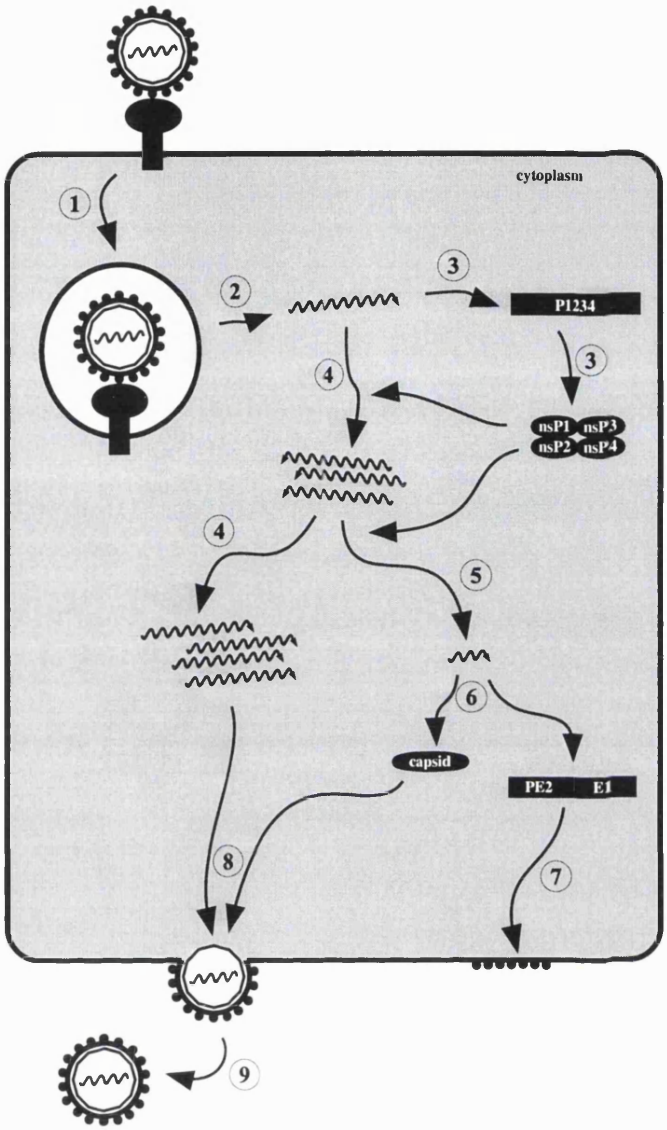

Figure 3. Life cycle of the Sindbis virus

The Sindbis virion enters the cell by receptor-mediated endocytosis (step 1). The (+)-stranded RNA genome is released from the vesicle (2) and translated to form P1234 (3). Maturation of this precursor protein results in active replicase nsP1234 that catalyses the synthesis of the (-) strand as well as the (+) RNA strand, thus amplifying the full-length viral genome (4). It also amplifies the subgenomic (+) RNA species (5), which is translated to form the structural proteins (6). Some of these proteins (the precursor protein PE2-6K-E1) enter the secretory pathway via the endoplasmic reticulum (ER) and the Golgi system to reach the cell membrane as glycoproteins E1 and E2 (7). The capsid protein assembles with the (+)-stranded genomic RNA to form capsids (8), which are released as virions upon assembly with the glycoproteins E1 and E2 (9) (adapted from Flint *et al.*, 2000).

icosahedral outer protein layer of the virions is composed of 240 heterodimers of the structural glycoproteins E1 and E2. Between the capsid and the outer protein layer of the virion lies the lipid bilayer of the cell membrane.

1.2.2 Sindbis viral expression systems

The expression of recombinant proteins in animal cells can be achieved using SV-based expression systems (for review see Frolov *et al.*, 1996). The strategy of this approach results from the replacement of the viral structural genes in the RNA genome with the coding sequence of the protein to be expressed. Transfection of a cell with this replicon RNA results in the amplification of the full-length genome and of the subgenomic RNA species that contains the recombinant sequences under the control of the subgenomic promoter (P_{SG}). However, this replicating RNA is packaging-incompetent, since it lacks the expression of the structural proteins. Instead, translation of the subgenomic RNA leads to the expression of the recombinant protein.

The generation of recombinant virions can be achieved, when replicon RNA is cotransfected with defective helper RNA that contains the sequences for the structural packaging proteins under control of the P_{SG}. However, the helper RNA lacks the nonstructural replicase sequence. Thus, amplification of the helper RNA and translation of the structural proteins only occurs when replicon RNA is cotransfected. Complementation between the two RNA species leads to copackaging of replicon and helper RNA in virions. These retain plaque-forming activity within their bipartite genome (Geigenmuller-Gnirke *et al.*, 1991). To generate infective virions that are replication-incompetent (i.e. the formation of new virions is prevented following infection), helper RNA species were engineered that lack the packaging signal (PS). Using these helper RNA species, most newly formed virions only contain the replicon RNA (pSinRep5 vector) that retains its PS. The virions can then be used for the delivery of replicon RNA into infected cells to achieve the expression of recombinant proteins. However, low rates of copackaging of defective helper RNA (e.g. DHBB) can still be observed in the absence of the PS (Bredenbeek *et al.*, 1993); for instance, DHBB is copackaged at a rate of 0.33% (Lu and Silver, 2001). Furthermore, recombination events between the replicon and helper RNA species can lead to replication-competent virions. Such recombination events include insertions, deletions,

and rearrangements of the parental RNA species. Eventually, these recombined viral genomes evolve to similar sizes as wildtype genomic viral RNA (Weiss and Schlesinger, 1991).

Neurovirulence of SV strains is influenced by mutations in the E1 and E2 glycoprotein sequences (Lustig *et al.*, 1988). The glycoprotein sequences of a neurovirulent strain were integrated into the helper construct pDH26S (Bredenbeek *et al.*, 1993). This expression system can be successfully employed for the specific heterologous expression of recombinant proteins in hippocampal interneurons, pyramidal, and granular neurons, with little infection of glial cells. Expression of green fluorescent protein allows to monitor the morphology of neurons in living rat hippocampal slice cultures (Ehrengruber *et al.*, 1999).

Recent approaches for the development of alphaviral expression systems with increased biosafety include the generation of tripartite trans-complementing RNA genomes. Cotransfection with replicon and two helper RNA species of the Semliki Forest virus (SFV), an alphavirus highly similar to SV, reduces the number of replication-competent virions since more independent recombination events are required for this to occur (Smerdou and Liljestrom, 1999). Alternatively, cell lines were stably transfected with constructs containing the sequences of the viral structural proteins under the control of the P_{SG}. Upon transfection with replicon RNA the expression of the structural proteins commences and leads to packaging of the replicon RNA with few replication-competent virions (Polo *et al.*, 1999). Further developments include the generation of SV expression systems with decreased cytopathic effects on the infected cells (Agapov *et al.*, 1998).

1.3 The NMDA receptor

1.3.1 General overview

Glutamate is the most common excitatory neurotransmitter in the mammalian CNS. It acts on postsynaptic glutamate receptors, transmitting sensory and motor information, but is also involved in higher brain functions such as learning and memory. Half a century ago, Donald Hebb had postulated a 'plastic synapse' as a cellular model for associative learning (Hebb, 1949):

> *'When an axon of cell A is near enough to excite a cell B and repeatedly or persistently takes part in firing it, some growth process or metabolic change takes place in one or both cells such that A's efficiency, as one of the cells firing B, is increased.'*

According to this model cellular learning is dependent on the efficacy of synaptic transmission. The discovery of long term potentiation (LTP) in the hippocampus showed that in a population of synapses the size of the postsynaptic responses is increased after tetanic presynaptic stimulation. Thus, these synapses perform according to the proposed model (Bliss and Lomo, 1973).

The first member of the NMDA receptor family, subunit NR1 was identified by expression cloning in *Xenopus laevis* oocytes (Moriyoshi *et al.*, 1991). By their characteristic involvement in signal processing, these ionotropic glutamate receptors have been implicated in synaptic plasticity. NMDA receptors act as coincidence detectors, by recognising two independent signals, the simultaneous release of glutamate from the presynaptic nerve terminal and the depolarisation of the postsynaptic terminal (chapter 1.3.4).

The activation of the NMDA receptor triggers a specific intracellular signal, the flow of Ca^{2+} ions into the postsynaptic terminal (Bourne and Nicoll, 1993). The Ca^{2+} influx can mediate a number of cellular responses, as for example LTP (chapter 1.3.6; for review see Bliss and Collingridge, 1993). Also, the influx of Ca^{2+} ions by overactivation of NMDA receptors can result in irreversible cell damage and delayed neuronal cell death. Proteases such as the calpains, nitric oxide (NO), or phospholipases are believed to be critically involved in these excitotoxic events (for review see Choi, 1988; Choi, 1992).

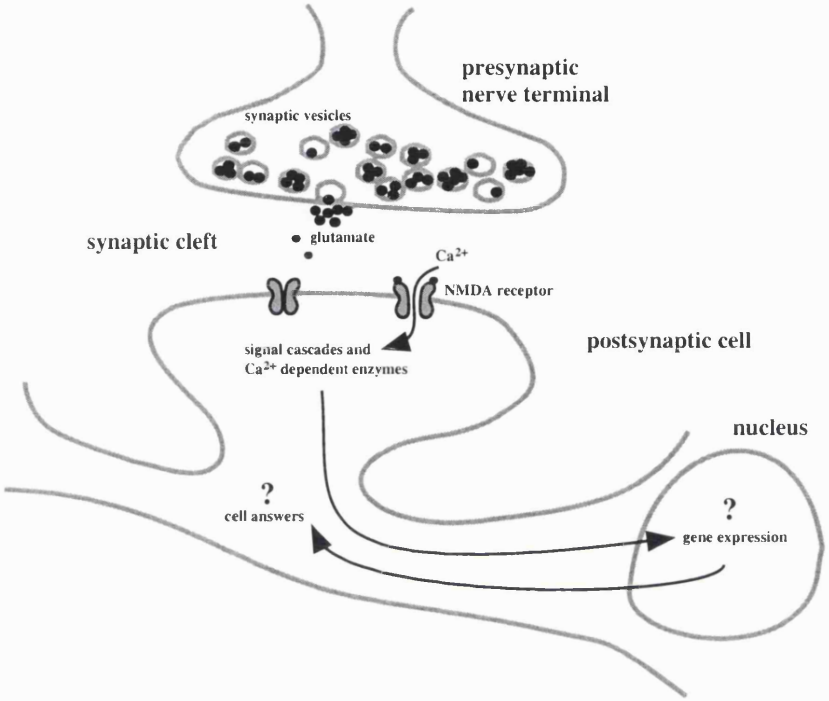

Figure 4. Schematic representation of the NMDA receptor function

The activation of NMDA receptors occurs through the simultaneous release of glutamate from presynaptic vesicles into the synaptic cleft and the depolarisation of the postsynaptic nerve terminal (coincidence detection). This leads to the influx of Ca^{2+} ions into the postsynaptic terminal. Ca^{2+} ions activate various signal cascades that alter the expression levels of a number of genes. mRNA expression changes underlie some of the cellular responses that are dependent on the activation of NMDA receptors, such as LTP or excitotoxic processes. It is the aim of the project to identify such differentially expressed genes and to characterise their function.

Although the molecular mechanism of coincidence detection has been well studied, many of the downstream effects that are brought about by the Ca^{2+} signal remain unknown (Fig.4).

1.3.2 Structure of NMDA receptors

NMDA receptors belong to the ionotropic glutamate receptor (iGluR) family (for review see Dingledine *et al.*, 1999). They include the subunits NR1 (Moriyoshi *et al.*, 1991), NR2A-D (Monyer *et al.*, 1992; Ishii *et al.*, 1993), and NR3A/B (Ciabarra *et al.*, 1995; Sucher *et al.*, 1995; Nishi *et al.*, 2001). The primary transcript of NR1 is processed by alternative splicing of three exons to result in a total of eight splice variants, adding further to the variability of NMDA receptors (Hollmann *et al.*, 1993). The protein sequence of NMDA receptor subunits comprises a cluster of four hydrophobic membrane domains M1 to M4. M2 is believed to form a loop within the cell membrane, lining the channel pore (Wo and Oswald, 1995). Functional NMDA receptors are heterooligomeric complexes, assembled from two NR1 subunits and a number of NR2 subunits (Behe *et al.*, 1995).

Furthermore, NMDA receptors interact with postsynaptic proteins such as postsynaptic density protein PSD-95 (Kornau *et al.*, 1995). They lie at the core of large multiprotein complexes, as demonstrated by proteomic analysis. These include glutamate receptors (e.g. NMDA, kainate, and metabotropic receptors), adaptor proteins (e.g. PSD-95), second messenger systems (e.g. PKA, PKC, CaM kinase, MAP kinase pathways), and cytoskeletal proteins (e.g. actin binding protein α-actinin 2) (Husi *et al.*, 2000). Many of these proteins are known to play a role in LTP (for review see Sanes and Lichtman, 1999).

1.3.3 Expression patterns of NMDA receptor subunits

The expression of NMDA receptor subunits follows distinctive temporal and regional patterns. Prenatal expression of rat NR1 is low, but gradually increases after birth to reach a maximum in the third postnatal week (Sheng *et al.*, 1994). In adult rats, NR1 subunits are expressed in most neurons, with highest mRNA expression levels in the hippocampus, cerebellum, bulbus olfactorius, and cortex (Moriyoshi *et al.*, 1991).

The regional expression of NR1 splice variants is differentially regulated, as for example in the hippocampus (Paupard *et al.*, 1997).

Expression of NR2A and NR2C subunits begins around birth, whereas NR2B and NR2D are also detected during embryonic development. Expression of NR2 subunits reaches a maximum in the first weeks of postnatal development and then decreases to a plateau. In the hippocampus, predominantly NR2A and NR2B subunits are expressed, while NR2C expression is restricted mainly to the cerebellum (Monyer *et al.*, 1994).

1.3.4 Electrophysiological properties of NMDA receptors

NMDA receptors display a characteristic electrophysiological profile (for review see Dingledine *et al.*, 1999). They are activated by agonists such as glutamate or N-methyl-D-aspartate (NMDA) and the simultaneous binding of the coagonist glycine (Curras and Pallotta, 1996). The receptors are permeable to Na^+, K^+, and also to Ca^{2+} ions (MacDermott *et al.*, 1986). In the presence of physiological Mg^{2+} concentrations the receptor channel is blocked in a voltage-dependent manner, and is inactive at the membrane resting potential of -70 mV. Depolarisation of the membrane generally occurs by the action of ionotropic excitatory receptors (e.g. AMPA receptors). This releases the Mg^{2+} ion from the channel pore (Mayer *et al.*, 1984; Nowak *et al.*, 1984). Thus, NMDA receptors act as a coincidence detector for the occurrence of two independent simultaneous events (Bourne and Nicoll, 1993), the release of glutamate from presynaptic vesicles into the synaptic cleft and the depolarisation of the postsynaptic terminal (release of Mg^{2+} ions from the channel pore). The permeability of NMDA receptors for Ca^{2+} ions and the Mg^{2+} block are controlled by a conserved asparagine residue N598 in the membrane domain M2 (N-site) that lines the channel pore. Indeed, mutant receptors of the subunit composition NR1(N598R)/NR2A are Ca^{2+}-impermeable and are not blocked by Mg^{2+} ions, since the positively charged arginine residue repels the divalent cations (Burnashev *et al.*, 1992). Such mutant receptors lack the coincidence detection capability of wildtype NMDA receptors.

1.3.5 Downstream signalling of the NMDA receptor activation

The coincidence detection of the NMDA receptor transforms two simultaneous synaptic events into a cellular signal, the influx of Ca^{2+} ions into the postsynaptic nerve terminal (Bourne and Nicoll, 1993). It is assumed that the cell distinguishes between the Ca^{2+} influx through NMDA receptors and from other sources, such as voltage-dependent Ca^{2+} channels (Bliss and Collingridge, 1993). Therefore, specific signalling cascades must exist that mediate appropriate responses to the NMDA receptor activation. The Ca^{2+} influx leads to the activation of Ca^{2+}-dependent enzymes and cellular signalling cascades. Some of these effects occur at the protein level and cause a fast cellular response, for example the Ca^{2+}-dependent inactivation of NMDA receptors by Ca^{2+}-calmodulin (Ehlers *et al.*, 1996). This interaction can be competitively inhibited by α-actinin 2 (Wyszynski *et al.*, 1997; Zhang *et al.*, 1998). However, long-lasting cellular responses such as LTP also rely on changes of the expression levels of a number of genes (for review see Davis and Laroche, 1998). These include immediate early genes (IEG) (Cole *et al.*, 1989), NMDA (Thomas *et al.*, 1994) and AMPA receptors (Nayak *et al.*, 1998), as well as the presynaptic proteins synapsin I and syntaxin 1B (Hicks *et al.*, 1997).

1.3.6 Long term potentiation

The hippocampus has been implicated in higher brain functions such as learning and memory. High frequency stimulation of excitatory hippocampal pathways leads to increased excitatory postsynaptic responses (Bliss and Lomo, 1973). Potentiation phenomena that exceed one hour in duration are referred to as long term potentiation (LTP). One condition for LTP is the simultaneous activation of the presynaptic and the postsynaptic terminal. Even weak presynaptic stimulation can lead to LTP if the postsynaptic terminal is artificially depolarised (Sastry *et al.*, 1986). The postsynaptic NMDA receptor acts as coincidence detector and is a prime candidate for playing a role in many forms of LTP. Following the activation of NMDA receptors Ca^{2+} ions enter the postsynaptic terminal. The fact that the intracellular application of Ca^{2+} chelators can inhibit LTP suggests that the Ca^{2+} influx represents the cytoplasmic signal for LTP (Lynch *et al.*, 1983). The expression of LTP involves the activation of

Ca^{2+}-dependent enzymes as well as translation and gene expression (for review see Davis and Laroche, 1998). Retrograde signals may mediate changes in the presynaptic cell. Among the candidates are nitric oxide (NO) and arachidonic acid (Williams *et al.*, 1989; Zhuo *et al.*, 1993). Also, morphological changes at the synapse are associated with LTP (Engert and Bonhoeffer, 1999).

Behavioural studies on mouse models with genetic modifications in the NMDA receptor genes address the relation between NMDA receptor-dependent forms of LTP and spatial learning. The absence of the NR1 subunit in homozygous knockout mice causes neonatal death within 8-15 hours after birth. Heterozygous animals express reduced NR1 mRNA and protein levels and appear phenotypically normal (Forrest *et al.*, 1994). Expression of very reduced levels of NR1 in mice (5-10%) was achieved by the insertion of a neo selection cassette into intron 20 of the NR1 gene, resulting in a hypomorphic allele. Homozygous animals display a number of behavioural phenotypes related to schizophrenia (Mohn *et al.*, 1999). The restricted deletion of NR1 in the CA1 field of the hippocampus abolishes NMDA receptor-mediated synaptic currents and LTP in CA1 synapses. Interestingly, these animals also display deficits in the water maze task (Tsien *et al.*, 1996). In this spatial learning paradigm, mice or rats have to locate a hidden platform in a water bath (Morris, 1984). Also, knock-in mice have been generated that express Ca^{2+}-impermeable NMDA receptors by introducing the point mutation N598R into the NR1 subunit (Kneussel, 1997; Single *et al.*, 2000). An alternative approach to the study of mutant mouse models is the pharmacological inhibition of NMDA receptors in animals. Application of the NMDA receptor antagonist D-aminophosphonovaleric acid (D-APV) inhibits dentate gyrus (DG) LTP and causes deficits in spatial learning in rats *in vivo* (Morris *et al.*, 1986).

1.3.7 The NR1 N598R mutant mouse model

The $NR1^{Rneo/+}$ knock-in mouse strain (Kneussel, 1997) carries the point mutation N598R in exon 15 and an insertion of a neomycin selection cassette (neo) in intron 18 of the NR1 gene (Fig.5A). The neo cassette was inserted by homologous recombination and is flanked by lox-P sites. It causes the disruption of full-length

transcription of the N598Rneo allele and leads to the hypomorphic expression of mutant N598R subunits, similar to a previously described mutant NR1 mouse model (Mohn *et al.*, 1999). Homozygous $NR1^{Rneo/Rneo}$ animals die postnatally. Heterozygous $NR1^{Rneo/+}$ animals are fertile and reach adulthood, but die at an earlier age than wildtype littermates. They also show deficits in spatial learning and an absence of LTP in the DG (Chen, b in preparation).

Matings between heterozygous $NR1^{Rneo/+}$ animals and a transgenic strain expressing Cre-recombinase (Schwenk *et al.*, 1995) lead to the global excision of the neo cassette in the offspring with the mutant NR1 allele (Fig.5). This results in the expression of 50% NR1 N598R subunits. The mutant subunits assemble into NMDA receptors that are Ca^{2+}-impermeable, not blocked by Mg^{2+} ions, and thus do not act as coincidence detectors. Therefore, these animals can be used to study the consequence of the absence of coincidence detection *in vivo*, but allowing the natural protein interactions of the NMDA receptor molecule to occur. The global activation of the mutant allele is dominant negative lethal, i.e. it causes heterozygous $NR1^{R/+}$ animals to die within several hours after birth. The gross morphology in the CNS of $NR1^{R/+}$ animals is unchanged in comparison to wildtype littermates. However, the formation of the whisker-related somatotopic map in the trigeminal pathway is impaired in mice exclusively expressing NR1 N598R subunits ($NR1^{R/-}$), but not in $NR1^{R/+}$ animals (Rudhard *et al.*, in preparation).

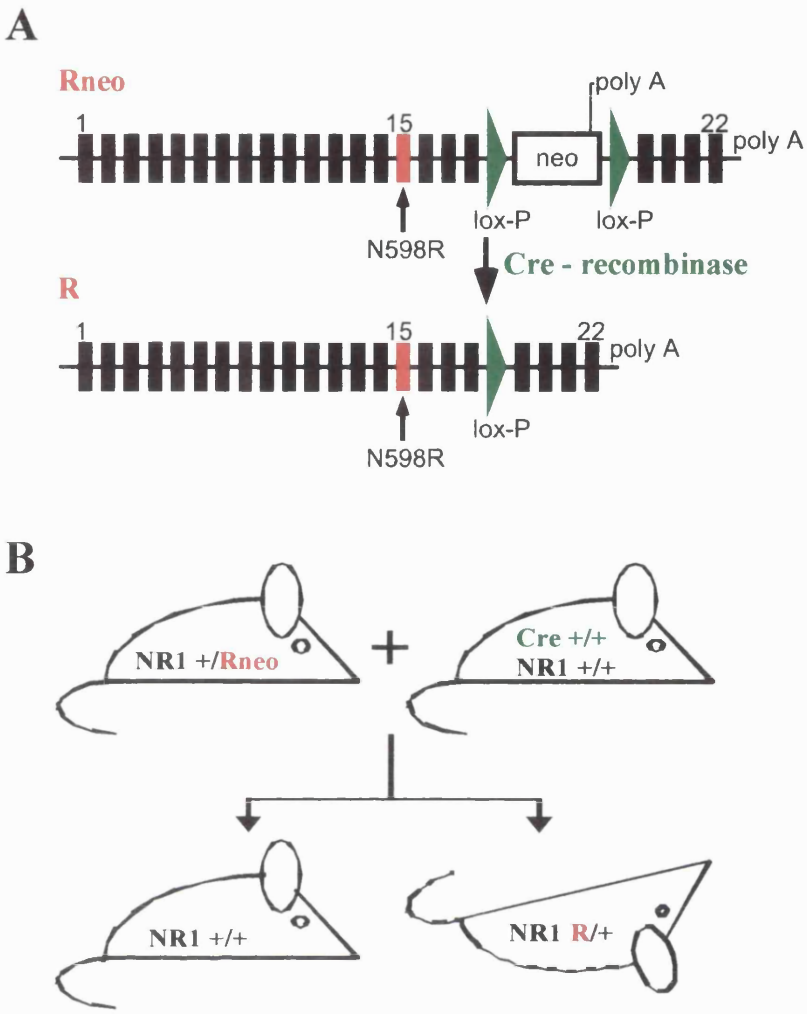

Figure 5. The NR1 N598R mutant mouse model

A. The $NR1^{Rneo/+}$ knock-in mouse strain (Kneussel, 1997) carries the point mutation N598R in exon 15 of the NR1 gene and the insertion of a neomycin selection cassette (neo) in intron 18, flanked by lox-P sites. The $NR1^{Rneo}$ allele (Rneo) leads to hypomorphic expression of mutant NR1 N598R subunits. The neo cassette is excised by Cre-recombinase. The $NR1^{R}$ allele (R allele) results in the expression of 50% mutant NR1 N598R subunits in heterozygous animals $NR1^{R/+}$.

B. Breeding scheme for the generation of mice expressing mutant NR1 subunits. The mating of $NR1^{Rneo/+}$ mice with a transgenic strain expressing Cre-recombinase ($Cre^{+/+}$) causes the excision of the neo cassette from the mutant allele in the offspring. Heterozygous animals $NR1^{R/+}$ die within several hours after birth. The comparison of mRNA expression levels in mice expressing the Ca^{2+}-impermeable N598R subunits ($NR1^{R/+}$) and their wildtype littermates ($NR1^{+/+}$) was chosen as an approach to identify genes whose expression is regulated by the influx of Ca^{2+} ions through NMDA receptors.

1.4 Aim of the project

1.4.1 Downstream effects to the NMDA receptor activation

The project was aimed at identifying genes whose expression is controlled by the NMDA receptor activation, and the characterisation of their functions. These genes represent candidates, which may be involved in the cellular responses to the NMDA receptor-mediated Ca^{2+} influx into the postsynaptic nerve terminal (Fig.4). Knock-in mice with the point mutation N598R in the NR1 gene were used as experimental model (Fig.5). This mutation causes the expression of Ca^{2+}-impermeable receptors that fail to act as coincidence detectors. It was expected that the N598R mutation would lead to a changed expression profile of those genes that are involved in mediating the cellular answer to the NMDA receptor activation. cDNA array technology was used for the quantification of expression levels of thousands of genes in a single experiment (for review see Colantuoni *et al.*, 2000).

While the screen failed to detect differentially expressed genes that are regulated by the NMDA receptor activation, it led to the discovery of a C57BL/6J substrain with a chromosomal deletion, which includes the α-synuclein gene locus (*Snca*). These findings were followed by functional research into downstream effects caused by the absence of α-synuclein. Some of the results have been published (Specht and Schoepfer, 2001; see appendix).

1.4.2 Viral expression system of α-synuclein

The second part of the project consisted in the generation of a Sindbis viral system for the expression of α-synuclein in neurons. In order to monitor the subcellular localisation of the recombinant protein in organotypic hippocampal neurons, α-synuclein was expressed as a fusion protein with red fluorescent protein (RFP) and enhanced green fluorescent protein (eGFP). These studies focus on the understanding of the physiological function of α-synuclein within neurons and its subcellular distribution. The emphasis of the presented data lies on the development of the viral expression system and the evaluation of its suitability for expression studies.

CHAPTER 2
Materials and methods

Molecular biological techniques were performed as described elsewhere (Sambrook *et al.*, 1989). Abbreviations of compounds and buffers are used according to this source.

2.1 Materials

2.1.1 Chemicals

All chemicals were purchased from Sigma-Aldrich and BDH-Merck, unless otherwise stated. Cell culture media, sera, and buffers were supplied by Gibco BRL, culture dishes by Nalge Nunc and Falcon (Becton Dickinson Labware). Milli-Q purified water (Millipore) was used throughout. Oligonucleotides (Sigma-Genosys) were diluted in TE buffer to 10 pmol/µl. Specific oligonucleotide sequences are listed in the appendix.

2.1.2 Standard buffers and solutions

50x Denhardt's reagent	1% Ficoll (type 400), 1% polyvinylpyrrolidone (PVP, MG 10000), 1% bovine serum albumin (BSA fraction V)
5x MOPS buffer	100 mM MOPS, 40 mM sodium acetate (NaAc), 5 mM EDTA, pH7
PB (0.1 M phosphate buffer)	77 mM Na_2HPO_4, 23 mM NaH_2PO_4, pH7.4
PBS	16 mM Na_2HPO_4, 4 mM NaH_2PO_4, 150 mM NaCl
20x SSPE	3 M NaCl, 200 mM NaH_2PO_4, 20 mM EDTA, pH7.4
TAE	40 mM Tris acetate, 1 mM EDTA, pH8
TBE (National Diagnostics)	89 mM Tris borate, 2 mM EDTA, pH8.3
TE	10 mM Tris, 1 mM EDTA, pH8

2.2 Standard molecular biology techniques

2.2.1 Bacterial cultures

DH5α cells (Gibco) were streaked onto LB agar plates (3.2%; Gibco) to obtain single colonies. For selection 150 µg/ml ampicillin were added to the agar.

Single colonies were inoculated in 2 ml LB medium (2%; Gibco) or TB medium (4.7%; Gibco). For selection 200 µg/ml ampicillin were added. Cultures were grown in a shaking incubator at 37°C (225 rpm). Salt-free LB medium (1% bacto-tryptone (Difco), 0.5% bacto-yeast extract (Difco), pH7.4) was used for amplification of plasmids containing eGFP and RFP coding sequences (CDS).

2.2.2 Small-scale preparation of plasmid DNA

Small-scale plasmid preparation was based on alkaline lysis protocols (Birnboim and Doly, 1979; Ish-Horowitz and Burke, 1981). Overnight (o/n) bacterial cultures (1.5 ml LB or TB medium) were pelleted (8000 x *g*, 30 s), resuspended in 150 µl of 50 mM glucose, 25 mM Tris, 10 mM EDTA, pH8, and lysed with 300 µl of freshly prepared 0.1 M NaOH, 1% SDS for 3 minutes on ice. The lysate was neutralised with 200 µl of 3 M potassium acetate (KAc), 2 M acetic acid (HAc) for 5 minutes on ice and cleared by centrifugation (15000 x *g*, 5 min). The supernatant was digested for 30 minutes at 37°C with 30 µg RNaseA. Proteins were removed by extraction with 400µl phenol:chloroform:isoamylalcohol (25:24:1; Gibco). The aqueous phase was transferred to a new tube and the plasmid DNA was precipitated with 850 µl ethanol, followed by centrifugation (15000 x *g*, 5 min). Pellets were washed with 70% ethanol, resuspended in 50 µl TE buffer, and stored at -20°C. Plasmid yields were ~25 µg.

2.2.3 Large-scale preparation of plasmid DNA

Highly purified plasmid DNA was obtained using a plasmid purification kit according to the manufacturer's protocol (Maxi-prep column kit; Qiagen). 100 ml LB or 40 ml TB medium were inoculated with a 1.5 ml o/n culture (high copy number

plasmids) and grown to an optical density of OD_{600}=0.5. The bacteria were pelleted (6000 x *g*, 15 min, 4°C) and the plasmid was purified by alkaline lysis, followed by affinity purification by gravity flow on anion-exchange columns. Preparations yielded 200-600 µg plasmid DNA and were resuspended in 400-500 µl TE buffer and stored at -20°C.

2.2.4 Polymerase chain reaction

cDNA fragments containing the coding sequences (CDS) of α-synuclein were generated by polymerase chain reaction (PCR). This was performed in 50 µl 1x Pfu polymerase PCR-buffer (Promega), containing 0.01-0.1 µg template DNA (α-synuclein clone GenBank W41663, NCBI; I.M.A.G.E. Consortium CloneID 353366, HGMP; Lennon *et al.*, 1996), 20 pmol of each primer, 10 nmol of each nucleotide, and 1.2 U Pfu polymerase (Promega). Cycling started with a denaturing step (94 °C / 5 min, hot start to prevent primer-dimer formation), followed by 25 cycles of denaturing (94 °C / 30 s), annealing (55 °C / 30 s) and polymerisation steps (72°C / 60 s). PCR products were purified by phenol / chloroform or gel extraction, and subjected to restriction digestion prior to subcloning. Specific primer sequences that were used for cloning are listed in the appendix.

2.2.5 Determination of the concentration of nucleic acids

The absorbance of diluted nucleic acid samples in H_2O was measured at 260 nm and 280 nm wavelengths in a quartz cuvette using a digital ultraviolet spectrophotometer (SmartSpec 3000; Biorad). An absorbance of A_{260nm}=1 is equivalent to 50 µg/ml double-stranded DNA and 40 µg/ml single-stranded DNA or RNA. The purity of nucleic acid samples was inferred from the ratio A_{260nm}/A_{280nm}; pure preparation of DNA or RNA have ratios of about 1.8 and 2.0, respectively.

2.2.6 Restriction digestion of DNA

1-5 µg plasmid DNA was digested with 5 U of the restriction enzyme(s), in the appropriate digestion buffer, under the conditions suggested by the enzyme suppliers

(Boehringer Mannheim; New England Biolabs). For subcloning of restriction fragments the reaction products were purified by gel extraction prior to ligation.

2.2.7 Agarose gel electrophoresis of DNA

DNA was analysed on gels containing 0.6%-1.2% agarose in TAE buffer and 0.6 µg/ml ethidium bromide. Different agarose qualities were used for analytical gels (SeaKem LE; FMC Bioproducts) and for purification of DNA fragments (SeaKem GTG, low-melting agarose SeaPlaque GTG or NuSieve GTG; FMC Bioproducts). Gels were run in TAE buffer at 5 V/cm. The loading buffer contained 15% Ficoll (type 400), 0.25% xylene cyanol FF, and 0.25% bromophenol blue. *Sty* I digested λ-phage DNA (including 7.7, 6.2, 4.3, 3.5, 2.7, 1.9, 1.5, and 0.9 kb fragments) or *Msp* I digested pBluescriptII KS(+) (Stratagene) plasmid (including 713, 489, 404, 367, 242, 190, 147, 118, 110, and 67 bp) were used as DNA standards.

2.2.8 Polyacrylamide gel electrophoresis of DNA

Polyacrylamide gels (6% or 8% acrylamide:N,N'-methylene-bisacrylamide (39:1), 0.1% ammonium persulphate in TBE, polymerised with 0.1% TEMED) were run in TBE buffer for the separation of DNA fragments smaller than 300 bp. Samples were loaded with 10x glycerol dye (30% glycerol, 5 mM EDTA, 0.25% bromophenol blue, 0.25% xylene cyanol FF), run at 5 V/cm, and stained in 1 µg/ml ethidium bromide for 15 minutes.

2.2.9 Gel extraction of DNA fragments

Bands containing DNA fragments were excised from agarose gels and purified using silica beads according to the supplier's protocol (Jetsorb; Genomed). Briefly, agarose slices were melted in high salt buffer (300 µl / 100 mg agarose), the DNA was bound to 5-10 µl bead suspension at 50°C for 15 minutes, washed, eluted with 20 µl TE buffer or H_2O, and stored at -20°C.

2.2.10 Phenol / chloroform extraction of DNA

Phenol / chloroform extraction was used to remove proteins and other impurities from DNA, following PCR or restriction digestion. Samples were mixed with an equal volume of phenol:chloroform:isoamylalcohol (25:24:1; Gibco), vortexed for 20 seconds, and centrifuged (15000 x *g*, 2 min). The aqueous phase was transferred to a new tube. If necessary, this procedure was repeated and followed by a chloroform extraction with 1/2 of the sample volume of chloroform:isoamylalcohol (24:1). Samples were then subjected to ethanol precipitation.

2.2.11 Ethanol precipitation of DNA

DNA samples were mixed with 1/10 of the volume of 3 M NaAc pH5.2 and 2.5 volumes ethanol, precipitated (at –20°C if critical), and collected by centrifugation (15000 x *g*, 20 min, 4°C). Pellets were washed twice with 70% ethanol and resuspended in TE buffer.

2.2.12 Ligation of DNA fragments

Ligation was carried out in 10 µl ligation buffer (50 mM Tris, 10 mM $MgCl_2$, 20 mM DTT, pH7.4) in the presence of 100 ng vector DNA, 10 ng of the DNA fragment to be subcloned, 2.5 U T4 ligase (Amersham Pharmacia), and 5 mM ATP. The reaction was incubated for 1-24 hours at 14°C-18°C. Prior to electroporation, reactions were desalted in 1% agarose (SeaKem GTG; FMC Bioproducts), 1.8% glucose for 30-60 minutes on ice, to reduce the salt concentration (Atrazhev and Elliott, 1996).

2.2.13 Preparation of frozen electrocompetent *E.coli*

Electrocompetent bacteria (Dower *et al.*, 1988) were prepared from the *E.coli* strain DH5α (Gibco). A single colony was inoculated in 200 ml fresh LB medium and grown for 14 hours. 50 ml of this culture was used to inoculate 1 l LB medium in two 2 l Erlenmeyer flasks and grown to an optical density of OD_{600nm}=0.5-1.0. The culture

was chilled on ice and cells were pelleted (4000 x *g*, 15 min, 4°C). Cells were washed several times (1x in 1 l sterile H_2O, 2x in 500 ml H_2O, 1x in 20 ml 10% glycerol) and finally resuspended in an equal volume of 10% glycerol (~5 ml final volume), with all steps being carried out at 4°C. Cells were frozen in liquid N_2 as 80 µl aliquots and stored at -80°C. Electrocompetence was tested by transforming pBluescriptII SK(-) plasmid (Stratagene). Usually, 1-2x10^7 colonies/µg DNA were obtained with ampicillin selection.

2.2.14 Transformation of competent *E.coli*

Frozen electrocompetent bacteria (40 µl) were thawed and mixed with 1-10 µl ligation reactions or plasmid preparations on ice. Electroporation was carried out in disposable cuvettes (1 mm gap; BTX Inc.) with 129 Ω and 1.6 kV (~5 ms pulse duration; ECM 600; BTX Inc.). Immediately, 600 µl prewarmed (37°C) SOC medium (2% bacto-tryptone (Difco), 0.5% bacto-yeast extract (Difco), 8.5 mM NaCl, 0.25 mM KCl, 10 mM $MgCl_2$, 20 mM glucose) was added to the cells. After an incubation period (20-40 min, 37°C, 225 rpm) the cell suspension was plated on a pre-warmed LB-plate containing 150 µg/ml ampicillin and grown in a 37°C incubator o/n.

Alternatively, chemically competent cells were used for transformation according to the manufacturer's protocol (one shot Top10 cells; Invitrogen). 50 µl cells were thawn on ice and mixed gently with up to 5 µl of the ligation reaction. After a 30 minute incubation on ice the cells were heat-shocked for 30 seconds in a 42°C water bath and placed on ice. 250 µl pre-warmed SOC medium was added to the transformed cells, which were then incubated (1 h, 37°C, 225 rpm) and plated.

2.2.15 DNA Sequencing

Purified DNA was sequenced using the dideoxy-method (BigDye terminator cycle sequencing kit; ABI Perkin Elmer) combined with automated sequencing (ABI 377 sequencer; ABI Perkin Elmer) according to the manufacturer's protocol.

PEG precipitation was used to purify small-scale plasmid preparations for sequencing. Approximately 4-8 µg plasmid DNA was precipitated in 20 µl volume containing 0.4 M NaCl and 6.5% PEG on ice for 15 minutes and pelleted (15000 x *g*, 15 min, 4°C). The pellet was washed with 70% ethanol and resuspended in 10 µl H_2O. Alternatively, DNA fragments were purified by gel extraction.

Sequencing of purified plasmid DNA (0.3-0.5 µg) or PCR products (100 ng / 100 bp) was performed in 10 µl volume containing 3.2-5 pmol sequencing primer, 1.5 µl BigDye terminator premix (ABI Perkin Elmer), and 2.5 µl of 900 mM Tris, 5 mM $MgCl_2$, pH9. Reactions were overlaid with mineral oil and subjected to 25-30 cycles of denaturing (96°C / 30 s), annealing (50-55°C / 15 s), and extension steps (60°C / 4 min). After addition of 30 µl $CHCl_3$, the 10 µl reaction was transferred to a new tube, precipitated with 25 µl ethanol and 1.5 µl 2M NaAc pH4.5 (15 min on ice) and pelleted (15000 x *g*, 15 min, 4°C). Pellets were washed with 70% ethanol and resuspended in 4 µl loading buffer (5 mM EDTA, 10 mg/ml Dextran blue, 80% deionised formamide). Samples were boiled for 3 minutes and 2 µl were loaded on the sequencing gel.

Denaturing sequencing gels contained a final concentration of 36% urea and 4.6% acrylamide:bisacrylamide (29:1; National Diagnostics). Gel mixes were deionised with 0.5 g ion-exchange resin (Amberlite MB-150), filtered through a 2 µm cellulose nitrate filter (Nalgene; Nalge Nunc), and degassed for 5 minutes. 5 ml 10x TBE buffer was added and the volume was adjusted to 50 ml. Polymerisation was started with the addition of 250 µl 10% ammonium persulphate and 35 µl TEMED. The gel was cast between two quartz glass plates, polymerised (≥2 h), and a 36-well comb was inserted. The gel was prerun for 20 minutes prior to sample loading. TBE was used as running buffer. Primary sequences were acquired using Prism 377 software (ABI Perkin Elmer) and analysed with Sequencher 3.1 software (Gene Codes Corporation Inc.). Generally 400–600 nucleotides of accurate sequence were obtained.

2.3 Genomic DNA techniques

2.3.1 Wildtype mouse strains / mutant mouse models

Animals of the inbred mouse strain C57BL/6J were obtained from Harlan UK (C57BL/6JOlaHsd). Mice from this source are referred to as BL6JHUK within the present thesis. C57BL/6 mice (Harlan, UK) are referred to as BL6, and C57BL/6N (Charles River) as BL6N. ICR and 129/Ola mice were obtained from Harlan UK. C57BL/6J genomic DNA was obtained from Jackson Laboratory (stock JR0664, preparation P34170) and is referred to as BL6Jax.

The $NR1^{Rneo/+}$ knock-in mouse strain (provided by M.Kneussel; Kneussel, 1997) carries the point mutation N598R and an insertion of a neomycin selection cassette (neo) in the NR1 gene (Fig.5). The global excision of the neo cassette was achieved by mating females from a Cre-recombinase expressing transgenic strain (provided by K.Rajewski; Schwenk *et al.*, 1995) with heterozygous $NR1^{Rneo/+}$ males. The $NR1^{Rneo/+}$ strain had been originally generated using ES cells from the inbred strain 129/Ola (cell line E14-1). Both the $NR1^{Rneo/+}$ and the $Cre^{+/+}$ strains were backcrossed into the inbred strain BL6JHUK at least six times, unless otherwise stated.

All mutant mouse strains were bred at the Biological Services Unit at University College London (UCL). All procedures on mice were carried out according to the Animal Scientific Procedures Act 1986 and under licence of the Home Office. Tissue of wildtype mouse strains was isolated from adult mice (generally three months old) obtained through their respective suppliers, or at developmental stages of up to three weeks from animals bred at UCL for less than two generations. Unless otherwise stated, material used in the experiments was obtained from individual animals. Generally, male animals were used.

2.3.2 Preparation of genomic DNA from mouse tail

Genomic DNA was isolated using a proteinase K / SDS protocol (Laird *et al.*, 1991). Approximately 30 mg tail tissue were digested in 500 µl lysis buffer (0.2 M NaCl, 0.1 M Tris pH8.5, 5 mM EDTA, 0.2% SDS, 0.1 µg/µl proteinase K) at 55°C o/n

with rotation. The sample was vortexed and undigested remnants were separated by centrifugation (15000 x *g*, 10 min). The DNA was precipitated with 500 µl isopropanol and pelleted (15000 x *g*, 2 min). Genomic DNA was washed with 70% ethanol and dissolved in 100 µl TE buffer, yielding ~0.5 µg/µl.

2.3.3 Genomic PCR

Genotyping PCR was performed in 25 µl volume of 1x Taq DNA polymerase buffer (with $MgCl_2$; Promega), containing 0.1-1 µg genomic DNA, 10 pmol of each primer, 5 nmol of each nucleotide, and 0.5-1 U Taq DNA polymerase (Promega). Cycling of genomic PCR started with a denaturing step (94°C / 5 min, hot start to prevent primer-dimer formation), followed by 30-35 cycles of denaturing (94°C / 30-60 s), annealing (50-55°C / 15-45 s), and extension steps (72°C / 30-60 s). Alternatively, a touchdown PCR protocol included 30 cycles of denaturing (94°C / 30 s), annealing (68°C / 30 s with ΔT= -0.5°C each cycle), and extension (72°C / 45 s), followed by 10 cycles with constant 52°C annealing. PCR was performed using a UnoII thermocycler (Biometra) with a heated lid (110°C). Oligonucleotide sequences are listed in the appendix.

Specific primers amplified exon 4 (mSynA-Seq9s / mSynA-Seq10a, 130 bp fragment) and exon 6 (mSynA-Seq2s / mSynA-Seq5a, 266 bp) of the mouse α-synuclein gene (*Snca*). *Snca* genotyping was performed using the primers mSynA-Seq2s and mSynA-Seq5a (266 bp), and mNR1-Seq38s and GluN-Seq3a (NMDA receptor subunit NR1, 404 bp) as internal control (touchdown protocol). Genotyping of NR1 mutant mice (Rudhard *et al.*, in preparation) identified the wildtype NR1 (508 bp), the N598Rneo (414 bp), and the N598R allele (excised neo, 651 bp), and was performed using the primers mNR1-Seq103s, mNR1-Seq10a, Neo-Seq4s, and Neo-Seq3a (touchdown protocol). The presence of Cre-recombinase was confirmed with the primers Cre-Seq1s and Cre-Seq2a (486 bp).

Amplification of the chromosome 6 genomic marker *D6Mit357* (UniSTS:130908, UniSTS database, NCBI) yielded a 100 bp product. Other markers used for the characterisation of the *Snca* locus included mouse atonal protein homologue 1 and 2 (*Atoh1*, GenBank D43694, 271 bp; *Atoh2*, GenBank U29086, 245

bp; NCBI), *Abcg2* (UniSTS:159513, 98 bp), *Grid2* (ionotropic glutamate receptor δ2, UniSTS:143256, 95 bp), and the markers *D6Mit120* (UniSTS:130662, 151 bp), *D6Mit122* (UniSTS:130664, 139 bp), *D6Mit299* (UniSTS:130849, 119 bp), and *32.MMHAP36PLC5.seq* (Whitehead Institute/MIT Center for Genome Research, 131 bp). Four PCR primer pairs were used to confirm the deletion of the *Snca* locus (PCR a-d; Fig.11A), covering 120 kb of chromosomal sequence (GenBank AF163865; Touchman *et al.*, 2001).

2.3.4 Yeast cultures

Yeast artificial chromosome (YAC) clones (YAC library, Whitehead Institute/MIT Center for Genome Research; Haldi *et al.*, 1996) were obtained as stab cultures (MRC HGMP Resource Centre). The vector arms pRML1 and pRML2 allow the selection with tryptophane and uracil (Spencer *et al.*, 1993) in the J57D yeast strain (*MAT*α, *ura*3-52, *trp*1 *ade*2-101 *can*1-100 *leu*2-3, 112 *his*3-6). Colonies were streaked onto DOBA-plates (2.5% agar in DOB medium) and grown at 30°C for 3 days. Single colonies were inoculated in 10 ml DOB medium (37.5 mM $(NH_4)_2SO_4$, 0.17% yeast nitrogen base (without amino acids and $(NH_4)_2SO_4$; Difco), 0.072% CSM-TRP-URA (without tryptophane and uracil; Bio 101), 2% glucose; filter sterilised) and grown with shaking for 30 hours at 30°C with closed lids (anaerobic metabolism). Cultures were vortexed occasionally to prevent sedimentation. 400 µl of the cultures were mixed with 100 µl glycerol, vortexed, and frozen as glycerol stocks at -80°C.

2.3.5 Small-scale purification of yeast genomic DNA

Yeast genomic DNA was prepared from 9.6 ml yeast cultures that had been grown for 30 hours in DOB medium (Johnston, 1994). Cells were harvested (3000 x *g*, 3 min) and washed in sterile H_2O by vortexing and centrifugation. Pellets were resuspended in 0.2 ml protoplasting buffer (1% ß-mercaptoethanol, 100 mM Tris pH7.5, 10 mM EDTA pH7.5, 200 U/ml lyticase) and incubated for 2 hours at 37°C with occasional mixing. Cell suspensions were mixed with 0.2 ml lysis buffer (0.2 M

NaOH, 1% SDS), incubated at 65°C for 20 minutes, and rapidly cooled on ice. After the addition of 0.2 ml 5 M KAc pH5.4, the lysate was incubated on ice for 15 minutes and cleared from protein precipitates and detergent (15000 x *g*, 3 min). DNA was precipitated from the supernatant with 0.6 volumes of isopropanol (5 min, room temperature), pelleted (15000 x *g*, 30 s), washed twice with 1 ml 70% ethanol for 10 minutes, and resuspended in 100 µl TE, resulting in ~0.5 µg/µl genomic yeast DNA.

2.3.6 Pulsed field gel electrophoresis

Agarose-embedded yeast genomic DNA was prepared from 30 ml yeast cultures that were grown in DOB medium (CHEF-DR III system, instruction manual; Biorad). Cells were collected (3000 x *g*, 10 min, 4°C), resuspended in 10 ml cold 50 mM EDTA pH8, and counted. Cells were then pelleted and resuspended in cell suspension buffer (10 mM Tris pH7.2, 20 mM NaCl, 50 mM EDTA) at a concentration of $6x10^8$/ml. 630 µl of the cell suspension were mixed with 200 U lyticase and 370 µl melted 2% agarose solution (at 50°C; SeaKem GTG; FMC Bioproducts), and solidified in plug moulds on ice. Agarose plugs were first incubated in 2.5 ml lyticase solution (10 mM Tris pH7.2, 50 mM EDTA, 200 U/ml lyticase) for 2 hours at 37°C with shaking. Plugs were then digested in 2 ml proteinase K solution (1 mg/ml proteinase K (Roche), 100 mM EDTA pH8, 0.2% sodium deoxycholate, 1% sodium lauryl sarcosine) at 50°C o/n without shaking. This was followed by washes for a total of four hours in an excess of wash buffer (20 mM Tris pH8, 50 mM EDTA). 1 mM PMSF was added during the second wash to inactivate proteinase K. Agarose plugs were finally washed and stored in 0.1x wash buffer at 4°C.

Agarose plugs were loaded onto a 1% agarose gel (SeaKem Gold; FMC Bioproducts) in 0.5x TBE buffer. YAC clones were sized using *S.cerevisiae* chromosomes as DNA standards (including 2200, 1600, 1125, 1020, 825, 680, 610, 450, 365, and 285 kb, Chef DNA standard plugs; Biorad). Pulsed field gel electrophoresis was performed at 14°C in 0.5x TBE running buffer with 6 V/cm (Chef DRIII system; Biorad). The pulsed field protocol included 12 hours at a 120° field angle with 60 seconds switch time, followed by 10 hours at 120° with 90 seconds switch time. The gel was stained in 0.5 µg/ml ethidium bromide.

2.3.7 Southern blotting and cDNA probes

Agarose gels were depurinated in 0.2 M HCl (15 min), denatured in 1.5 M NaCl, 0.5 M NaOH (90 min), and neutralised in 1.5 M NaCl, 0.5 M Tris pH7.2, 1 mM EDTA (20 min) with gentle agitation. Southern blotting of DNA onto Hybond-N membranes (Amersham Pharmacia) by capillary force and the probing of the membrane was performed as described for Northern blotting (chapter 2.4.6/7).

YAC clones were characterised using a radiolabelled probe directed at the β-lactamase sequence (Amp probe, 1.1 kb fragment, *Alw*N I/*Apa*L I restriction digest of plasmid pGEM-T) that is contained in the YAC construction vectors pRML1 and pRML2 (Spencer *et al.*, 1993). A second probe was generated using a cDNA fragment from the 3'-untranslated region of α-synuclein (3'UTR; *Bgl* II/*Not* I, 557 bp fragment of clone GenBank W41663, NCBI; I.M.A.G.E. Consortium CloneID 353366, HGMP; Lennon *et al.*, 1996).

2.4 RNA techniques

2.4.1 General considerations

RNA was handled in RNase-free conditions using gloves, autoclaved tips, and fresh Eppendorf tubes. All solutions were prepared in autoclaved glass bottles washed with DEPC-H_2O (0.1% DEPC in H_2O, incubated o/n, and autoclaved) and were made up using DEPC-H_2O or fresh Milli-Q-H_2O. For Northern blotting only dedicated gel trays, combs, and tanks were used.

2.4.2 Preparation of total RNA

Total RNA preparation was based on extraction with guanidine isothiocyanate, phenol, and chloroform (Chomczynski and Sacchi, 1987). Mice from postnatal day P0 to P8 were killed by decapitation. For RNA preparations of early developmental stages, mouse embryos from embryonic day E15.5 to E18.5 were obtained by

caesarean section. Embryos were culled by cutting the umbilical cord and then washed in ice-cold PBS. Brains were prepared (including cerebellum and brainstem; ~50-100 mg tissue before P0, 250 mg at P8) and homogenised with an 18G syringe in a total volume of 1.5 ml Trizol reagent (Gibco). If the RNA was to be used in cDNA array experiments a second homogenisation step was performed optionally, in which the sample was applied on a QIA-shredder column (Qiagen) and centrifuged (15000 x *g*, 2 min). The sample was then incubated for 5 minutes at room temperature and centrifuged (15000 x *g*, 2 min). The supernatant was transferred to a new tube, mixed with 300 µl $CHCl_3$ for 15 seconds, and incubated for 3 minutes. Phase separation was attained by centrifugation (15000 x *g*, 15 min, 4°C). The aqueous phase (900 µl) was mixed with 750 µl isopropanol. After 10 minutes, the precipitated total RNA was collected by centrifugation (15000 x *g*, 10 min, 4°C). The pellet was washed with 75% ethanol, resuspended in 250 µl nuclease-free H_2O, and stored at -80°C. An A_{260nm}/A_{280nm} ratio of 1.6-1.8 and a yield of 100-250 µg total RNA were reached.

Adult mice were killed by dislocation of the neck. Total RNA was prepared from the hippocampus (~50 mg tissue) as described, with an estimated yield of 100 µg. Alternatively, RNA was prepared from 0.5 g adult brain, scaling up the volumes of the above protocol by the factor six. The yield was ≥500 µg total RNA.

2.4.3 Preparation of polyA$^+$-RNA

PolyA$^+$-RNA was prepared from 100-200 µg total RNA using oligo-dT mRNA isolation columns according to the manufacturer's protocol (Oligotex; Qiagen). After binding to the oligo-dT resin the polyA$^+$-RNA was washed, eluted with 100 µl 5 mM Tris pH7.5 at 70°C, and stored at –80°C. If the sample was used in cDNA array experiments, a second round of purification was performed. The yield was estimated using a DNA dipstick kit (Invitrogen) and generally reached 0.5-1 µg polyA$^+$-RNA. The polyA$^+$-RNA was precipitated from the eluate (100 µl) at –80°C by adding 5 µl glycogen (2mg/ml, type II from oyster), 10 µl 3 M NaAc pH5.2, and 300 µl ethanol, and collected by centrifugation (15000 x *g*, 15 min, 4°C). The pellet was resuspended in sample buffer for Northern blotting. For cDNA array experiments polyA$^+$-RNA was shipped as wet ethanol precipitate on dry ice.

2.4.4 cDNA array experiments

cDNA array technology allows the expression profiling of thousands of genes in a single experiment (for review see Colantuoni *et al.*, 2000). The experiment itself was performed by Genome Systems Inc. (now Incyte Genomics) on the mouse GEM1 microarray (GEM-5200). First, a reverse transcriptase reaction on 200 ng polyA$^+$-RNA was performed to incorporate fluorescent nucleotides into single-stranded cDNA. Wildtype and mutant samples were labelled with two different fluorophores (cyanine dyes Cy3 and Cy5) and then hybridised simultaneously to the array chip, on which ~9000 expressed sequence tags (EST; cDNA fragments of 0.5-5 kb length) were immobilised. The expression levels were measured by reading the fluorescence intensities at the wavelenghts of the two fluorophores. The resulting data were then forwarded to us by the company.

2.4.5 Agarose gel electrophoresis of RNA

Using a microwave oven, 0.8 g agarose (SeaKem LE; FMC Bioproducts) were dissolved in 62 ml H_2O. Sequentially, 20 ml cold 5x MOPS buffer (at 4°C) and 18 ml of 40% formaldehyde were added. The 0.8% agarose gel was poured in a large tray (16.5 cm). After solidifying for 30 minutes, the gel was prerun for 10 minutes before loading the samples.

RNA samples (100-500 ng polyA$^+$-RNA or 10 µg total RNA in up to 5 µl volume) were denatured in 11 µl preheated sample buffer (1.5 µl 5x MOPS buffer, 2.6 µl formaldehyde, 7.5 µl deionised formamide) at 65°C for 10 minutes. Then, 2.5 µl of preheated loading buffer (12% Ficoll (type 400), 2 mg/ml xylene cyanol FF, 2 mg/ml bromophenol blue, 0.2 mg/ml ethidium bromide) were added. Samples were loaded at 65°C. As RNA standard, 4 µg of *in vitro* transcribed RNA (Promega) was treated in the same way. It contained λ-phage fragments (6583, 4981, 3638, 2604, 1908, 1383, 955, 623 nucleotides) and a mouse β-actin fragment (281 nucleotides). Gels were run in 500 ml 1x MOPS buffer at 0.6-1.2 V/cm for 15-18 hours, stirring both buffer chambers. A photo of the gel was taken under UV illumination before the blotting procedure. Analytical gels were run at 10 V/cm for at least 25 minutes without stirring the buffer chambers.

2.4.6 Northern blotting

RNA was transferred from agarose gels onto a nylon membrane (Hybond-N; Amersham Pharmacia) in 10x SSPE buffer by capillary force o/n. Then, the RNA was cross-linked to the membrane with 120000 µJ by UV irradiation (Stratalinker 2400; Stratagene). A prehybridisation step was performed under rotation for 6-18 hours at 42°C in a glass-tube containing 20 ml hybridisation solution (6x SSPE, 5x Denhardt's reagent, 50 µg/ml yeast RNA (from Torula yeast, type IX), 50 µg/ml denatured (at 96°C) salmon sperm DNA, 50% formamide, 0.5% SDS). The membrane was hybridised at 42°C o/n with a denatured radiolabelled probe in 4-6 ml fresh hybridisation solution. This was followed by three washes in a volume of 250 ml at 65°C with shaking, once in 5x SSPE / 0.1% SDS (30 min) and twice in 0.3x SSPE / 0.1% SDS (10 min; high stringency washes). The bound radioactivity was detected by autoradiography (Kodak X-OMAT-AR) at -80°C with exposure times in the range of 1-48 hours. Membranes were stripped in 0.1% SDS at 90°C for 30 seconds and stored at -80°C. Membranes were not allowed to dry at any stage of the procedure.

2.4.7 Generation of radiolabelled cDNA probes

Appropriate DNA fragments in a range of 0.2-1.5 kb were generated by PCR or restriction digestion of plasmid DNA, separated on 0.5-0.7% agarose gels (low melting NuSieve GTG for <1kb fragments; FMC Bioproducts), excised, and denatured in 1-2 ml H_2O / g agarose (96°C, 3 min).

Radiolabelling was performed by random priming using a Prime-It II kit according to the manufacturer's protocol (Stratagene). Up to 50 ng template DNA in a 24 µl volume were mixed with 10 µl random hexamers or nonamers, denatured (96°C, 3 min), and placed at 37°C for 10 minutes for annealing. Then, 10 µl 5x Primer Buffer for dATP, 5 µl (α^{32}P)dATP (specific activity 3000 Ci/mmol), and 1 µl Klenow fragment of DNA polymerase I (5 U/µl) were added. The 50 µl reaction was incubated for 20-60 minutes at 37°C. ^{32}P-radiolabelled probes were purified with a QIAquick nucleotide removal kit (Qiagen). Binding of the DNA to spin columns was followed by three washes and elution with 200 µl 10 mM Tris pH8.5. Radiolabelled probes were denatured (96°C, 3 min) and used for hybridisation. Generally, activities of 10^7-10^8 cpm were reached.

2.4.8 Templates for radiolabelled cDNA probes

Restriction fragments of an α-synuclein cDNA clone (GenBank W41663, NCBI; I.M.A.G.E. Consortium CloneID 353366, HGMP; Lennon *et al.*, 1996) were used to generate radiolabelled probes. A probe to the 3'-untranslated region (3'UTR) of α-synuclein resulted from a 557 bp fragment (*Bgl* II/*Not* I). The 201 bp 5'UTR *Eco*R I/*Nco* I fragment (data not shown) and the 469 bp *Nco* I/*Nco* I fragment (coding sequence CDS) led to identical results. The cDNA clone W41663 was verified by sequencing (data not shown).

A 3'UTR γ-synuclein probe was obtained from a 393 bp restriction fragment (*Eco*R I/*Not* I) of a cDNA clone (GenBank BE133521, I.M.A.G.E. Consortium CloneID 1533487). Consistent results were obtained using a full-length cDNA probe (745 bp *Eco*R I/*Not* I fragment of clone GenBank AA981984, I.M.A.G.E. Consortium CloneID 1348635; data not shown). Both cDNA clones were verified by sequencing (data not shown). A γ-synuclein probe to the CDS was generated as RT-PCR fragment (primers mSynG-Seq1s and mSynG-PCR4a) and subcloned into the construct pSin-EG-N1 (chapter 3.4.1) with *Nco* I and *Bgl* II. After confirmation of the clone (pSin-gSyn-EG) by sequencing, the 376 bp *Nco* I/*Bgl* II fragment was excised and used to generate radiolabelled probes with identical results (data not shown).

A CDS probe to synphilin-1 was generated using a 1.5 kb RT-PCR fragment (primers hSynph-Seq2s and hSynph-Seq10a). Same results were obtained with a slightly overlapping 290 bp synphilin-1 RT-PCR fragment (primers hSynph-Seq1s and hSynph-Seq3a; data not shown). Primers were designed using the human synphilin-1 sequence (GenBank AF076929). Sequencing of the RT-PCR products revealed ~90% and 85% identity between the human and mouse sequences within two stretches of ~500 bp on the cDNA level (data not shown).

An NR1-specific probe was directed against exons 15-17 of the NMDA receptor subunit, recognising a doublet at 4.2 / 4.4 kb. Identical results were obtained using an NR1 probe for exons 19-22 (data not shown). A murine 0.9 kb probe to the actin CDS served as positive control, revealing a band of 2.2 kb in brain.

2.4.9 Reverse transcriptase PCR

Reverse transcriptase (RT) reactions were performed at 42°C for 30 minutes with 50 ng total RNA, using Ready-To-Go RT-PCR beads (Amersham Pharmacia) in a volume of 25 µl, containing 0.25 µg oligo-dT primer. This was followed by a denaturing step (94°C / 5 min) and PCR cycling (94°C / 30 s, 55°C / 30 s, 72°C / 45 s) with 5 pmol of each specific primer.

The primers mSynA-PCR1s and mSynA-PCR2a were used to amplify a 568 bp mouse α-synuclein fragment (exons 1 to 6 on cDNA). Amplification of a 473 bp mouse tubulin α1 (*Tuba1*) fragment with the primers mTubA1-Seq1s and mTubA1-Seq2a served as a positive control (exons 2 to 4 on cDNA, as judged from the rat genomic sequences).

2.5 Techniques for protein analysis

2.5.1 SDS-PAGE

100 µg mouse tissue were homogenised in 1 ml boiling lysis buffer (1% SDS, 1 mM Na_3VO_4, 10 mM Tris pH7.4) with a Dounce homogeniser (IKA Labortechnik), microwaved for 15 seconds, and cleared by centrifugation (15000 x *g*, 5 min). Protein concentrations, generally ~5-15 µg/µl were measured using a Lowry assay according to the manufacturer's protocol (DC protein assay; Biorad). Samples were denatured (96°C, 3 min) in an equal amount of 2x SDS-PAGE sample buffer (100 mM Tris pH6.8, 20% glycerol, 4% SDS, 10% β-mercaptoethanol, 0.2% bromophenol blue).

SDS-PAGE (Laemmli, 1970) was carried out on 7.5%, 10%, 12.5%, 15%, or gradient (4-20%) polyacrylamide gels with 4% stacking gels in running buffer (25 mM Tris, 200 mM glycine, 0.1% SDS, pH8.8), using Mini-ProteanII systems (Biorad). Gel mixes contained the appropriate concentration of acrylamide:N,N'-methylene-bisacrylamide (29:1) in 375 mM Tris pH8.8 (separating gel) or 125 mM Tris pH6.8 (stacking gel), 0.1% SDS, 0.1% fresh ammonium persulphate, and 0.1% TEMED. Protein samples (10-30 µg per lane) were separated at 40 mA and sized using prestained markers (MW of 10, 15, 25, 37, 50, 75, 100, 150, and 250 kDa; Biorad).

2.5.2 Coomassie blue / silver staining

SDS-PAGE gels were stained in 35% methanol, 15% HAc, 0.1% Coomassie brilliant blue R-250 (Biorad), and destained in 35% methanol, 15% HAc. The detection limit of this method lies at 500 ng protein.

Silver staining increased the sensitivity of detection to 1-5 ng protein. Gels were fixed for 1 h in 50% methanol with shaking and washed with H_2O for a total of 2 hours. This was followed by steps of 20 minutes in 3.5 μM DTT, and in 6 mM $AgNO_3$. After a rinse in H_2O, colour development was carried out in 0.05% formaldehyde, 280 mM Na_2CO_3. The reaction was stopped by the addition of citric acid to a final concentration of 0.2 M.

Gels were washed in water and dried between sheets of gel drying film (BDH).

2.5.3 Western blotting

Proteins were blotted onto PVDF membranes (Hybond-P; Amersham Pharmacia) in blotting buffer (50 mM Tris, 40 mM glycine, 20% methanol, ~pH8) with 6 V/cm / 90 mA for 12-20 h with cooling, using a Transblot System (Biorad). Membranes were blocked in buffer containing 50 mM Tris pH8, 2 mM $CaCl_2$, 80 mM NaCl, 0.2% Igepal CA-630, and 5% non-fat dried skimmed milk (Marvel; Premier Brands) for 1-2 hours. For some antibodies, a different blocking buffer (PBS containing 0.05% Tween20 and 3% BSA) was used to reduce the nonspecific binding. Primary antibodies were applied for one hour in blocking buffer, followed by three washes of 10 minutes with blocking buffer. Membranes were then incubated with horseradish peroxidase (HRP)-conjugated secondary antibodies for one hour at a dilution of 1:10000 in blocking buffer, followed by washes in blocking buffer (1x 10 min) and PBS (3x 15 min). Membranes were developed with ECL Plus reagent (Amersham Pharmacia) according to the supplier's protocol and exposed on film for up to 1 hour (X-OMAT-AR; Kodak). Membranes were stripped at 50°C for 30 minutes in 62.5 mM Tris pH6.7, 2% SDS, 100 mM β-mercaptoethanol, washed, and re-probed.

2.5.4 Antibodies

Monoclonal mouse anti rat α-synuclein IgG1 (S63320; Transduction Laboratories) was used for Western blotting at concentrations of 1:500-1000. Polyclonal rabbit anti human α-synuclein antibody PER4 (provided by M.Goedert; Spillantini *et al.*, 1998b) was used at a titer 1:500. Polyclonal rabbit anti human β-synuclein IgG (1:2500; SA3405; Affiniti) and polyclonal rabbit anti human synphilin-1 IgG (1:1000; ab6179; Abcam) were used in alternative blocking buffer. A second anti human synphilin-1 antibody was used unsuccessfully on mouse proteins (ab6178; Abcam; data not shown).

Polyclonal rabbit anti Sindbis virus IgG (anti-SV; provided by D.Griffin; Jackson *et al.*, 1987) was used at a concentration of 1:5000. Polyclonal rabbit antibodies against GFP (1:2500; ab290; Abcam) and RFP (1:1000; No.8370; Clontech), and monoclonal mouse anti-GFP IgG1 (1:1000; No.1814460, clones 7.1 and 13.1; Roche) were used to detect recombinant proteins.

Monoclonal mouse anti chick α-tubulin IgG1 (1:20000; T9026; Sigma) detected a 55 kDa band, which was used as positive control. HRP-conjugated secondary antibodies (goat anti rabbit or goat anti mouse IgG; Jackson ImmunoResearch Laboratories) were used at a dilution of 1:10000.

2.6 Sindbis viral expression system

2.6.1 Culturing of BHK cells

Baby hamster kidney cells BHK-21 were cultured according to the supplier's protocol (Sindbis expression system; Invitrogen). Cells were cultured at 37°C, 5% CO_2 in MEM alpha medium (with L-glutamine), 5% fetal bovine serum (FBS), and penicillin / streptomycin (100 U/ml / 0.1 mg/ml final concentration, respectively). Cells were generally split when subconfluent (~80-90%) by trypsinisation (1 ml 0.05% trypsin, 0.5 mM EDTA solution (Gibco) in PBS) for a few minutes, followed by neutralisation of the trypsin in two volumes of medium. Cells were collected by

centrifugation (250 x *g*, 5 min), resuspended in medium, counted with a hemocytometer, and plated.

For the preparation of frozen stocks, cells were brought to a concentration of $4x10^6$/ml medium. 0.5 ml of the cell suspension was mixed with an equal volume of ice cold freezing medium (20% DMSO, 80% medium) in cryotubes, placed in a freezing block (cooled to 4°C), transferred to –80°C o/n, and then stored in liquid N_2. Frozen aliquots were thawn in a water bath (37°C, 1-2 min). Cells were washed in 10 ml prewarmed medium, resuspended in medium, and plated.

2.6.2 cRNA synthesis

10-20 µg plasmid DNA was digested at 37°C for 1 hour in a volume of 100 µl containing 30 U of the respective restriction enzyme under the appropriate reaction conditions. Linearisation of the plasmid was confirmed by running 1 µl of the digest on a DNA agarose gel. The product was purified by phenol / chloroform extraction, chloroform extraction, and ethanol precipitation, and resuspended in 8.5 µl DEPC-H_2O. Expression constructs based on the pSinRep5 plasmid (Invitrogen; Bredenbeek *et al.*, 1993) were linearised with *Not* I, adding 15 U *Pvu* I to the restriction digest. The deficient helper plasmid pDH26S (Invitrogen; Bredenbeek *et al.*, 1993) was linearised with *Xho* I.

In vitro transcription was performed in 20 µl 1x SP6 polymerase buffer (Promega) containing ~5 µg linearised plasmid DNA, 5 mM each of ATP, UTP, and CTP, 1.6 mM GTP, 0.75 mM $m^7G(5')ppp(5')G$ (capping reagent; Amersham Pharmacia), and 2 µl SP6 polymerase mix (Promega) for 1 hour at 37°C. 1 µl of the reaction product was analysed on an 0.8% agarose DNA gel.

For purification, the cRNA reaction was brought to a volume of 100 µl with DEPC-H_2O, followed by phenol / chloroform extraction with 20 µl 2 M NaAc pH4, 50 µl H_2O-saturated phenol pH4, and 10 µl chloroform. cRNA was precipitated from the aqueous phase with an equal volume of isopropanol (≥1 h, –20°C) and pelleted (15000 x *g*, 5 min). To remove unincorporated nucleotides, the cRNA was resuspended in 100 µl DEPC-H_2O and precipitated with 30 µl 8 M NH_4Ac and 260 µl ethanol. After centrifugation, the pellet was washed with 70% ethanol and resuspended in 50 µl DEPC-H_2O. 1 µl of the final product was run on an analytical denaturing RNA agarose gel. cRNA yields were in the range of 100 µg.

2.6.3 Transfection of BHK cells / virion preparation

Transfection of BHK cells was performed according to the Sindbis expression system protocol (Invitrogen). The PBS buffer used here was free of divalent cations (137 mM NaCl, 2.7 mM KCl, 10 mM Na_2HPO_4, 1.8 mM KH_2PO_4, pH7.4 in DEPC-H_2O). Cells were harvested by trypsinisation, counted, washed twice in PBS and resuspended in PBS at a concentration of 10^7/ml. For transfection $5x10^6$ cells were mixed with *in vitro* transcribed cRNA in a volume of 0.5 ml PBS, and electroporated in a disposable cuvette (4mm gap; BTX Inc.) with 129 Ω and 0.8 kV (~0.8 ms pulse duration; ECM 600; BTX Inc.). BHK cells were then plated in culture medium.

The medium containing the virions was collected at 24 hours and 48 hours post-transfection and frozen at –80°C. The resulting virion harvests were referred to as vXX(24) and vXX(48), where XX indicates the recombinant fusion protein and the time point of harvest is indicated in brackets.

2.6.4 Plaque assay

BHK cells were plated at a concentration of $5x10^4$/ml medium in 48-well plates in a volume of 1 ml/well. After attachment to the plate (12 h post-plating), monolayers were infected with diluted virion preparations in a volume of 25 µl PBS (1 h, 4°C, with shaking). The cells were then overlaid with 0.25 ml/well pre-warmed agarose (1% low melting SeaPlaque GTG (FMC Bioproducts) in culture medium with 2% serum, equilibrated to 37°C). Plaque-forming units (PFU) were counted at 48 hours post-infection, when cytopathic effects were visible on the monolayer. The infectious unit titers (IU) were established by counting isolated cells expressing eGFP fusion proteins. Cells expressing RFP fusion proteins were not counted due to the high autofluorescence background of the top agarose.

2.6.5 Immunohistochemistry

The surface of 3-well slides (Scientific Laboratory supplies Ltd.) was coated with 10 µg/ml poly-D-lysine in PBS at 37°C for 1-3 hours, washed twice with PBS, and dried. For immunohistochemistry, BHK cells were plated onto these slides

($2x10^4$/well in 250 µl medium) and infected 18 hours post-plating (10 µl virion harvest in 100 µl PBS, 1 h, 4°C). The cells were then washed with PBS and incubated o/n in 250 µl medium. At 24 hours post-infection the cells were washed with PBS and fixed in 4% paraformaldehyde (PFA) in PBS for 30 minutes. After three washes in PBS the cells were permeabilised with 0.1% TritonX100 in PBS for 15 minutes and blocked in blocking buffer (0.1% TritonX100, 2% BSA in PBS) for 15 minutes. The primary antibody incubation (polyclonal rabbit anti-SV at a dilution of 1:1000; provided by D.Griffin; Jackson *et al.*, 1987) was performed in blocking buffer for 2 hours. After three washes of 10 minutes in blocking buffer, the fixed cells were incubated with labelled secondary antibody (Cy5-conjugated goat anti rabbit IgG at 1:20; Jackson ImmunoResearch Laboratories) in blocking buffer for 1 hour. Cells were washed for 10 minutes in blocking buffer, in PBS containing 0.1% TritonX100, and three times in PBS, and mounted with Fluorsave (Calbiochem).

2.6.6 Metabolic labelling

The incorporation of ^{35}S-methionine into proteins in infected BHK cells was performed according to the Sindbis expression system protocol (Invitrogen). Briefly, $2.5\text{-}5x10^5$ cells were plated in 6-well plates in 2 ml culture medium per well and incubated until the cells had attached and reached 60% confluence (8-18 h). The medium was removed and cells were infected with recombinant Sindbis virions in a volume of 500 µl medium (1 h with gentle rocking at room temperature or 4°C). 2.5 ml medium were added to each well, and cells were grown to 85% confluence (18-24 h post-infection). Monolayers were then washed twice with PBS and depleted of methionine (in 1 ml/well MEM Eagle medium (with Earle's salts, without L-methionine and L-glutamine), 2 mM glutamine) for 30 minutes (5% CO_2, 37°C). Cells were then pulsed for 1 hour in a 37°C rocking incubator by the addition of 10 µCi ^{35}S-methionine (~1 pmol; Amersham Pharmacia) per well. A 30 minute chase was performed after the addition of 2 ml MEM alpha medium per well at 37°C with rocking. The cells were then washed three times with 2 ml PBS and collected in 2 ml PBS by scraping with subsequent centrifugation (15000 x *g*, 1 min). Cell pellets were denatured in 2x SDS-PAGE sample buffer, subjected to SDS-PAGE, blotted onto PVDF membranes, and analysed by autoradiography prior to Western blotting. Exposure times were in the range of 1-24 hours.

2.6.7 Organotypic hippocampal slice cultures

Rat organotypic hippocampal slices were cultured on porous membranes as previously described (Stoppini *et al.*, 1991). A male Sprague Dawley rat was decapitated at postnatal day P7-9. The head was cooled on ice for 5 minutes, sprayed with 70% ethanol, and the brain prepared and transferred into cold dissecting solution (35 mM D(+)-glucose in GBSS, filter sterilised). The hippocampus was prepared on ice, aligned on the chopping block, and excess dissecting solution was removed. The hippocampus was cut into slices of 250-400 µm with razor blades (previously stored in acetone, washed in 70% ethanol, and sterilised by flaming; Boots), using a McIlwain tissue chopper (Mickle Laboratory Engineering). Slices were rinsed into a 50 ml tube with dissecting solution, separated by gentle shaking, transferred into a Petri dish with fresh dissecting solution, and allowed to rest for 30 minutes at 4°C.

Cell culture plates (6-well plates) were prepared with 1 ml culture medium (35 mM D(+)-glucose in 49% MEM, 24.5% EBSS, 24.5% heat inactivated horse serum, 2% supplement B27, filter sterilised). TC inserts (0.4 µm, Millicell CM filter; Millipore) were placed in each well, overlaid with 0.5 ml culture medium, and equilibrated in the incubator. 1-3 selected slices were placed on each insert and excess medium was removed. Organotypic slices were cultured at 36°C with 5% CO_2. The culture medium was changed at day *in vitro* DIV1 and then twice a week, supplementing the medium with 10 µM cytosine ß-arabinofuranoside after DIV4. Organotypic slices were used for experiments between DIV7 and DIV15.

2.6.8 Morphology of organotypic slice cultures

Nissl staining was performed to stain cell nuclei. Cultured hippocampal slices were rinsed in PBS and fixed for 1 hour in 4% PFA in PBS. After washes with PBS (2x 5 min), slices were stained in 0.1% cresyl violet in 1% HAc for 10 minutes and destained in 95% ethanol. Stained slices were washed twice for 5 minutes in PBS, cut out on the supporting TC membrane, and mounted in Fluorsave (Calbiochem) on glass slides.

Alternatively, OsO_4 staining was used to label lipids such as cell membranes. Fixed slices were stained with 0.1% OsO_4 in PBS for 1 hour with rocking, washed twice in PBS for 5 minutes, and incubated for 10 minutes in 10 mM DTT in PBS. Stained slices were then washed twice for 5 minutes in PBS, cut out on the TC membrane and mounted in PBS.

2.6.9 Preparation of antibody-coupled Protein G-Sepharose beads

Monoclonal antibodies were coupled to Protein G-Sepharose beads for immunoprecipitation of antigen (Lane and Harlow, 1988). 250 µl of a Protein G-Sepharose bead suspension (~150 µl packed beads; Amersham Pharmacia) were washed three times in 1 ml binding buffer (50 mM Tris pH7.5, 150 mM NaCl, 1 mM EDTA, 1 mM EGTA), collected (15000 x *g*, 1 min), and resuspended in 875 µl binding buffer. 125 µl monoclonal mouse anti-GFP IgG1 (0.4 µg/µl; No.1814460, clones 7.1 and 13.1; Roche) were added and the mix was rotated o/n at 4°C. The beads were then washed (3x 1 ml) and resuspended in 1.5 ml 0.2 M sodium borate pH9. Dimethylpimelimidate was added to a final concentration of 20 mM. The crosslinking reaction was performed at room temperature with rotation for 30 minutes. Beads were then washed twice in 1 ml 0.2 M ethanolamine pH8, rotated for 1 hour in 1.5 ml 0.2 M ethanolamine pH8, washed twice in 1 ml sterile filtered PBS, and resuspended in a total volume of 250 µl PBS containing 0.01% thimerosal. Aliquots were taken throughout the procedure and the crosslinking efficiency was confirmed by SDS-PAGE. Antibody-coupled beads were stored at 4°C and, prior to use, washed once in 1 ml binding buffer.

2.6.10 Immunoprecipitation

Infection of organotypic hippocampal slice cultures (P8/DIV7, 300 µm thickness) was performed by application of virions onto the slice (bulk infection). At 24 hours post-infection slices were excised on the supporting TC membrane, rinsed in PBS, and frozen at –20°C. Three slices were pooled and homogenised in 600 µl binding buffer (50 mM Tris pH7.5, 150 mM NaCl, 1 mM EDTA, 1 mM EGTA) containing 1% TritonX100 and 1x protease inhibitor mix (Complete inhibitor cocktail

tablets; Boehringer Mannheim) by ultrasonication (maximum intensity on ice, 10 s). The homogenate was cleared by centrifugation (15000 x *g*, 15 min, 4°C), mixed with 25 µl antibody-coupled Protein G-Sepharose bead suspension (equivalent to 5 µg monoclonal anti-GFP IgG1), and rotated at 4°C o/n. Beads were collected by centrifugation (100 x *g*, 1 min) and washed three times in 1 ml binding buffer with TritonX100 and protease inhibitors. Bound proteins were eluted with 100 µl 100 mM glycine pH2.5 with vortexing and centrifugation (15000 x *g*, 1 min). The eluate was neutralised with an equal volume of 2x SDS-PAGE sample buffer, denatured (96°C, 3 min), and subjected to SDS-PAGE, followed by silver staining or Western blotting.

2.6.11 Confocal microscopy

The cellular localisation of recombinant fluorescent fusion proteins in organotypic hippocampal slice cultures was examined by confocal microscopy. Slice cultures (P9/DIV7-10, 300 µm thickness) were infected in bulk with 2-10 µl virion harvest and fixed at 12-48 hours post-infection. To retain the cellular morphology, slices were fixed at 36°C in PB containing 4% PFA, 0.5% glutaraldehyde for 15 minutes, washed twice in PBS (5 min, room temperature), and mounted in Fluorsave (Calbiochem).

A Leica system was used for confocal microscopy (TCSSP multi band confocal imaging spectrophotometer) on a Leica DMRE microscope with the oil-immersion objectives 25x (0.75NA numerical aperture; PL Fluotar), 40x (1.25NA; HCX PLAPO), and 63x (1.32-0.6NA; HCX PLAPO). The 488 nm and 568 nm Ar/Kr (Argon/Krypton) laser lines were used for the excitation of eGFP and RFP, respectively. The 633 nm HeNe (Helium/Neon) laser line was used for the excitation of the cyanine fluorophore Cy5. Fluorescence was acquired at 500-550 nm (for eGFP), 580-620 nm (for RFP), and 650-750 (for Cy5) with Leica TCSNT software. The pinhole was set to 1 Airy disc unit. Analysis of confocal images was performed using the public domain ImageJ software (available from http://rsb.info.nih.gov/ij; NIH). Stacks of images were compressed by a z-projection.

CHAPTER 3
Results

3.1 Overview

Initially, a cDNA array experiment was performed on an $NR1^{R/+}$ and a wildtype whole brain $polyA^{+}$-RNA sample to identify genes that are regulated downstream to the NMDA receptor activation. This led to the finding that α-synuclein mRNA was differentially expressed in the two samples. However, α-synuclein expression was not regulated by the NMDA receptor function, but was dependent on the genomic background of the inbred mouse strain BL6JHUK, used for backcrossing of the $NR1^{Rneo/+}$ colony (chapter 3.2).

Expression of α-synuclein was not detected in BL6JHUK samples by Northern and Western blotting (chapter 3.3.1). The mechanism for the absence of α-synuclein was a deletion of the α-synuclein gene locus (*Snca*) in the BL6JHUK strain (chapter 3.3.2). The chromosomal deletion was characterised by genomic PCR analysis combined with database searches (chapter 3.3.3-5). To explain the lack of a noticeable phenotype in the α-synuclein-deficient animals, downstream effects of the deletion were analysed by Northern and Western blotting. However, no compensatory upregulation was observed for the related proteins β- and γ-synuclein. Also, the expression of synphilin-1, an interacting partner of α-synuclein was not altered (chapter 3.3.6-8).

The initial aim of the project was further addressed by mRNA profiling in the adult $NR1^{Rneo/+}$ model (chapter 3.3.9). Furthermore, the influence of the mutation in the NMDA receptor and the deletion of the *Snca* locus on the life expectancy of affected animals was analysed (chapter 3.3.10).

A Sindbis viral (SV) system for the expression of fluorescent α-synuclein fusion proteins in organotypic cultures was established. Recombinant virions were produced and tested on plaque assays (chapter 3.4.1-3). The expression of the fusion proteins in BHK cells was analysed by Western blotting (chapter 3.4.4). Hippocampal slices retained their organotypic organisation during culturing (chapter 3.4.5) and were

used for the expression of α-synuclein-eGFP fusion protein. The expression of the recombinant proteins was analysed by immunoprecipitation and Western blotting (chapter 3.4.6). Finally, initial experiments were performed to address the subcellular localisation of α-synuclein-eGFP (SG) fusion proteins in hippocampal neurons (chapter 3.4.7).

3.2 Screening for downstream effects of the NMDA receptor activation

3.2.1 Identification of α-synuclein by mRNA profiling in the $NR1^{R/+}$ mouse model

It was the aim of the project to identify genes whose expression is controlled by the Ca^{2+} influx through NMDA receptors (Fig.4). A knock-in mouse model with the point mutation N598R in the NR1 subunit of the NMDA receptor served as experimental model (Fig.5). $PolyA^{+}$-RNA samples were isolated from mutant $NR1^{R/+}$ mice and wildtype littermates and were compared by mRNA profiling using cDNA array technology.

The animals needed for the experiment were generated through matings of $NR1^{Rneo/+}$ x $Cre^{+/+}$ (Fig.5) and genotyped for the mutant NR1 allele (data not shown). Since $NR1^{R/+}$ animals die postnatally the experiment was performed using animals that were obtained by caesarean section at embryonic day E18.5. To reach the highest possible degree of comparability between the two samples, total RNA from individual wildtype and $NR1^{R/+}$ animals from the same litter was isolated in parallel. Total RNA samples were used to generate $polyA^{+}$-RNA. Northern blot analysis was performed on a fraction of these samples, to control for RNA degradation. Hybridisation with a mouse actin probe revealed no sign of degradation of the two samples. The intensity of the signal was almost identical, indicating that the two RNA samples were highly comparable (Fig.6C).

The cDNA array experiment was performed by Genome Systems Inc. on mouse microarray GEM1, using the $NR1^{R/+}$ and the wildtype $polyA^{+}$-RNA samples. A reverse transcriptase reaction generated complementary single-stranded cDNA probes that were labelled with two different fluorophores. The $NR1^{R/+}$ sample was labelled

with Cy3, the wildtype sample with Cy5. The two samples were then simultaneously hybridised to the immobilised cDNA fragments on the cDNA array chip. The fluorescence intensity of each cDNA fragment on the array corresponds to the expression level of that gene. The comparison of the intensities in the two fluorescent channels is a measurement for the differential expression of a gene.

The data obtained from the cDNA array experiment were analysed by plotting the value corresponding to the intensity of fluorescence of Cy3 against the value for Cy5 for all cDNA fragments that were immobilised on the chip. From almost 9000 cDNA fragments only mouse α-synuclein was differentially expressed with 3495 units of fluorescence in the wildtype sample and 457 in the mutant $NR1^{R/+}$ sample, implying a differential expression factor of 7.6 fold (Fig.6A). The significance of this result was validated by comparing the scan images of the respective chip area obtained in the two fluorescent wavelengths (Fig.6B). It appeared that the chip surface was not damaged or dirty, thus an artefact could be excluded. The expression of all other genes on the cDNA array was not significantly altered, with expression levels lying within the range of twofold. However, the data points corresponding to lower expressed genes deviated slightly from the diagonal line, which may be caused by the use of two cyanine dyes with different fluorescence spectra. These values are so minimal though that it is unlikely that these genes are expressed at all. Rather, the values reflect the background fluorescence, since the data were analysed without background subtraction.

To verify the obtained result α-synuclein expression was analysed by Northern blotting on the same samples that had been used in the cDNA array experiment. A radiolabelled probe directed at the 3'-untranslated region (3'UTR) of α-synuclein (chapter 2.4.8) was hybridised to the membrane that had been previously probed for actin. A 1.5 kb transcript signal was only detected in the wildtype and not in the $NR1^{R/+}$ $polyA^{+}$-RNA sample (Fig.6C). This result could be further validated at a later time using probes directed at the 5'UTR and the coding sequence (CDS) of α-synuclein (data not shown). These data are in agreement with the 7.6 fold differential expression of α-synuclein as suggested by the cDNA array experiment. However, the results that were obtained by Northern blotting could not be quantified. This is due to the fact that the intensity of the signal depends on the probe and the saturation of the signal, and that the linear dynamic range of the Northern blotting technique is in the range of only one order of magnitude.

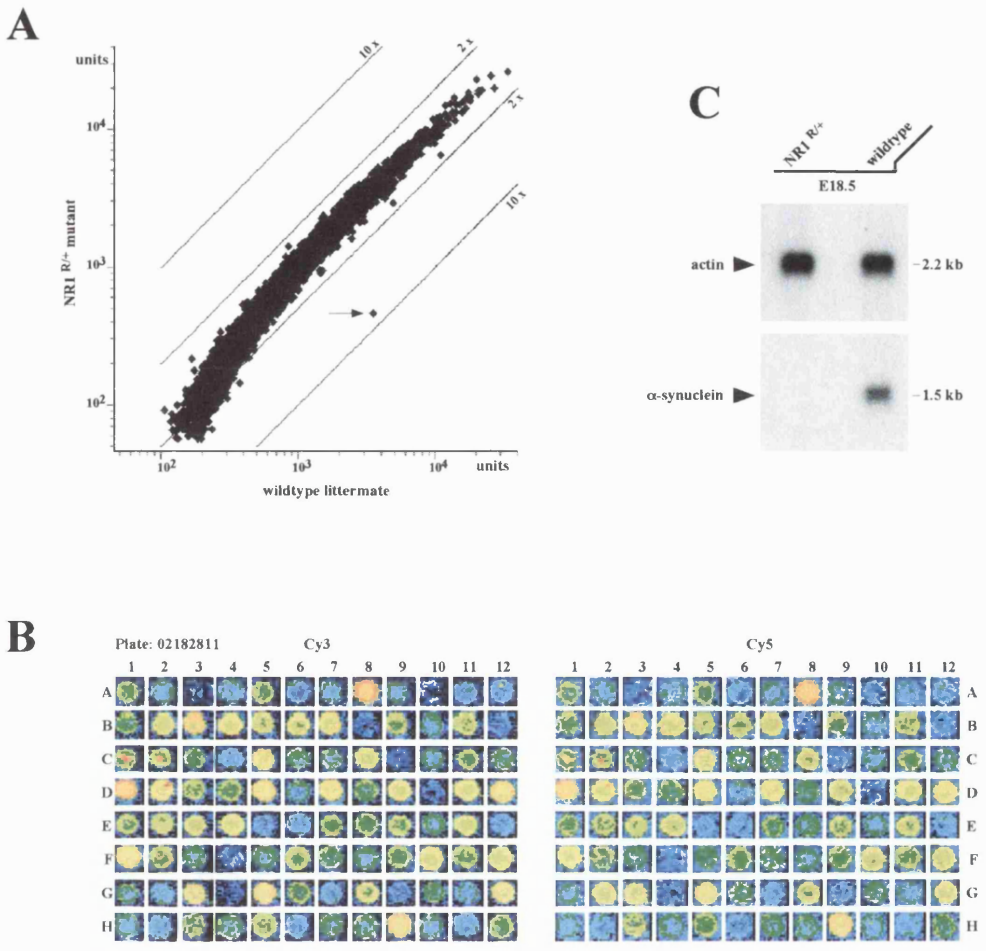

Figure 6. Identification of α-synuclein in the NR1$^{R/+}$ mouse model using cDNA array technology

A. cDNA array experiment using brain polyA$^+$-RNA from an NR1$^{R/+}$ mouse and a wildtype littermate at E18.5. From all analysed genes (~9000 ESTs) only the expression of α-synuclein (GenBank W41663, NCBI) was significantly altered (indicated by an arrow; differential expression factor 7.6x). The data are represented without background subtraction. Expression is quantified as units of fluorescence intensity. Diagonals indicate differential expression by 2x and 10x, respectively.

B. Example of one plate from the cDNA array experiment, showing the fluorescence in the Cy3 (left, NR1$^{R/+}$ sample) and Cy5 channels (right, wildtype). False colours represent the intensity of fluorescence, with bright colouring used for strong signals. α-synuclein is located in position G2.

C. Northern blot of brain polyA$^+$-RNA (160 ng per lane), using the same mutant NR1$^{R/+}$ and wildtype samples as in the cDNA array experiment. Probing for α-synuclein 3'UTR confirmed the result obtained in the cDNA array experiment. The expression of α-synuclein (1.5 kb transcript size) is not detected in the NR1$^{R/+}$ sample. Previously, the membrane had been probed with an actin probe (2.2 kb transcript) to control for the quality of the isolated polyA$^+$-RNA.

3.2.2 Inconsistent expression of α-synuclein mRNA in $NR1^{R/+}$ mutant mice

Northern blot analysis was used to test the reproducibility of the previous finding on a different set of samples. When α-synuclein mRNA expression was compared between a mutant $NR1^{R/+}$ sample from a newborn animal (P0) with a wildtype littermate it appeared, however, that the transcript was present in comparable amounts in both samples (Fig.7A). The membrane was also probed for actin. This showed that the concentration of RNA was comparable in both samples. Furthermore, the membrane was probed for the NR1 subunit of the NMDA receptor using a probe that contained exons 15-17 of the cDNA sequence. It appeared that the expression levels of this gene were similar in the wildtype and the $NR1^{R/+}$ animal. This result was confirmed with a probe directed against NR1 exons 19-22 (data not shown).

From the result obtained with P0 samples it was hypothesised that the expression of α-synuclein may be delayed in the mutant $NR1^{R/+}$ animals and would only be different within a specific time window before birth. To test this assumption, a number of Northern blot experiments were performed to characterise the temporal expression pattern of mouse α-synuclein mRNA in mutant $NR1^{R/+}$ and wildtype animals. Samples from $NR1^{R/+}$ animals were compared with their wildtype littermates throughout development, from E16.5 to P8. When the expression of α-synuclein was analysed by Northern blotting, a very confusing picture emerged (Fig.7B). It appeared that no consistency in the expression pattern of α-synuclein could be obtained within the group of animals used in the experiment. The presence of the transcript did not correlate with the presence of the mutation in the NMDA receptor subunit NR1. Therefore, the observed differential expression of α-synuclein was unlikely to be linked to the mutation in the NR1 subunit. Instead, it was speculated that the inconsistent expression of α-synuclein may be caused by the genomic background of the mutant mouse model.

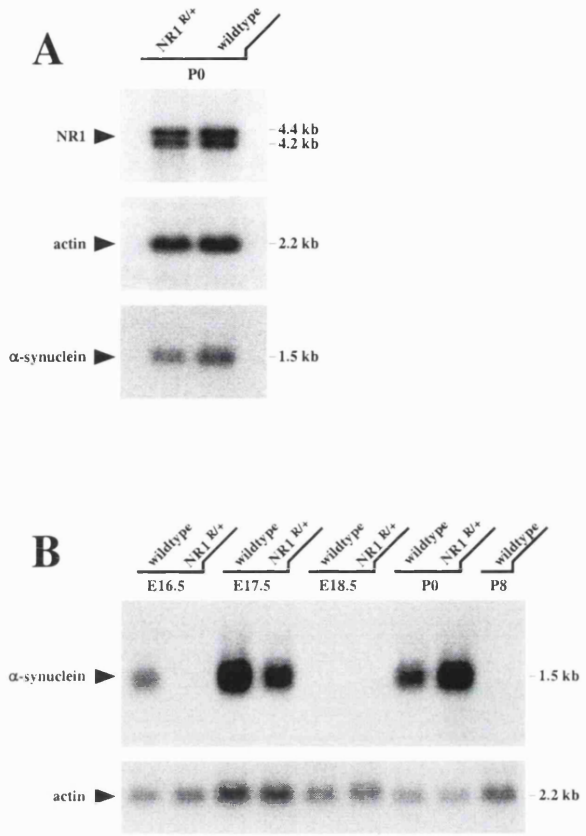

Figure 7. Inconsistent expression of α-synuclein in NR1$^{R/+}$ mutant mice

A. Northern blot using brain polyA$^+$-RNA (500 ng per lane) from an NR1$^{R/+}$ mouse and a wildtype littermate at P0. Probing for exons 15-17 of subunit NR1 shows no differences in the expression levels of the transcripts (doublet band at 4.2 and 4.4 kb). After stripping, the membrane was probed for actin (2.2 kb), showing that comparable amounts were loaded in both lanes. Probing for the CDS of α-synuclein suggested no significant difference in the expression of the 1.5 kb transcript in this set of samples.

B. Timecourse of expression of α-synuclein in brain polyA$^+$-RNA samples (400-500 ng per lane) from NR1$^{R/+}$ and wildtype animals between E16.5 and P8. Probing for the 3'UTR region of α-synuclein shows that the expression of the transcript is not correlated to the NR1 genotype. Re-probing for actin served as positive control.

3.3 The strain BL6JHUK carries a chromosomal deletion of α-synuclein

3.3.1 α-synuclein expression levels in different mouse strains

The $NR1^{Rneo/+}$ knock-in mouse model was originally generated using embryonic stem cells from the inbred strain 129/Ola (ES cell line 14-1). The resulting chimeric animals were then backcrossed into the inbred strain BL6JHUK for several generations. The mutant animals used in the previous cDNA array experiment and the Northern blot studies were obtained from matings of the $NR1^{Rneo/+}$ strain with the $Cre^{+/+}$ transgenic strain, that had also been backcrossed into the BL6JHUK strain. Since the previous investigation on the mutant model had led to contradictory results, α-synuclein mRNA expression levels were compared between the inbred strains that had been used for the generation of the knock-in mice, namely 129/Ola and BL6JHUK, as well as the outbred strain ICR for control.

Expression of α-synuclein mRNA in brains of 129/Ola, ICR, and BL6JHUK mice was compared by Northern blot analysis at time points throughout development. Consistently, the α-synuclein signal was absent in BL6JHUK samples, whereas the other strains expressed equal amounts of the transcript (Fig.8A). In 129/Ola and ICR mice α-synuclein mRNA expression increased between P0 and P15 as previously described (Hong *et al.*, 1998; Hsu *et al.*, 1998). Expression of α-synuclein mRNA was observed as early as on embryonic day E14 (on total embryo RNA) and E17 (brain RNA) in ICR but not in BL6JHUK mice (data not shown). Probing for the actin gene was used to control for the amounts of RNA that were loaded in each lane.

Subsequently, it was tested if the expression differences of the α-synuclein transcript would be reflected on the protein level. Therefore, Western blotting experiments were performed on total brain homogenates from the three mouse strains. Consistent with the result obtained by Northern blotting, no detectable expression of α-synuclein protein was observed in BL6JHUK samples (Fig.8B). This was in contrast to the 129/Ola and ICR samples where a single protein band was detected at 19 kDa. Protein levels increased during postnatal development in agreement with previous studies (Hsu *et al.*, 1998), but were consistently absent from BL6JHUK samples. At prenatal stages (using homogenates from embryo at E14 and brain at E17) α-synuclein

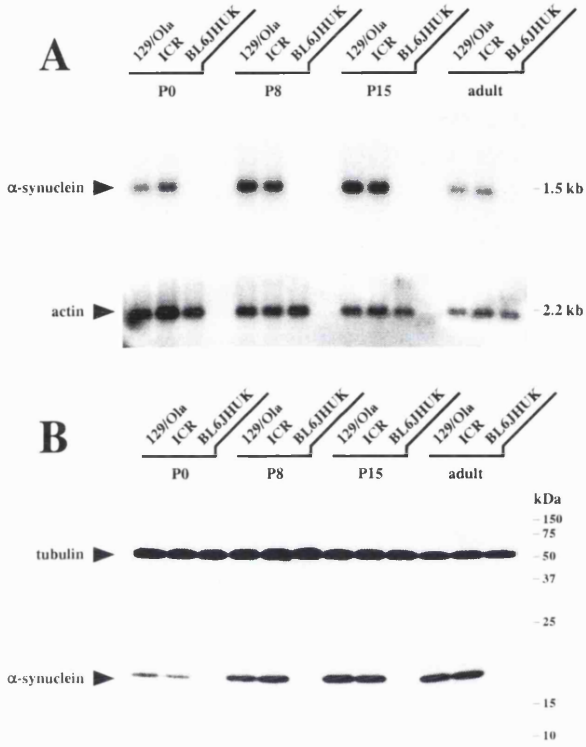

Figure 8. α-synuclein expression levels in different mouse strains

A. Northern blot of brain polyA$^+$-RNA (500 ng per lane) from 129/Ola, ICR, and BL6JHUK mice at the developmental time points P0, P8, P15, and adult, probed with an α-synuclein 3'UTR probe. The α-synuclein transcript (1.5 kb) is consistently absent from the BL6JHUK samples. RNA samples were pooled from 4 animals (at P0), or from 2 animals (at P8 and P15) from the same litter. After stripping, the membrane was re-probed for actin.

B. Brain homogenates from 129/Ola, ICR, and BL6JHUK mice at P0, P8, P15, and adult age were separated by 15% SDS-PAGE (20 µg protein per lane). The Western blot membrane was simultaneously probed with monoclonal anti-α-synuclein (S63320; Transduction Laboratories) and anti-α-tubulin antibodies, identifying protein bands of apparent molecular weights of 19 kDa and 55 kDa, respectively. α-synuclein protein was not detected in BL6JHUK samples at any developmental time point.

expression was below detection levels in ICR and BL6JHUK animals (data not shown).

These results suggested that the differential expression of α-synuclein identified in the $NR1^{R/+}$ mouse model was not caused by the mutation in the NMDA receptor, but was due to the genomic background of the animals used in this study.

3.3.2 Deletion of the α-synuclein gene locus in BL6JHUK animals

Although α-synuclein was not detected in the BL6JHUK strain by Northern and Western blotting, the detection of low expression levels could require methods of greater sensitivity. Therefore, α-synuclein mRNA expression was determined by semi-quantitative RT-PCR analysis (Fig.9A). Amplification on brain total RNA of an ICR mouse at P15 with specific α-synuclein primers resulted in a detectable cDNA fragment after as few as 20 PCR cycles. However no product was detected using BL6JHUK RNA, even with 35 cycles. When BL6JHUK RNA was spiked with low levels of ICR RNA the appearance of the α-synuclein product could be observed after 35 cycles at a dilution factor of 10^4. This indicated that expression of α-synuclein in BL6JHUK RNA is decreased by at least this factor compared to the ICR strain, on the assumption that the RNA concentration in the two samples was comparable. The amplification of a tubulin sequence was used as positive control. The obtained result was found to be consistent when repeated on sets of samples from P8 and E14 (data not shown). Since the expression of α-synuclein was decreased to such an extent, the α-synuclein locus (*Snca*) in the BL6JHUK strain must be considered a null allele. This result was unexpected for a number of reasons that are discussed at a later point (chapter 4.1.1).

To further elucidate the underlying mechanism, the presence of the *Snca* locus was analysed by PCR experiments on tail genomic DNA (Fig.9B). It was found that the α-synuclein locus was absent in BL6JHUK mice. In contrast to the ICR and 129/Ola strains, amplification of genomic DNA fragments corresponding to the exons 4 and 6 of the α-synuclein gene yielded no PCR product in the BL6JHUK sample. PCR amplification spanning intronic α-synuclein sequences (exons 1 to 2, exons 5 to 6) produced identical results (data not shown). Reproducibility was confirmed on a number of BL6JHUK mice (n = 8) from four batches of animals. A genomic PCR

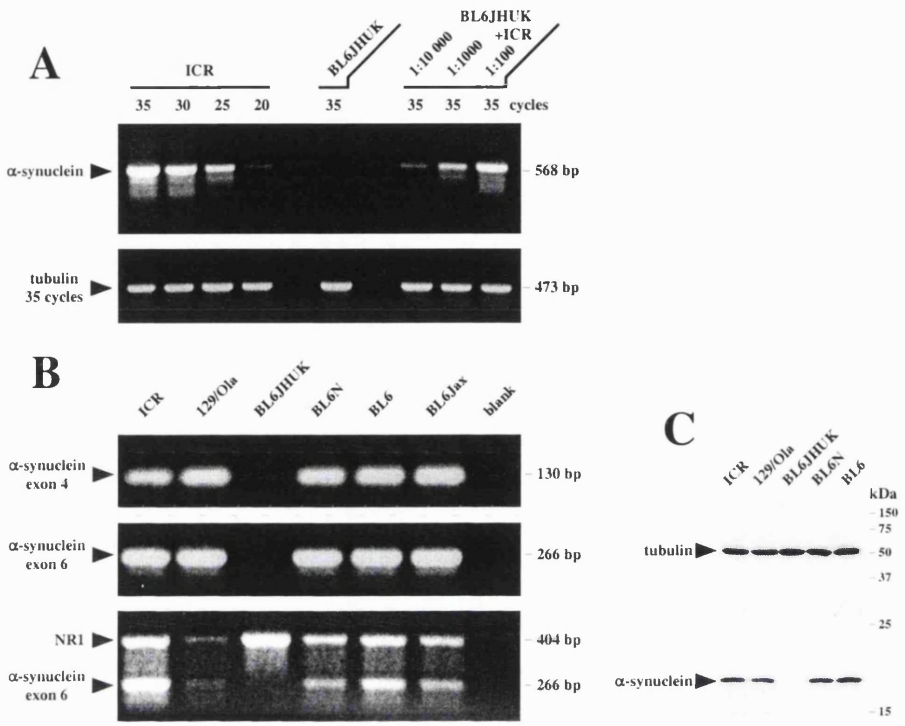

Figure 9. Deletion of the *Snca* locus in BL6JHUK animals

A. Semi-quantitative RT-PCR analysis of α-synuclein expression in BL6JHUK mice, sized on a 1.5% agarose gel. A 568 bp α-synuclein band was detected after as few as 20 PCR cycles on brain total RNA of an ICR mouse at P15, but not in the P15 BL6JHUK sample after 35 cycles. When the BL6JHUK sample was spiked with as little as 0.01% ICR RNA the α-synuclein band was detected after 35 cycles. The control shows the amplification of a 473 bp tubulin fragment with constant 35 PCR cycles.

B. Probing for the presence of the *Snca* locus in the ICR, 129/Ola, BL6JHUK, BL6N, BL6, and BL6Jax strains. Genomic α-synuclein DNA fragments of exon 4 (130 bp fragment) and of exon 6 (266 bp) were amplified by PCR and separated on a 2% agarose gel. Amplification of α-synuclein sequences was absent in the BL6JHUK sample. A genotyping PCR protocol for the *Snca* locus amplified exon 6 of α-synuclein and a fragment of the NR1 gene as internal control. Fragment sizes are 266 bp and 404 bp, respectively.

C. Western blot analysis of α-synuclein expression in brain homogenates (20 μg protein per lane) from adult ICR, 129/Ola, BL6JHUK, BL6N, and BL6 animals, separated by 15% SDS-PAGE. Blots were simultaneously probed with monoclonal anti-α-synuclein (S63320; Transduction Laboratories) and anti-α-tubulin antibodies, recognising proteins of 19 kDa and 55 kDa, respectively. Expression of α-synuclein was absent in the BL6JHUK sample.

protocol was established for genotyping, in which the amplification of the exon 6 α-synuclein sequence was combined with the amplification of NR1 as an internal control (Fig.9B).

Further PCR analysis revealed that mouse strains related to BL6JHUK, namely BL6N and BL6, did not carry the deletion (Fig.9B). Western blotting confirmed that α-synuclein protein was expressed in adult BL6N and BL6 animals (Fig.9C). To establish whether the entire C57BL/6J strain was affected by the deletion, C57BL/6J DNA samples from two different sources were compared. It appeared that BL6Jax DNA (C57BL/6J provided by Jackson Laboratory) was not affected by the deletion (Fig.9B), in contrast to BL6JHUK DNA (C57BL/6J from Harlan UK). Therefore, only a subpopulation of C57BL/6J mice carries the deletion of the *Snca* locus.

In retrospect, α-synuclein genotyping was performed on the DNA samples from the animals that had been used in the cDNA array experiment. This revealed that the mutant $NR1^{R/+}$ mouse had indeed carried the *Snca* deletion, whereas the wildtype mouse was not affected by the deletion (data not shown).

3.3.3 Initial characterisation of the chromosomal *Snca* deletion

The screening of a C57BL/6J yeast artificial chromosome (YAC) library (Whitehead Institute/MIT Center for Genome Research; Haldi *et al.*, 1996) with α-synuclein probes led to the identification of YAC clone #326H11 (M.Peters, personal communication). This YAC clone is positive for the chromosome 6 genomic marker *D6Mit357* (Fig.11C). Sequence alignment with the mouse α-synuclein chromosomal sequence (GenBank AF163865, NCBI; Touchman *et al.*, 2001) locates the genomic marker *D6Mit357* to the sequence between exons 4 and 5. Exon 1 and exon 6 of the *Snca* gene are 97 kb apart (Fig.11A).

This information was used to characterise the size of the *Snca* deletion in BL6JHUK animals (Fig.10A). Using genomic PCR analysis C57BL/6J DNA samples from two different sources were compared, BL6Jax DNA (provided by the Jackson Laboratory) and BL6JHUK DNA (animals provided by Harlan UK). The BL6JHUK sample was negative for *D6Mit357* and other genomic markers within 120 kb sequence of the *Snca* locus (PCR a-d, primers designed on *Snca* sequence GenBank

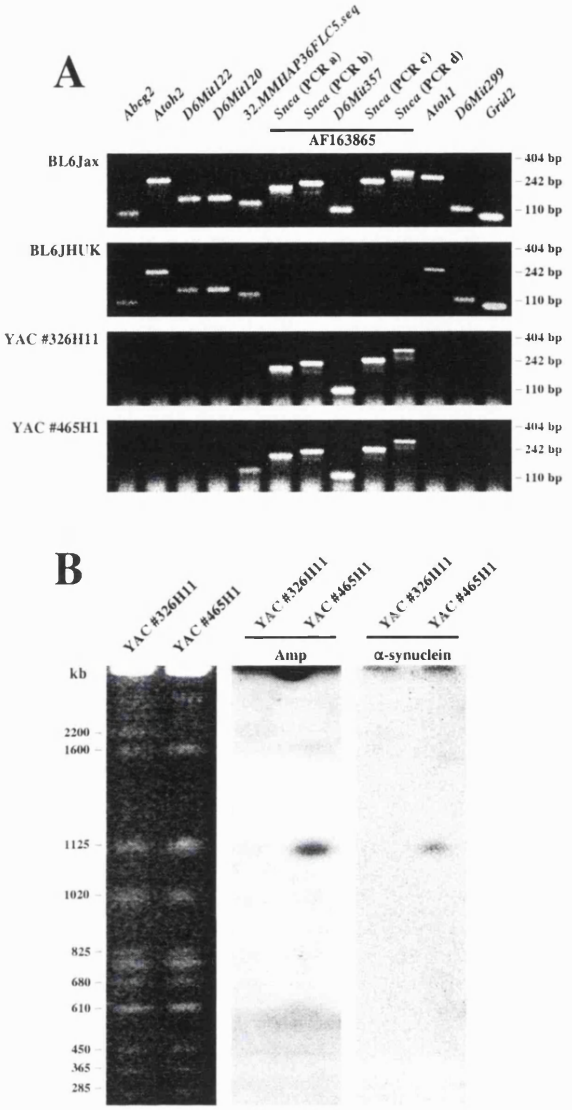

Figure 10. Characterisation of the *Snca* chromosomal deletion in the BL6JHUK strain

A. Genomic PCR on BL6JHUK and BL6Jax mouse tail DNA and genomic DNA from YAC clones #326H11 and #465H1, separated on a 2% agarose gel. The *D6Mit357* marker and a number of PCR primer pairs designed on the *Snca* sequence AF163865 (PCR a-d) were negative on BL6JHUK DNA, whereas all other markers amplified on both mouse DNA samples, namely *Abcg2*, *Atoh2*, *D6Mit122*, *D6Mit120*, *32.MMHAP36FLC5.seq*, *Atoh1*, *D6Mit299*, and *Grid2*. The YAC clones #326H11 and #465H1 are positive for all markers located within the sequence AF163865 (Touchman *et al.*, 2001), *D6Mit357* and PCRa-d. Also, YAC #465H1 is positive for marker *32.MMHAP36FLC5.seq*.

B. Yeast genomic DNA of the YAC clones #326H11 and #465H1, separated by pulsed field gel electrophoresis and analysed by Southern blotting. YACs were sized by ethidium bromide staining (left) using *S.cerevisiae* chromosomes as DNA standards. Probing for β-lactamase (Amp probe) and the 3'UTR of α-synuclein detected the 1.1 MB artificial chromosome YAC #465H1. YAC clone #326H11 was not detected, probably due to low YAC DNA yields obtained from the yeast culture.

AF163865, NCBI; Fig.11A). However, genomic loci that are known to be in close proximity to *Snca*, including the genes *Atoh1* and *Atoh2* proved to be unaffected by the deletion. *Atoh1* and *Atoh2* are believed to be located at 1.1 cM (centiMorgan) at either side of *Snca* on mouse chromosome 6 (Touchman *et al.*, 2001). Also, the gene loci *Abcg2* and *Grid2* were not affected by the deletion (Fig.10A, Fig.11A). Furthermore, a number of polymorphic genomic markers were not affected by the deletion in the BL6JHUK strain (Fig.10A). *D6Mit122* and *D6Mit299* are mapped on mouse chromosome 6 (Fig.11B; MGSC mouse genomic sequencing consortium, Ensembl database), and *D6Mit120* and *32.MMHAP36FLC5.seq* are part of the YAC contig WC6.20 (Fig.11C; Whitehead Institute/MIT Center for Genome Research). According to these results, the deletion found in the BL6JHUK strain covers at least 120 kb including the entire *Snca* locus, and is smaller than 2.2 cM. The initial characterisation of the chromosomal deletion was completed in March 2001 and has been published (Specht and Schoepfer, 2001). Currently (December 2001) the loci *Abcg2*, *Atoh2*, *Grid2*, and *Atoh1* are mapped to close locations of *Snca* at around 29 cM on mouse chromosome 6 (*Abcg2* at 28.5 cM; *Atoh2* at 29 cM; *Snca* at 29 cM; *Grid2* at 29.65 cM; *Atoh1* at 29.69 cM; human-mouse homology map, NCBI; Fig.11A).

3.3.4 Mapping of the *Snca* deletion using YAC clones

YAC clone #326H11 is mapped to contig WC6.20, which includes a number of YAC clones (Whitehead Institute/MIT Center for Genome Research). The contig is linked by the genomic markers *D6Mit357* (*Snca* locus), *32.MMHAP36FLC5.seq*, and *D6Mit120* (Fig.11C). Consistent with the database information, it was confirmed that the YAC clones #326H11, #117H3, and #465H1 are positive for the marker *D6Mit357*, clones #465H1 and #293D6 for *32.MMHAP36FLC5.seq*, and #293D6 for marker *D6Mit120* (Fig.11C; experimental data not shown).

Yeast genomic DNA from the YAC clones #326H11 and #465H1 was separated by pulsed field gel electrophoresis and subjected to Southern blotting (Fig.10B). Probing for the β-lactamase YAC sequence (Amp probe; Spencer *et al.*, 1993) and the 3'UTR of the α-synuclein gene showed that YAC #465H1 has an overall size of approximately 1.1 MB and is positive for α-synuclein. The experiment

did not yield any information on the YAC clone #326H11. DNA from both YAC clones was subjected to genomic PCR analysis (Fig.10A). Both YAC clones were positive for the markers *D6Mit357* and PCR a-d, and thus contain the entire 120 kb sequence of the *Snca* locus (Fig.11A). While YAC #326H11 proved negative for all other genomic loci tested, YAC #465H1 was positive for the marker *32.MMHAP36FLC5.seq*, consistent with the information available for contig WC6.20 (Fig.11C). This genomic marker was not affected by the deletion in the BL6JHUK strain (Fig.10A). Thus, it was concluded that the 1.1 MB sequence of YAC clone #465H1 contains the entire genomic sequence of the *Snca* locus and includes at least one of the two breaking points of the deletion. This clone should therefore be useful to obtain further information on the *Snca* deletion.

3.3.5 Recent mapping data of the *Snca* deletion

Recent database searches (December 2001; MGSC mouse genomic sequencing consortium, Ensembl database) revealed a more detailed organisation of the chromosomal region around position 68 MB on mouse chromosome 6 (Fig.11B). Chromosomal sequences are assembled into contigs #2757 and #291, which cover the area from 55 MB to 85 MB on mouse chromosome 6. Since the *Snca* locus has not yet been aligned to these chromosomal sequences, it is likely that the *Snca* deletion is contained in the segment between the two contigs, estimated to be 0.5 MB in size. Further mapping experiments were performed with a range of genomic markers that are mapped to contigs #2757 and #291. These included *D6Jcs25*, *D6Mit241*, *D6Mit123*, *D6Mit126*, *D6Mit245*, *D6Mit186*, *D6Mit243*, *D6Mit124*, *D6Mit244*, *D6Mit96*, *D6Mit95*, *D6Mit162*, *D6Mit125*, *D6Mit175*, and *D6Mit121* (Fig.11B). All these loci were not affected by the deletion in BL6JHUK animals (experimental data not shown). Thus, together with the previous information the data suggest that the size of the deletion is likely to be smaller than 0.5 MB, between the genomic markers *D6Mit122* (at 67.91 MB) and *D6Mit126* (at 68.42 MB).

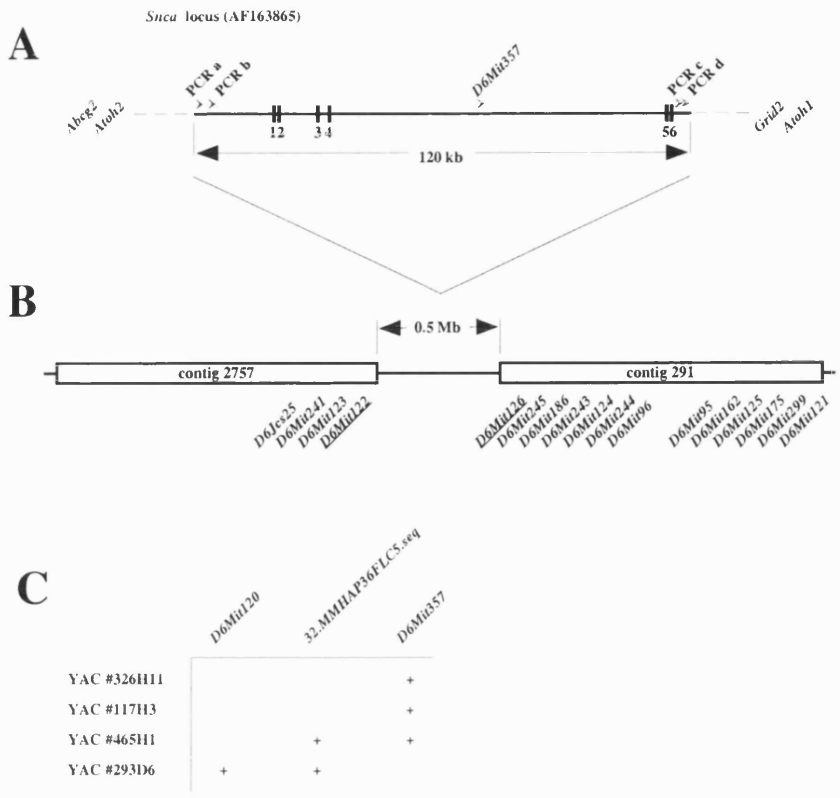

Figure 11. Mapping of the *Snca* locus in the BL6JHUK strain

A. Scheme of the exonic organisation (exons numbered 1-6) of the *Snca* locus sequence AF163865 (Touchman *et al.*, 2001) and the location of the genomic markers *D6Mit357* and PCR a-d (indicated by arrows). *Atoh2* and *Atoh1* are mapped to 1.1 cM at either side of *Snca* (Touchman *et al.*, 2001). Currently (December 2001; human-mouse homology map, NCBI), *Snca* is mapped to 29 cM on mouse chromosome 6 in close proximity to *Abcg2* (at 28.5 cM), *Atoh2* (29 cM), *Grid2* (29.65 cM), and *Atoh1* (29.69 cM). The orientation of the *Snca* sequence on the chromosome is arbitrary.

B. Schematic representation of contigs #2757 and #291 on mouse chromosome 6 (December 2001; MGSC Ensembl database) with the genomic markers *D6Jcs25*, *D6Mit241*, *D6Mit123*, *D6Mit122*, *D6Mit126*, *D6Mit245*, *D6Mit186*, *D6Mit243*, *D6Mit124*, *D6Mit244*, *D6Mit96*, *D6Mit95*, *D6Mit162*, *D6Mit125*, *D6Mit175*, *D6Mit299*, and *D6Mit121*. All these genomic markers were used for PCR analysis and were not affected by the deletion in the BL6JHUK strain. The deletion is likely to be smaller than 0.5 MB between *D6Mit122* at 67.91 MB and *D6Mit126* at 68.42 MB (underlined).

C. Scheme of contig WC6.20 (Whitehead Institute/MIT Center for Genome Research), containing the YAC clones #326H11, #117H3, #465H1, and #293D6. The contig is linked by the genomic markers *D6Mit357*, *32.MMHAP36FLC5.seq*, and *D6Mit120* (positive YACs are indicated by +). These markers have not yet been mapped within the mouse chromosome 6 sequence (December 2001; MGSC Ensembl database). The data shown here were confirmed by genomic PCR on YAC DNA (experimental data not shown).

3.3.6 Expression of β-synuclein is unaffected by the α-synuclein deletion

α-synuclein null mice do not display any obvious phenotypes (Abeliovich *et al.*, 2000; Chen *et al.*, a in preparation). This could be caused by a compensatory upregulation of functionally related genes. β-synuclein or γ-synuclein represent potential candidates due to their high degree of sequence identity and structural similarity (Fig.1).

However, Western blot analysis with a specific antibody against β-synuclein revealed that expression levels of the 19 kDa protein remained unaffected in the absence of α-synuclein at any stage of postnatal development (Fig.12A). Protein expression was uniform in the 129/Ola, ICR, and the BL6JHUK strain and increased noticeably during postnatal development. The antibody PER4 (provided by M.Goedert) recognises both α- and β-synuclein (Spillantini *et al.*, 1998b), which run at virtually identical molecular weights on SDS-PAGE. Probing with this antibody (Fig.12A) yielded the combined results obtained from the selective Western blotting for α-synuclein (Fig.8B) and β-synuclein (Fig.12A).

3.3.7 Expression of γ-synuclein is unaffected by the α-synuclein deletion

Northern blotting indicated that the expression of γ-synuclein was not significantly altered by the absence of α-synuclein in BL6JHUK mice during postnatal development compared to the strains 129/Ola and ICR (Fig.12B). The specificity of the γ-synuclein probe was confirmed using two different cDNA probes (data not shown). It could be argued that the signals on the Northern blot membrane do not appear to be of equal strength, being slightly weaker in the BL6JHUK sample at the time points P8 and P15 in relation to the actin control probing. However, this was not observed on a second Northern blot membrane at P15 (data not shown). Thus, it probably represented an experimental artefact, caused by the extensive probing that had been previously performed on the membrane. However, compensatory upregulation of the γ-synuclein gene could certainly be ruled out. Also, this had been already indicated by the cDNA array experiment (Fig.6A), in which a γ-synuclein EST

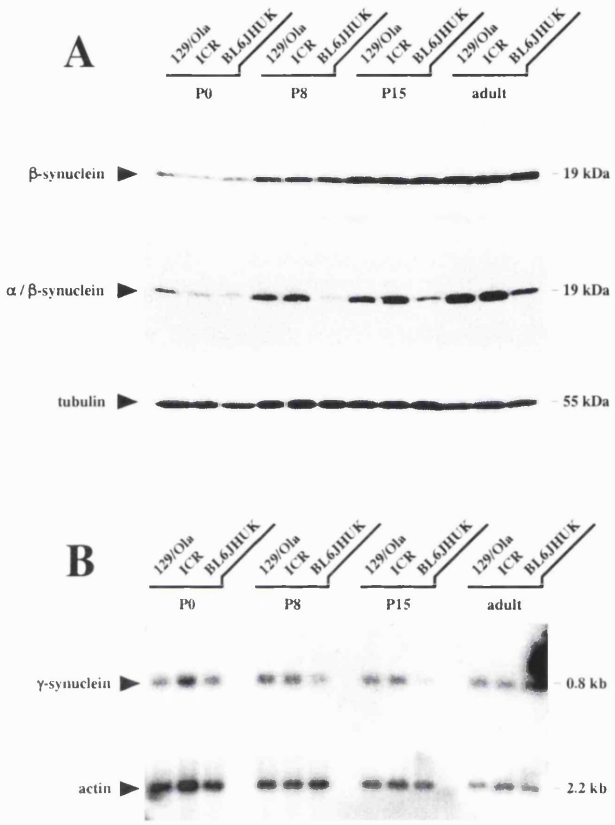

Figure 12. Developmental expression of β- and γ-synuclein in different mouse strains

A. 15% SDS-PAGE on brain homogenates from the 129/Ola, ICR, and BL6JHUK strains at P0, P8, P15, and adult (20 μg protein per lane). The Western blot membrane was sequentially probed with polyclonal anti-β-synuclein IgG (SA3405; Affiniti), detecting the 19 kDa protein, and monoclonal anti-α-tubulin antibody for control. PER4 antibody detected both α- and β-synuclein. This was performed on a different membrane using the same protein samples.

B. Northern blot of brain polyA$^+$-RNA (500 ng per lane) from 129/Ola, ICR, and BL6JHUK mice at different developmental stages (P0, P8, P15, and adult). Probing with a 3'UTR γ-synuclein probe detected a transcript of ~0.8 kb that is similarly expressed in the three strains. RNA samples were pooled from 4 animals (at P0) or from 2 animals (at P8 and P15) from the same litter. The same membrane as in Fig.8A was used for this experiment; the actin control is identical to Fig.8A.

clone had been present (GenBank AA272342, NCBI). The γ-synuclein signal intensities in this experiment were almost identical with 2325 (wildtype) and 2492 arbitrary expression units ($NR1^{R/+}$ mutant animal with *Snca* deletion).

3.3.8 Synphilin-1 expression is unaffected by the α-synuclein deletion

Human α-synuclein has been shown to specifically interact with human synphilin-1 protein (Engelender *et al.*, 1999). Therefore, the influence of the α-synuclein deletion on the expression levels of synphilin-1 in mice was tested. Synphilin-1 mRNA expression was found to be unaffected by the absence of α-synuclein in BL6JHUK animals (Fig.13A). Equal levels of the synphilin-1 transcript were detected in the 129/Ola, ICR, and BL6JHUK strains by Northern blotting. This result was confirmed using different cDNA probes to synphilin-1 (data not shown).

Likewise, protein expression levels were unaltered between the strains as judged by Western blot analysis (Fig.13B). The antibody used in this experiment (ab6179; Abcam) was raised against the epitope ASKGKNKAA of the human synphilin-1 protein (amino acids 911-919) that is identical in the corresponding mouse sequence. The antibody detected a protein of approximately 85 kDa, together with a number of other protein bands. Since the 85 kDa band was of the expected size and expressed throughout postnatal development, it was taken as the mouse homologue of synphilin-1. The expression of synphilin-1 showed a slight increase during postnatal development (Fig.13B). A different antibody (ab6178; Abcam) was used unsuccessfully on mouse tissue (data not shown). It was raised against the human epitope SLELNGEKDKDKGR**TL**QRT, which has three mismatches when aligned to the respective mouse sequence **G**LELNGEKDKDKGR**AP**QRT. The alignment was done using the mouse synphilin-1 sequence GenBank AF348447 (NCBI) that was corrected by sequencing information obtained from RT-PCR fragments (data not shown) and the human synphilin-1 sequence GenBank AF076929 (NCBI).

Taken together, the results consistently showed that the expression of synphilin-1 was not affected by the deletion of α-synuclein.

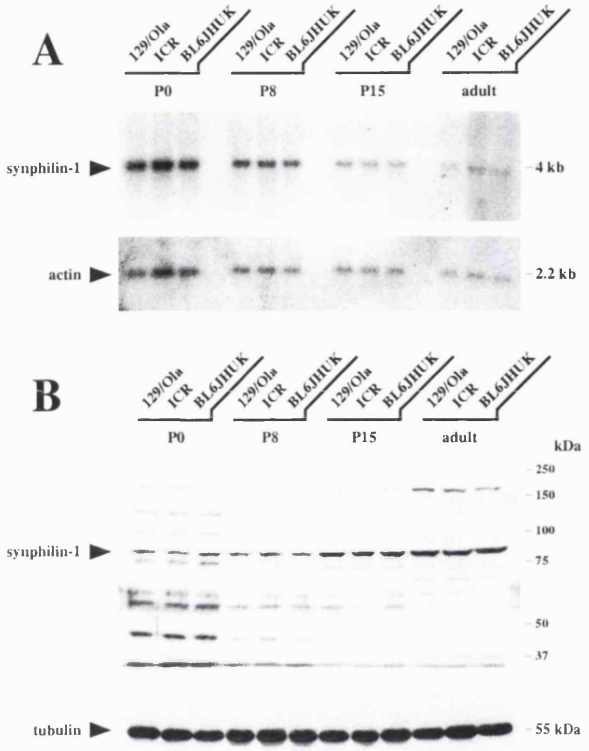

Figure 13. Developmental expression of synphilin-1 in different mouse strains

A. Northern blot of brain polyA$^+$-RNA (500 ng per lane) from 129/Ola, ICR, and BL6JHUK mice at P0, P8, P15, and adult age. The 1.5 kb synphilin-1 probe detected a transcript of ~4 kb, expressed equally in the three mouse strains throughout postnatal development. RNA samples were pooled from 4 animals (at P0) or from 2 animals (at P8 and P15) from the same litter. After stripping, the membrane was re-probed for actin.

B. Brain homogenates from 129/Ola, ICR, and BL6JHUK mice at P0, P8, P15, and adult age were separated by 7.5% SDS-PAGE (30 µg protein per lane). The Western blot membrane was sequentially probed with polyclonal anti-synphilin-1 (ab6179; Abcam) and monoclonal anti-α-tubulin antibodies. The recognised proteins have apparent molecular weights of approximately 85 kDa and 55 kDa, respectively. The synphilin-1 antibody detected a number of non-specific protein bands.

3.3.9 Adult $NR1^{Rneo/+}$ mouse model

While other experiments were in progress, a number of electrophysiological and behavioural phenotypes had been identified in adult $NR1^{Rneo/+}$ animals in comparison to wildtype animals (Chen, b in preparation). These could be caused by the hypomorphic expression of mutant NR1 N598R subunits in the mutant animals, similar to an earlier study (e.g. Mohn *et al.*, 1999). The expression of the N598R subunits is reduced by the insertion of the neo selection cassette to ~5% compared to the wildtype allele (Chen, b in preparation). Therefore, a second cDNA array experiment was performed to address the original aim of the project, the identification of genes that are regulated downstream to the NMDA receptor. To this end, mRNA expression profiles in adult $NR1^{Rneo/+}$ animals and wildtype littermates were compared. Since the observed electrophysiological phenotype was present in the dentate gyrus (DG) area of the hippocampus, the cDNA array experiment was performed on $polyA^+$-RNA isolated exclusively from the hippocampus. To obtain the necessary yields and to control for preparation artefacts, three hippocampal preparations of each genotype were pooled for RNA isolation. Northern blotting on 150 ng $polyA^+$-RNA from each of the two pooled samples with an actin probe confirmed the integrity of the material (data not shown).

However, the cDNA array experiment suggested, that none of the genes that were present on the cDNA array chip was differentially expressed (Fig.14A). Only the expression levels of few genes showed a slight deviation from the diagonal line of equal expression, lying within the range of twofold. In retrospect, genotyping for the *Snca* deletion was performed on the animals used in this experiment. This showed that in the wildtype group only one out of three animals expressed α-synuclein, in contrast to three out of three animals expressing α-synuclein in the mutant $NR1^{Rneo/+}$ group (data not shown). This finding (expression ratio 1:3) is reflected by the ratio of the fluorescence intensities of α-synuclein on the cDNA array (expression ratio 1.8x; 5595 units of fluorescence in the $NR1^{Rneo/+}$ sample compared to 3107 in the wildtype sample).

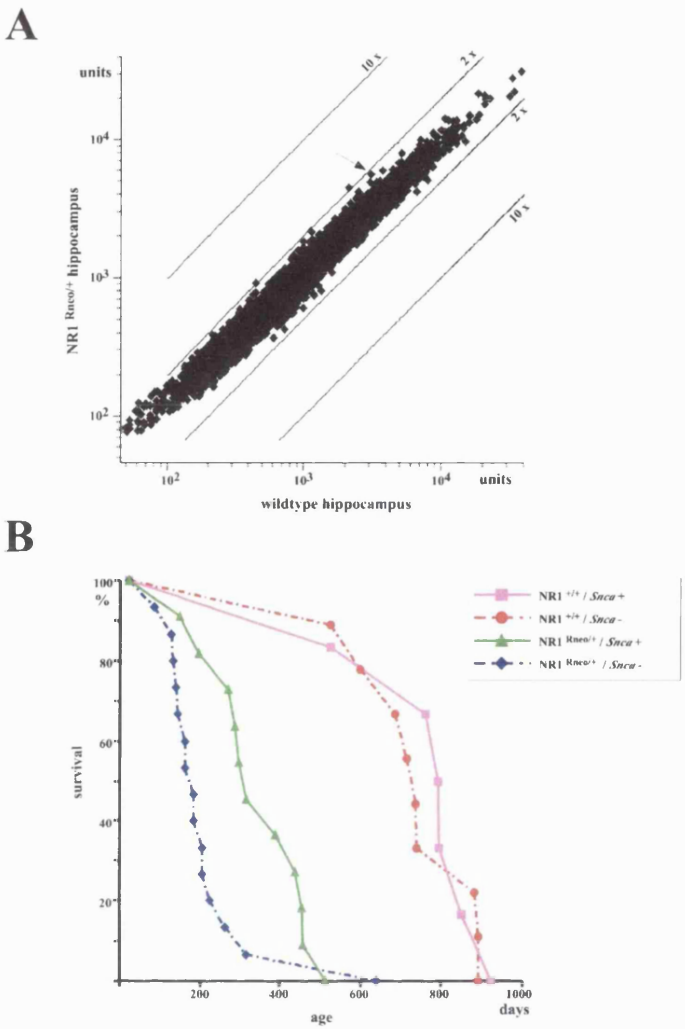

Figure 14. Studies on the adult NR1$^{Rneo/+}$ mouse model

A. cDNA array experiment using 600 ng hippocampus polyA$^+$-RNA, isolated from three adult (8 months old) mutant NR1$^{Rneo/+}$ mice (Cy3 sample) and three wildtype littermates (Cy5). No expression changes were observed in any of the analysed genes (~9000 ESTs). No animal in the NR1$^{Rneo/+}$ group but two in the wildtype group carried the *Snca* deletion. This is reflected by a differential expression factor of 1.8x (α-synuclein, indicated by an arrow; 5595 and 3107 units, respectively). Expression is quantified as arbitrary fluorescence units without background subtraction. Diagonals indicate 2x and 10x differential expression.

B. The survival of NR1$^{Rneo/+}$ animals (trace of green triangles, n=11) is decreased compared to their wildtype littermates (pink squares, n=6). However, life expectancy is further decreased in NR1$^{Rneo/+}$ animals with the deletion of the α-synuclein locus (*Snca*-, blue diamonds, n=15) compared to NR1$^{Rneo/+}$ animals expressing α-synuclein (*Snca*+, green triangles). No significant difference was observed between wildtype NR1$^{+/+}$ animals with (red circles, n=9) and without the *Snca* deletion (pink squares). Each data point corresponds to one animal. Animals were backcrossed four times into the BL6JHUK strain (F4 generation). Only male animals are included that were believed to have died from normal causes rather than from disease.

3.3.10 Survival of $NR1^{Rneo/+}$ animals

During the maintenance of the $NR1^{Rneo/+}$ colony it became apparent that mutant animals died younger compared to wildtype animals. Therefore, survival data were collected on animals of the colony, in order to quantify this effect (with the help of P.Chen). These animals resulted from the fourth backcross (F4 generation) of the $NR1^{Rneo/+}$ colony. The animals were grouped according to their genotype concerning the $NR1^{Rneo/+}$ mutation and the *Snca* deletion. When the life times of the different genotypes were compared it appeared that indeed, $NR1^{Rneo/+}$ animals had a drastically reduced life expectancy compared to $NR1^{+/+}$ wildtype animals (Fig.14B). However, it also was shown that animals with the combined mutations $NR1^{Rneo/+}$ and $Snca^{-/-}$ died at an earlier age (~1/2 year) than $NR1^{Rneo/+}$ animals without the *Snca* deletion (~1 year). The significance of this finding was confirmed using a Mann-Whitney U-test ($P<0.02$). Thus, the deletion of the *Snca* locus aggravates the phenotype observed in the $NR1^{Rneo/+}$ animals. However, the mechanism that is responsible for the interaction of the two mutations is not known. In contrast to this, the life expectancy of $NR1^{+/+}$ wildtype animals is not affected by the presence of the *Snca* deletion.

3.4 Sindbis viral expression system

3.4.1 Cloning of SV contructs for the expression of α-synuclein fusion proteins

The discovery of the deletion of the *Snca* gene in the inbred mouse strain BL6JHUK proved that the differential expression of α-synuclein that was identified in the initial cDNA array screen was not caused by a downstream effect of the NMDA receptor. However, the involvement of α-synuclein in a range of neurodegenerative diseases justified further studies on this protein. To address its physiological role, a Sindbis viral (SV) expression system was chosen for the expression of recombinant α-synuclein protein. To observe the distribution of the recombinant protein within infected cells α-synuclein was expressed as a fusion protein with enhanced green fluorescent protein (eGFP) or red fluorescent protein (RFP).

The eGFP-containing sequence of the plasmid pEGFP-N1 (GenBank U55762, NCBI; Clontech) was excised with the restriction enzymes *Hind* III and *Not* I, and ligated into the pTN-HGESin backbone (provided by C.Tigaret) that had been generated by the digest with *Hind* III and *Kpn* I, using an adapter oligonucleotide (GGCCGTAC). The RFP sequence of pDsRed1-N1 (GenBank accession in preparation; No. 6923-1; Clontech) was inserted into pTN-HGESin in the same way. The eGFP sequence of pEGFP-C1 (GenBank U55763, NCBI; Clontech) was shuttled into pTN-HGESin with the restriction enzymes *Nco* I and *Kpn* I. The resulting intermediate constructs were named pTN-GN1Sin, pTN-RN1Sin, and pTN-GC1Sin, respectively. The construct pTN-GN1Sin was linearised with *Hind* III and *Nco* I, and the multiple cloning site (MCS) was replaced with the *Hind* III/*Pst* I fragment (~120 bp) from pRSSP6012 (provided by R.Schoepfer), using the adapter CATGTGCA. This generated the intermediate construct pSin-EG-N1, with an altered MCS bearing a *Sty* I restriction site for the insertion of the start codon of the coding sequence (CDS).

In the second cloning step the CDS of α-synuclein was generated as PCR fragment and then subcloned into the intermediate constructs. The primers mSynA-PCR7s and mSynA-PCR8a amplified a 457 bp product that was cut with the restriction enzymes *Bgl* II and *Xba* I and ligated into the *Bgl* II/*Kpn* I backbone of pTN-GC1Sin using the adapter CTAGGTAC. This yielded the construct pSin-EG-aSyn. The 491 bp PCR product of mSynA-PCR1s and mSynA-PCR9a was shuttled into pSin-EG-N1

with *Nco* I and *Bgl* II, to produce the construct pSin-aSyn-EG. By replacing the *Hind* III/*Bam*H I fragment in pTN-RN1Sin for the 480 bp *Hind* III/*Bgl* II α-synuclein sequence from pSin-aSyn-EG, a third construct was generated, namely pSin-aSyn-RFP. The fusion protein constructs pSin-EG-aSyn, pSin-aSyn-EG, and pSin-aSyn-RFP were confirmed by double-stranded sequencing using a variety of oligonucleotides for the entire CDS (α-synuclein, eGFP, and RFP sequences) as well as the 5'- and 3'-untranslated regions (UTR; data not shown).

The CDS from the three fusion protein constructs was shuttled into the pSinRep5 plasmid (Invitrogen; Bredenbeek *et al.*, 1993) with the restriction enzymes *Xba* I and *Not* I. The final expression constructs pSinR5-EG-aSyn, pSinR5-aSyn-EG, and pSinR5-aSyn-RFP were verified by restriction digestion (data not shown). The cDNA sequences and the resulting fusion protein sequences are listed in the appendix.

3.4.2 Preparation of recombinant Sindbis virions

The pSinRep5-based expression constructs contain the sequence information for the viral packaging signal (PS), the nonstructural proteins P1234 (replicase), and the recombinant α-synuclein fusion proteins under the control of the subgenomic promoter sequence (P_{SG}). The remaining plasmid sequence contains the SP6 polymerase sequence for transcription, the ColE1 origin of replication, and the β-lactamase gene for ampicillin selection (Fig.15A; Bredenbeek *et al.*, 1993).

pSinRep5 expression constructs were linearised with *Not* I, adding *Pvu* I to optimise the restriction digest (Fig.15A). cRNA was generated from the linearised constructs by *in vitro* transcription. This yielded cRNA fragments of approximately 9.2 kb, containing the PS, replicase, P_{SG}, and fusion protein expression sequences (replicon RNA; Fig.15B). The helper plasmid pDH26S (Invitrogen; Bredenbeek *et al.*, 1993) was linearised with *Xho* I and yielded a 6.2 kb cRNA transcript. This RNA species carries the sequence for the expression of the viral structural proteins that are needed for the packaging of Sindbis virions (Fig.3). Also, the helper RNA retains the PS, but is not efficiently incorporated into virions (Bredenbeek *et al.*, 1993).

Both *in vitro* transcribed cRNA species were introduced into BHK cells by electroporation (30 μg replicon RNA together with 20 μg DH26S helper RNA). The

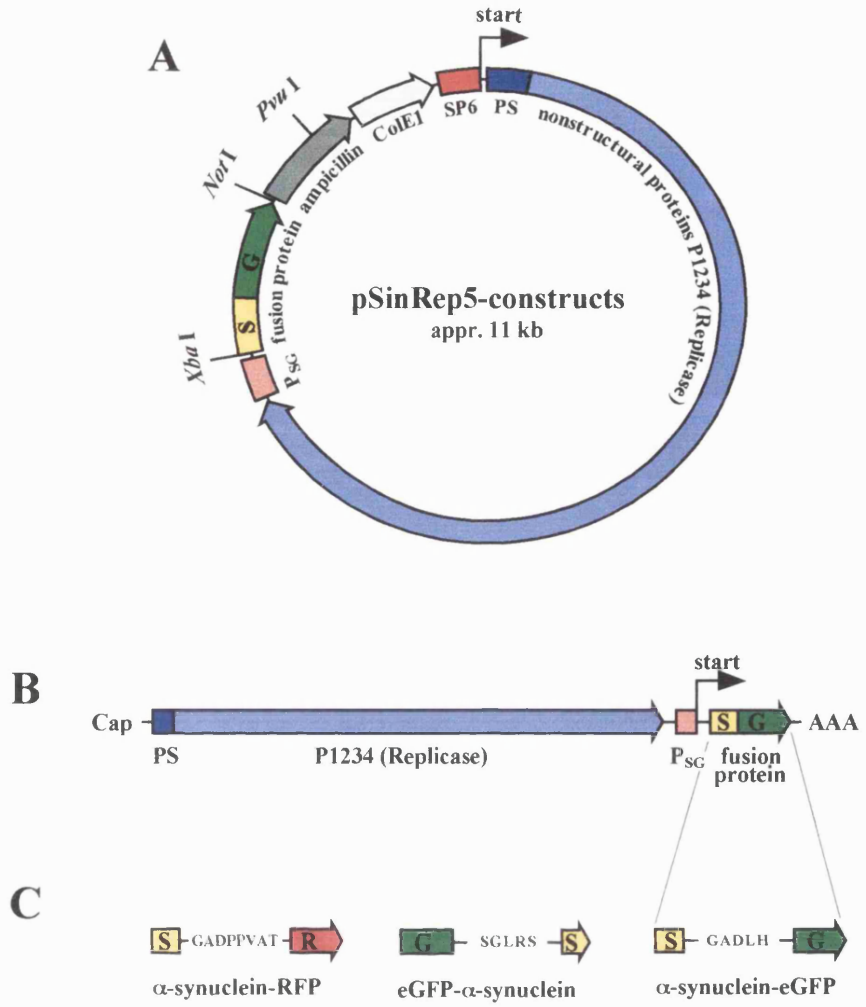

Figure 15. Sindbis viral constructs for the expression of α-synuclein fusion proteins

A. SV constructs for the expression of recombinant proteins are based on plasmid pSinRep5 (Invitrogen; Bredenbeek *et al.*, 1993), containing the sequences for ampicillin resistance and the origin of replication (ColE1). Recombinant sequences were introduced into the MCS with the restriction enzymes *Xba* I and *Not* I. Plasmids were linearised with *Not* I and *Pvu* I, and used for *in vitro* transcription with SP6 polymerase.

B. cRNA transcripts (replicon RNA) contain the viral packaging signal (PS), the sequence for the nonstructural proteins P1234 (replicase), and the recombinant sequences under the control of the subgenomic promoter (P_{SG}). The transcript begins with a 5'-cap signal (cap) and terminates with a polyA sequence (AAA).

C. In transfected BHK cells replicon RNA leads to the expression of the fluorescent α-synuclein fusion proteins under the control of P_{SG}. Three different replicon species produce α-synuclein-RFP (SR), eGFP-α-synuclein (GS), and α-synuclein-eGFP (SG). The amino acid sequences of the linking peptides are inserted between the two domains of the fusion proteins.

expression of the recombinant fusion proteins eGFP-α-synuclein (GS), α-synuclein-eGFP (SG), or α-synuclein-RFP (SR) could be observed after 8 hours post-transfection by the appearance of green and red fluorescence in the transfected cells. The fusion proteins GS, SG, and SR contain linker peptide sequences that arise from the MCS used for the generation of the expression constructs (Fig.15C).

The expression of the fluorescent proteins showed that transfected cells expressed the replicase that is needed for the amplification of the genomic RNA as well as the subgenomic RNA (Fig.3). BHK cells had been cotransfected with the helper RNA species for expression of the viral structural proteins. Therefore, replicon and helper RNA in cotransfected cells led to the packaging of the genomic replicon RNA into virus particles that were then released into the culture medium. The virions were expected to be replication-incompetent, and mainly to contain the replicon RNA but not the helper RNA, since this RNA species is packaged inefficiently (Bredenbeek *et al.*, 1993). The medium containing the virions was collected at 24 hours and 48 hours. These virion harvests were used to infect BHK cells or neurons for the expression of the recombinant fusion proteins GS, SG, and SR (Fig.15C). They are referred to as vGS(24), vGS(48), vSG(24), vSG(48), vSR(24), and vSR(48), respectively.

3.4.3 Plaque assay of recombinant Sindbis virions

The Sindbis virion preparations were tested for infectivity on BHK cell monolayers. This could be monitored by the detection of green fluorescence as early as 6 hours post-infection using the preparations vSG and vGS. Since RFP undergoes a process of maturation (Baird *et al.*, 2000), red fluorescence in cells infected with vSR was delayed to ~12 hours. However, in these initial tests it was noted that after longer incubations (24 hours post-infection), patches of fluorescent cells appeared within the monolayer. This seemed to be caused by replication-competent virions that could undergo an amplification step by the formation of infectious particles. Therefore, plaque assays were performed to characterise the different viral preparations.

In these assays, the BHK monolayer was infected and then covered with a layer of agarose, to restrict the diffusion of newly formed virions. Green fluorescence appeared in isolated cells within the monolayer after only 6 hours post-infection with

vSG or vGS preparations. However, after 24 hours plaques started to appear in the monolayer, with BHK cells displaying cytopathic effects. At 48 hours post-infection these plaques were typically in the range of 200-400 μm in diameter. Cells in many of these plaques also expressed green fluorescent proteins, but at lower levels compared to the isolated bright fluorescent cells (Fig.16A). Plaque-forming units (PFU) were counted at 48 hours post-infection by the presence of cytopathic effects in the monolayer of BHK cells, and infectious units (IU) were counted as isolated cells with bright green fluorescence (Fig.16B). A big variation in the titers between the different preparations (vSG, vGS) and virion harvests (harvest at 24 and 48 h post-transfection) was noted. The harvest vSG(24) contained only 1 PFU per 500 IU, and therefore generally infected isolated cells, without the formation of plaques. In contrast to this, vGS(24) contained 1 PFU in every 10 IU. Therefore, infection with this preparation led to the appearance of many plaques and comparatively few isolated fluorescent cells (Fig.16A). Generally, the IU counts were higher by two orders of magnitude in the 48 hour harvests compared to the 24 hour virion harvest. However, the PFU counts in the 48 hour harvest were increased by approximately three orders of magnitude. Thus, the harvests at 48 hours post-transfection contained a higher ratio of PFU/IU than the 24 hour virion harvests. Cells expressing red fluorescent proteins were difficult to detect due to the autofluorescence of the agarose. Therefore, for vSR preparations only the PFU titers were established in the plaque assays (Fig.16B).

The observation of replication-competent virions was in contradiction to the expected behaviour of the viral expression system, since the helper RNA species had been shown to be only inefficiently packaged into newly formed virions. However, some copackaging of helper RNA and replicon RNA (Bredenbeek *et al.*, 1993) or recombination events between the two RNA species (Weiss and Schlesinger, 1991) have been previously described. Virions that had gained replication competence should express the viral structural proteins in infected cells. To test this hypothesis, immunohistochemistry with anti-SV antibody and a Cy5-labelled secondary antibody was performed on BHK cells that had been infected with vGS(24). This showed that viral proteins were expressed in patches of cells on the monolayer (Fig.16C). Many of these cells also expressed low levels of green fluorescence, although the eGFP and the Cy5 signals were not necessarily colocalised in all cases. In contrast to this, infection with vSG(24) led mainly to the expression of bright green fluorescence in isolated cells, without the expression of viral proteins (data not shown).

A

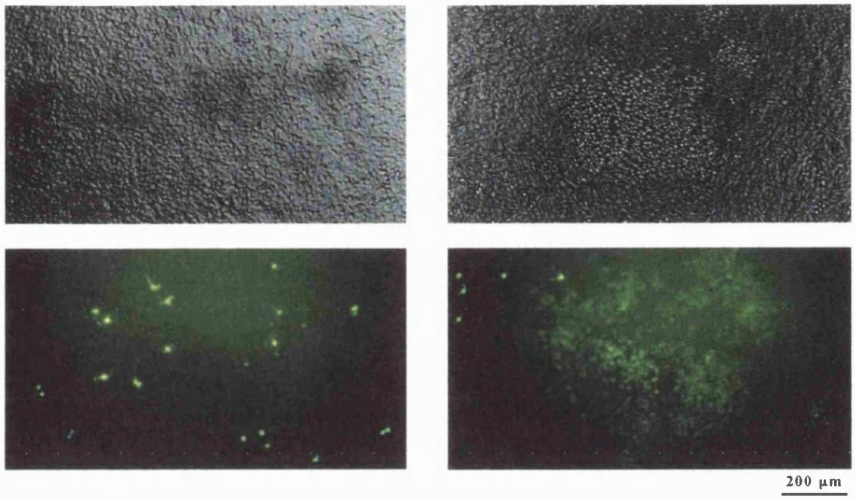

B

virion preparation	harvest	titer (PFU / ml)	titer (IU / ml)	ratio
vGS(24)	24 h	2×10^4	2×10^5	1 : 10
vSG(24)	24 h	1×10^3	5×10^5	1 : 500
vSR(24)	24 h	1×10^4	ND	ND
vGS(48)	48 h	2×10^7	3×10^7	1 : 1.5
vSG(48)	48 h	5×10^5	2×10^7	1 : 40
vSR(48)	48 h	1×10^7	ND	ND

C

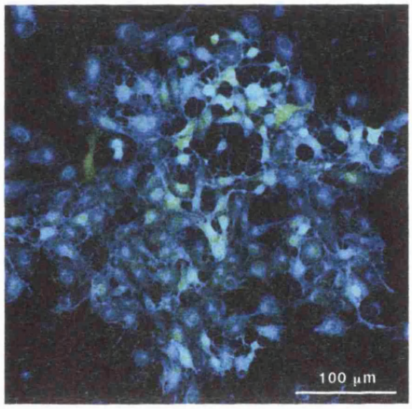

Figure 16. Plaque assay of recombinant Sindbis virions

A. Infection of BHK cell monolayers with vSG(24) led to the presence of mainly isolated cells that expressed fluorescent proteins at 48 hours post-infection (left). Infection with vGS(24) caused the appearance of many plaques within the monolayer (right), where cells displayed cytopathic effects. Plaques were often associated with the expression of green fluorescence.

B. Virus titers obtained for the different virion preparations (vGS, vSG, vSR) and harvests (24 h, 48 h). Plaque-forming units (PFU) were counted at 48 hours post-infection by the appearance of plaques, many of which also expressed green fluorescence. The infectious unit titer (IU) was established by counting isolated cells expressing green fluorescence. Cells expressing red fluorescent proteins were not counted due to the high autofluorescence of the top agarose.

C. BHK cells infected with vGS(24) were subjected to immunohistochemistry using anti-SV antibody and Cy5-coupled secondary antibody at 24 hours post-infection. A part of the monolayer is shown in which cells not only express green fluorescent proteins (green signal), but also viral proteins (blue signal).

3.4.4 Biochemical analysis of expressed α-synuclein fusion proteins in BHK cells

Metabolic labelling was performed to further characterise the protein expression patterns in BHK cells that had been infected with different virion preparations. It appeared that infection for 18 hours with low titers of vGS(24), vSG(24), and vSR(24) did not change the overall protein expression pattern in BHK cells compared to the incorporation of ^{35}S-methionine into proteins in uninfected cells (Fig.17). However, when 10x higher concentrations of vGS(24), vSG(24), and vSR(24) were used, a dramatic change in the expression patterns could be observed at 24 hours post-infection. With vGS(24) and vSR(24), a near total shutdown of host cell protein synthesis was observed (Fig.17). Instead, cells produced predominantly a small number of highly expressed proteins. The patterning of these protein bands suggested that they include the structural viral proteins capsid (~30 kDa), E2 (~48 kDa), and E1 (~52 kDa). Therefore, it was concluded that almost the totality of cells was infected with replication-competent virions that drive the expression of viral proteins. The observed shutdown of the host cell protein synthesis was less dramatic in cells infected with vSG(24), where only a small band of the size of the capsid protein (30 kDa) was visible in the normal protein pattern (Fig.17). This could be caused by the reduced PFU titer of this preparation (Fig.16B). Therefore, reinfection with newly formed virions occurred to a lesser extent with the virion preparation vSG(24) compared to vGS(24) and vSR(24), and did not affect the totality of the BHK cells.

In order to confirm the results obtained by metabolic labelling, the expression of viral structural proteins in infected cells was analysed by Western blotting with anti-SV antibody (Fig.17). Viral proteins were predominantly expressed in the infected cells that displayed the strongest effect of host cell protein synthesis shutdown, namely in cells infected with high concentrations of vGS(24) and vSR(24) for 24 hours. The observed banding pattern that was detected with anti-SV antibody paralleled that observed by metabolic labelling. Therefore, it was concluded that these protein bands represented the viral structural proteins capsid (30 kDa), E2 (48 kDa), E1 (52 kDa), and possibly a precursor protein at around 100 kDa. The expression of viral proteins could also be detected in cells infected for 24 hours with vSG(24), but to a lesser extent. Also, traces of capsid protein were detected in cells infected with low concentrations of vGS(24) and vSR(24) for 18 hours (Fig.17).

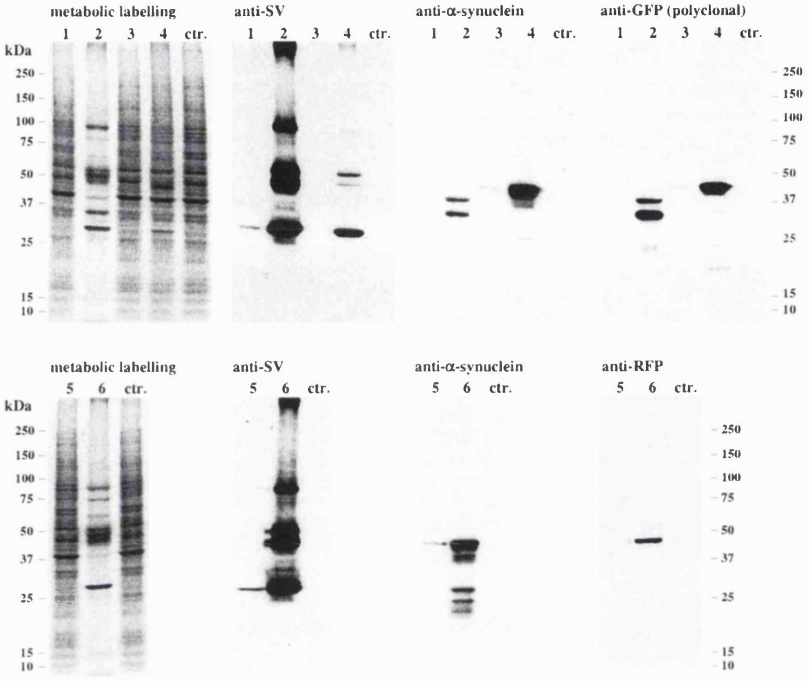

Figure 17. Biochemical analysis of expressed α-synuclein fusion proteins in BHK cells

BHK cells were infected with 10 µl vGS(24), vSG(24), and vSR(24) for 18 hours (lanes 1, 3, 5, respectively) and with 100 µl vGS(24), vSG(24), and vSR(24) for 24 hours (lanes 2, 4, 6, respectively). Uninfected cells served as negative control (ctr.). Metabolic incorporation of ^{35}S-methionine was performed and cell homogenates were separated by 4-20% gradient SDS-PAGE (10 µg protein per lane), followed by Western blotting. Membranes were used for autoradiography of labelled proteins and then sequentially probed with anti-RFP or anti-GFP (polyclonal), anti-α-synuclein, and anti-SV antibodies.

Metabolic labelling showed that infection with high concentration of vGS(24) and vSR(24) leads to a total shutdown of the host cell protein synthesis (lanes 2 and 6, respectively). In these cells, and to a lesser extent in cells infected with vSG(24) (lane 4), viral structural proteins were expressed as judged by anti-SV probing. Antibodies directed against α-synuclein and GFP detected two main recombinant fusion proteins in cells infected with high concentrations of vGS(24) (lane 2). The expressed fusion proteins SG (lanes 3 and 4) and SR (lanes 5 and 6) were of the expected size of 45 kDa and were recognised by anti-α-synuclein antibody and by anti-GFP or anti-RFP antibodies, respectively.

The expression of recombinant fluorescent α-synuclein fusion proteins GS, SG, and SR was analysed by Western blotting with antibodies raised against α-synuclein, GFP, and RFP (Fig.17). Infection with high concentrations of vGS(24) led to the expression of detectable amounts of two recombinant proteins of approximately 35 kDa and 40 kDa that were both recognised by anti-α-synuclein and anti-GFP antibodies. However, the size of the expected fusion protein GS was approximately 45 kDa. The expression of the two smaller products could have been caused by recombination events during the virion preparation or by protein degradation of the GS fusion protein within the BHK cells. In contrast to this, infection with high concentrations of vSG(24) led to the expression of predominantly one single protein band that was recognised by the anti-α-synuclein and the anti-GFP antibodies. This product had the expected molecular weight of the fusion protein SG of approximately 45 kDa. Both antibodies detected a low proportion of protein degradation of the SG product. The expression of the fusion protein SG could also be detected in cells infected with lower virion titers. Similarly, the infection of BHK cells with high titers of vSR(24) led to the expression of one main product that was recognised by antibodies against α-synuclein and RFP. This product had the expected size of the SR fusion protein of 45 kDa. However, a significant proportion of the product underwent protein degradation as judged from the α-synuclein probing. The SR protein could also be detected with anti-α-synuclein antibody in cells infected with low virion titers.

Taken together, the results suggested that in contrast to the constructs vGS(24) and vSR(24), the virion harvest vSG(24) was the most suitable for further expression studies of fluorescent α-synuclein fusion proteins. The infection with vSG(24) was shown to lead to the expression of the expected fusion protein SG with only minimal protein degradation (Fig.17). Also, this virion preparation had the lowest ratio of PFU/IU (Fig.16B). Therefore, the problems associated with the presence of replication-competent virions were limited with this preparation (Fig.17). However, the duration of the following expression experiments was kept to a minimum to prevent reinfection as much as possible.

3.4.5 Morphology of cultured organotypic hippocampal slices

Organotypic rat hippocampal slice cultures were chosen as experimental model for the expression of α-synuclein fusion proteins. The expression of mouse α-synuclein fusion proteins in rat tissue was not expected to represent a major problem, since the mouse and rat sequences of α-synuclein are virtually identical, with a single amino acid difference in position 121 of the protein (Fig.1).

As a first approach, organotypic hippocampal slices were cultured for one week (day *in vitro* 7, DIV7) and used to study their general morphology (Fig.18). After fixation, whole slices were subjected to Nissl staining with cresyl violet to outline the distribution of cell nuclei. The staining showed that the cell body layers in the dentate gyrus (DG) as well as in the CA1, CA2, and CA3 fields of the hippocampus retained their organotypic organisation throughout one week of culture. Alternatively, slices were stained with OsO_4, which is incorporated into lipids such as cell membranes. The strongest staining occurred in the areas containing the neuropil from the pyramidal CA neurons, confirming the organotypic organisation of the cultured slices. In addition, this technique also stained isolated cells on the slice, which probably represented dying cells. This could be expected to occur in organotypic cultures, following the injuries of neurons during the preparation of the slice, and caused by the culture conditions.

3.4.6 Immunoprecipitation of α-synuclein-eGFP expressed in slice cultures

The expression of α-synuclein-eGFP fusion protein (SG) in organotypic slices was analysed by immunoprecipitation of the recombinant protein, in combination with silver staining and Western blotting. Organotypic hippocampal rat slices were cultured for one week (DIV7) and infected with vSG(48). The infection with this preparation was chosen because of its high IU titers (Fig.16B). Homogenates of slices at 24 hour post-infection were subjected to immunoprecipitation with monoclonal anti-GFP antibody. The purified antigen SG was then analysed together with aliquots of the purification procedure by SDS-PAGE. Silver staining of gels showed that predominantly one protein of the expected size of 45 kDa was purified with the GFP antibody from the protein homogenate (Fig.19). The purified protein was absent in the

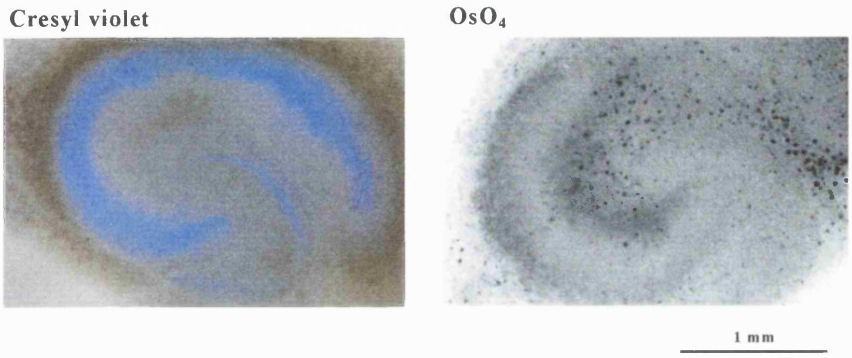

Figure 18. Morphology of cultured organotypic hippocampal slices

Rat P9 hippocampal 300 µm slices were cultured for one week (DIV7), fixed, and stained in cresyl violet (left). The overall distribution of cell nuclei in the cell body layer of the hippocampus was preserved in the slice, with intensive staining of the nuclei in the DG and the fields CA1, CA2, and CA3. Alternatively, fixed slices were stained with OsO_4 (right). Intensive staining of lipids was observed in the hippocampal areas containing the dendritic arborisations. Also, isolated cells were heavily stained with OsO_4, probably representing dying cells in the slice culture.

last washing step, as well as in the control experiment, in which antibody-coupled beads were incubated without homogenate from infected slices. This was designed to control for the stability of the chemical coupling of the GFP antibody to the Protein G-Sepharose beads and did not control for unspecific antibody binding. The total yield of purified GFP antigen was estimated to be approximately 1 μg protein when 5 μg monoclonal anti-GFP (coupled to beads) had been used for purification.

The expression of SG fusion protein in hippocampal slices and its purification by immunoprecipitation were also analysed by Western blotting. In the protein homogenate anti-α-synuclein antibody detected the expression of a 45 kDa band. This protein was also recognised with antibodies against GFP (Fig.19). A second protein of ~19 kDa was detected by anti-α-synuclein antibody in the homogenate, which was likely to represent the endogenous expression of rat α-synuclein. The 45 kDa protein that was purified by immunoprecipitation with GFP antibody was also detected with antibodies against α-synuclein and GFP, confirming that it was the expected SG fusion protein. However, two main degradation products were recognised with the polyclonal and the monoclonal anti-GFP antibodies and not with anti-α-synuclein, suggesting that these truncated proteins retained the GFP domain, but underwent protein degradation within the α-synuclein domain of the fusion protein.

Taken together these results proved that infection of hippocampal slice cultures with vSG(48) led to the expression of the α-synuclein-eGFP fusion protein (SG). Although some degradation of the expressed protein occurred, the expected 45 kDa band represented the predominant product. Protein degradation of such highly overexpressed proteins is an event that is likely to occur. Attempts to use immunoprecipitation as an approach to copurify and identify proteins that interact with α-synuclein fusion protein were unsuccessful (data not shown). It is likely, that much larger amounts of purified fusion protein SG would be necessary to be used as bait for the detection of protein interaction partners.

3.4.7 Expression of α-synuclein-eGFP fusion protein in organotypic slice cultures

Initial expression experiments were performed on organotypic hippocampal slice cultures using the virion preparation vSG(24). This was done to establish the cellular distribution of recombinant SG fusion protein. The infection of slices led to

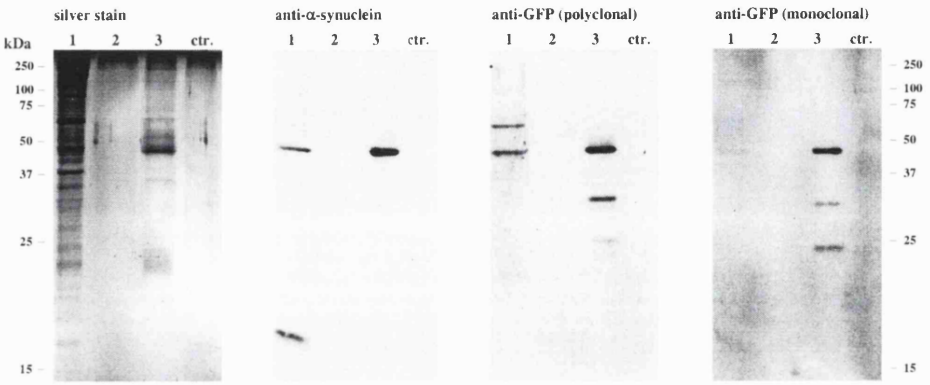

Figure 19. Immunoprecipitation of α-synuclein fusion proteins expressed in hippocampal cultures

Rat P8 hippocampal 300 μm slices were infected at DIV7 with 20 μl vSG(48) and collected at 24 hours post-infection. The expressed fusion protein SG was purified by immunoprecipitation with monoclonal anti-GFP antibody. Proteins were separated by 12.5% SDS-PAGE. Silver staining and Western blotting was performed using gels and membranes with identical protein samples.

A 45 kDa protein was expressed in the whole homogenate (lane 1; ~5 μg protein) and was recognised with antibodies against α-synuclein and GFP. This SG fusion protein was specifically purified by immunoprecipitation (lane 3; 200 ng protein), but was absent from the final washing step before the elution of the antigen (lane 2). However, two major truncated SG proteins that retained their eGFP domain were also purified by immunoprecipitation. The α-synuclein antibody also detected a ~19 kDa band in the homogenate that was likely to be endogenous rat α-synuclein. Polyclonal GFP antibody detected a band of higher molecular weight, probably an aggregation product of SG in the homogenate. As a test for the stability of the chemical coupling of the GFP antibody to Protein G-Sepharose beads a control experiment was run in parallel, in which the homogenate was omitted from the immunoprecipitation protocol (ctr. lane).

the appearance of green fluorescence after as little as six hours predominantly in neurons, but also in some glial cells. Infected hippocampal neurons were identified according to their morphology as mostly interneurons and also pyramidal neurons. Slices were fixed at various time points post-infection and analysed by confocal microscopy. The general cellular distribution of expressed fusion protein SG appeared unchanged at time points between 12 hours and 48 hours post-infection. The overexpression of SG fusion protein led to a fluorescent signal in the soma and the dendritic arborisations of infected neurons (Fig.20A/B). Also, strong fluorescent signals were detected in isolated spots in close proximity to the cells. Since infected cells on the slices were often distant from one other, these clusters of fluorescent spots were most likely to originate from the closest infected fluorescent cell itself. Also, this location of fluorescence was not observed in cells expressing recombinant eGFP protein alone (C.Tigaret, personal communication; data not shown).

A more detailed analysis of the subcellular distribution of SG protein in hippocampal neurons revealed that within the soma, a bright fluorescent signal was present in the cell nucleus. Furthermore, axons and dendrites emerging from the soma could be identified by their morphology (Fig.20D). While the dendrites often displayed spines along their axis, the axonal compartment contained beaded structures of intensive fluorescence, which produced the spotted distribution of fluorescence observed in the proximity of the infected cells (Fig.20C). Thus, it was concluded that these fluorescent signals represented presynaptic boutons. Furthermore, judging from the high fluorescence intensity of these spots in comparison to the weakly labelled axons, it was concluded that the expression product SG accumulated at these locations. This observation is in agreement with the described presynaptic localisation of α-synuclein. In contrast, the detection of fluorescence in the soma and the dendrites of infected cells might not reflect a specific distribution of SG protein caused by a localisation signal for these compartments, but rather result from the overexpression of the recombinant protein.

These studies showed that the infection of hippocampal neurons with vSG(24) led to the expression of the recombinant α-synuclein-eGFP fusion protein (Fig.19). The SG protein was overexpressed and was therefore present in most cellular compartments. However, confocal analysis suggested that an accumulation of the SG fusion protein occurred in presynaptic locations (Fig.20).

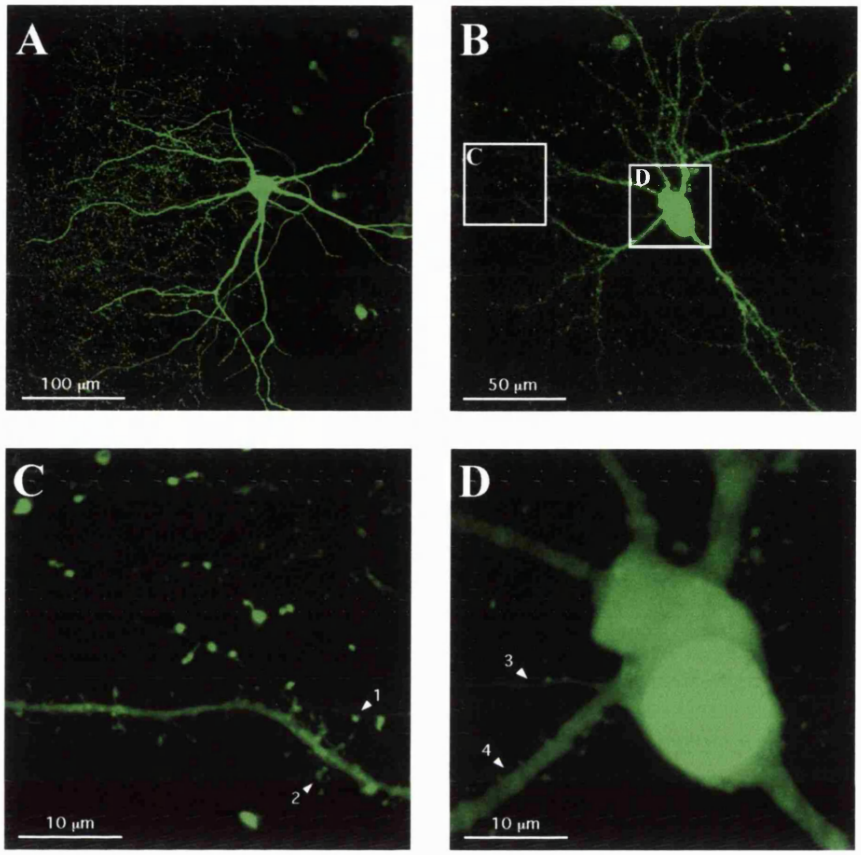

Figure 20. Expression of α-synuclein-eGFP fusion protein in hippocampal cultures

A / B. Overview of hippocampal interneurons infected with vSG(24), expressing SG fusion protein. Slices (P9/DIV10, 300 µm) were fixed at 22 hours post-infection and analysed by confocal microscopy at 25x magnification. SG protein is detected in the cell soma and the dendritic arborisations. Also, a beaded pattern of strong fluorescent signals is present in the proximity of the infected cells.

C / D. Details of structures from the cell shown in B, at 63x magnification with an electronic zoom of 4x. SG protein is detected in the axonal (arrow 3) and dendritic cellular compartment (4) that emerge from the soma, as well as in the cell nucleus. A beaded structure of strong fluorescent signals is associated with the axonal compartment (1). Spines are visible along the axis of the dendrite (2).

Stacks of images (A. 50 µm stack size with 45 frames at an accumulation of 2; B. 22 µm/ 22x2 frames; C. 17 µm/ 85x4 frames; D. 12 µm/ 59x2 frames) were compressed by a z-projection using maximal intensity signals with ImageJ software.

CHAPTER 4
Discussion

4.1 Identification of a mouse strain with a deletion of the α-synuclein gene locus

4.1.1 Deletion of the α-synuclein gene locus in C57BL/6J inbred mice

Analysis of the mRNA expression profiles in the $NR1^{R/+}$ mouse model by cDNA array technology identified a single gene, α-synuclein, as being differentially expressed. However, no consistent correlation between α-synuclein mRNA expression and the NMDA receptor mutation was observed. Instead, α-synuclein expression was dependent on the genomic background of the inbred mouse strain C57BL/6J that had been used for backcrossing of the $NR1^{Rneo/+}$ mouse colony. These animals are referred to as BL6JHUK within the present thesis, according to their source (C57BL/6JOlaHsd from **H**arlan **UK**).

Consistently, α-synuclein mRNA and protein were not detected in the BL6JHUK strain in contrast to the strains 129/Ola, ICR, BL6N (C57BL/6N), and BL6 (C57BL/6). In the strains 129/Ola and ICR the expression of the mRNA transcript increased during postnatal development and peaked at P15. Similarly, α-synuclein protein expression increased during development to reach a plateau at P15 in these animals. The observed temporal expression patterns of mouse α-synuclein were in agreement with previous studies (Hong *et al.*, 1998; Hsu *et al.*, 1998). A semi-quantitative estimation of α-synuclein mRNA expression levels was achieved by RT-PCR. This showed that the expression of the transcript was decreased by a factor $\geq 10^4$ in the BL6JHUK strain compared to the ICR strain. Thus, the α-synuclein gene locus (*Snca*) in the BL6JHUK strain can be considered a null allele.

The underlying mechanism of the null allele was analysed by genomic PCR. It resulted that the absence of α-synuclein expression in BL6JHUK mice was caused by a chromosomal deletion of the *Snca* locus in this strain. In contrast, a number of other mouse strains were not affected by the deletion, including the strains ICR, 129/Ola, BL6N, BL6, and BL6Jax (C57BL/6J DNA obtained from Jackson Laboratory). These

results unequivocally show that BL6JHUK animals, a subpopulation of the C57BL/6J strain, carry a chromosomal deletion of the *Snca* locus.

The discovery of a chromosomal deletion of α-synuclein in C57BL/6J DNA was unexpected for various reasons. Firstly, the protein had been previously detected in brain from wildtype C57BL/6 mice (Kahle *et al.*, 2000). Furthermore, α-synuclein cDNA clones had been isolated from C57BL/6J libraries (GenBank W41663 and AA266446, NCBI), implying the presence of the α-synuclein gene. Also, the screening of a C57BL/6J YAC library had identified an α-synuclein positive YAC clone (M.Peters, personal communication). Finally, the initial cDNA array experiment had suggested a differential mRNA expression of 7.6 fold rather than the complete absence of the gene (clone W41663 was present on the array).

Indeed, it was found that the deletion of α-synuclein only affected a subpopulation of C57BL/6J animals, namely C57BL/6JOlaHsd animals that had been obtained from Harlan UK (BL6JHUK). The deletion was not present in the C57BL/6J DNA provided by the Jackson Laboratory (BL6Jax). Also, the deletion did not occur in the related strains C57BL/6N and C57BL/6. It remains to be established how widespread this deletion is within different C57BL/6J colonies. All animals obtained from Harlan UK that were analysed during the years 2000 and 2001 were shown to carry the mutation (n = 8 from four batches of animals), suggesting that a majority of the colony is affected. However, it can not be excluded that the colony remains heterogeneous regarding the deletion. From the available information it appears that the mutation has been present in this colony as early as 1997. Further investigation will be needed to determine the prevalence of the deletion within the mouse colony and the time point at which it occurred.

4.1.2 Size of the *Snca* deletion in a C57BL/6J substrain

A total of 120 kb genomic sequence information is available for the *Snca* locus in the mouse strain 129/SvJ (Fig.11A; GenBank AF163865, NCBI; Touchman *et al.*, 2001). Genomic PCR analysis of the chromosomal deletion in BL6JHUK DNA proved that it covers ≥120 kb sequence including the *Snca* locus. However, the deletion was shown not to affect loci mapped at a distance of only 1.1 cM to each side of *Snca*, namely *Atoh1* and *Atoh2* (Touchman *et al.*, 2001), as well as the genes *Abcg2* and

Grid2. Currently (December 2001), these loci are mapped to close locations of *Snca* at 29 cM on mouse chromosome 6 (*Abcg2* at 28.5 cM; *Atoh2* at 29 cM; *Grid2* at 29.65 cM; *Atoh1* at 29.69 cM; human-mouse homology map, NCBI).

The sequence analysis of mouse α-synuclein positive YAC clones offered a separate approach to obtain more information about the deletion of the *Snca* locus in BL6JHUK animals. These included the clones #326H11 and #465H1, members of the YAC contig WC6.20 (Fig.11C; Whitehead Institute/MIT Center for Genome Research). Pulsed field gel electrophoresis in combination with Southern blotting suggested that YAC clone #465H1 had an estimated size of 1.1 MB. Genomic PCR showed, that both YAC clones contained the entire 120 kb sequence AF163865. However, most other genomic markers tested were absent from the YAC sequences. So far only one marker, *32.MMHAP36FLC5.seq* proved positive for BL6JHUK and BL6Jax mouse genomic DNA as well as YAC clone #465H1. This suggests that clone #465H1 contains within its 1.1 MB sequence at least one of the two breaking points of the chromosomal deletion.

Database information on chromosomal sequences could allow a more exact characterisation of the deletion. Current searches (December 2001; MGSC Ensembl database) combined with genomic PCR analysis suggest that the deletion is located between the genomic markers *D6Mit122* and *D6Mit126*. It is estimated that these markers are separated by as little as 0.5 MB at position 68 MB along the mouse chromosome 6 sequence (Fig.11B). However, further information is needed to establish the exact size and the breaking points of the chromosomal deletion of the α-synuclein locus in the BL6JHUK strain.

At present, it can not be fully established if gene loci other than *Snca* are affected by the chromosomal deletion. However, it can for instance be excluded that the genomic locus *Grid2* is deleted in BL6JHUK animals. This locus is affected by the naturally occurring Lurcher (*Lc*) mutation in the membrane domain M3 of the mouse ionotropic glutamate receptor δ2 (Zuo *et al.*, 1997). Heterozygous *Lc*/+ animals develop ataxia caused by apoptotic death of cerebellar Purkinje cells, and homozygous *Lc*/*Lc* animals die shortly after birth. Mapping locates the *Grid2* gene between the markers *D6Mit121* and *D6Mit175* (Zuo *et al.*, 1995). However, both these loci, currently mapped to position 80 MB on mouse chromosome 6 are not covered by the *Snca* deletion in BL6JHUK animals (Fig.11B).

4.1.3 Nomenclature of the *Snca* deletion in a C57BL/6J substrain

Within the present thesis, the C57BL/6J substrain with a deletion of the *Snca* locus has been referred to as BL6JHUK according to its source (C57BL/6JOlaHsd animals from **H**arlan **UK**). Also, it has been previously referred to as C57BL/6S (S for α-**s**ynuclein; Specht and Schoepfer, 2001). This arbitrary denomination could be justified, since the exact size of the deletion is not known. In particular, it remains elusive, if other genes are affected by the deletion.

However, a genomic nomenclature has now been introduced for the chromosomal deletion, Del(6)*Snca*1Slab, according to the general rules and guidelines for mouse nomenclature (MGI Mouse Genome Informatics, Jackson Laboratory). This nomenclature describes the **del**etion on mouse chromosome **6** that includes the **1**st mutation identified in the ***Snca*** locus. The laboratory registration code (Slab) states the laboratory name (**S**choepfer **Lab**oratory) and was registered at the Institute of Laboratory Animal Research (ILAR). Following this nomenclature, the C57BL/6J substrain with a deletion of the *Snca* locus is now referred to as C57BL/6JOlaHsd-Del(6)*Snca*1Slab. The advantage of this terminology is that the deletion can be easily referred to when backcrossed into a different mouse strain.

4.1.4 Frequencies of chromosomal deletions

Currently, the deletion Del(6)*Snca*1Slab is estimated to be in the range of 120-500 kb. The deletion is phenotypically silent, which might explain why it has escaped detection so far. It is interesting to investigate how frequent such deletions are in different mouse strains or colonies, and to consider the likelihood that a deletion might escape detection.

The entire mouse genome contains approximately $3x10^9$ bp of sequence information (December 2001; MGSC Ensembl database). A deletion of a specific sequence can be identified by genomic PCR in animals that are homozygous for that locus. However, a large number of genomic markers would be needed to exclude all deletions of minor sizes. For example, 6000 **equally spaced** markers would be needed to exclude all deletions larger than 0.5 MB (i.e. $3x10^9$ bp / $0.5x10^6$ bp). When 1000 equally spaced markers were used for screening, the probability that a deletion of exactly 0.5 MB was detected would be as low as 16.7% (i.e. 1000 / 6000).

The probability p_n that a deletion of x bp is detected in a genome of y bp is reduced if a number of n **randomly distributed** markers are used. It can be calculated according to the following formula, based on the assumption that the markers are infinitesimally small.

$$p_n = \sum_{i=0}^{n-1} \frac{x}{y}\left(1-\frac{x}{y}\right)^i$$

With 6000 randomly distributed markers the probability to detect a deletion of exactly $0.5\text{x}10^6$ bp in a genome of $3\text{x}10^9$ bp would be 63%, with 1000 markers it would drop to only 15%.

The exact definition of the genomic background in inbred mouse strains is crucial for scientific research. For example, C57BL/6 is probably the most widely used inbred mouse strain. However, genomic variations in different substrains or subpopulations may underlie contradictory experimental results. In the future, large-scale screening of expression profiles (e.g. Sandberg *et al.*, 2000) by cDNA array technology or proteomics is likely to identify unexpected genomic variants. It will be interesting to see how frequently such deletions occur and whether they play an important role in evolution. For the moment, the occurrence of such deletions has implications on the number of genomic markers needed to validate mouse strains.

4.1.5 Lack of an obvious phenotype in animals with the *Snca* deletion

BL6JHUK animals carrying the α-synuclein deletion appear to be phenotypically normal. No differences were noticeable in their general health, development, breeding behaviour, or fertility, and the life expectancy of α-synuclein-deficient mice was not significantly altered compared to wildtype animals. These findings are consistent with previous reports on the phenotype of α-synuclein knockout animals (Abeliovich *et al.*, 2000). Furthermore, the performance of *Snca*$^{-/-}$ animals is not altered in the spatial learning paradigm of the water maze (data not shown; Chen *et al.*, a in preparation).

Also, tyrosine hydroxylase (TH) staining had shown that the number and morphology of dopaminergic neurons is not affected in *Snca*$^{-/-}$ animals (Abeliovich *et al.*, 2000). This finding was confirmed by an initial immunohistochemical experiment.

TH staining of dopaminergic neurons in the substantia nigra (SN) of adult BL6JHUK animals was not altered in comparison to wildtype BL6N control animals (data not shown; performed by R.Singh Jolly and S.W.Davies). The absence of a severe phenotype in the *Snca*$^{-/-}$ animals could explain why the chromosomal deletion affecting the BL6JHUK colony has not been previously identified.

4.1.6 Potential compensatory effects in animals with the *Snca* deletion

To explain the lack of a noticeable phenotype in the absence of α-synuclein, potential compensatory mechanisms can be taken into account. It is possible that the function of α-synuclein is compensated by the upregulation of a gene that encodes a protein with a similar function and that this would be reflected by increased mRNA or protein levels. Likely candidates are the members of the synuclein family of proteins, β- or γ-synuclein. Particularly β-synuclein is a possible compensatory factor, since its structure is highly similar to α-synuclein (Fig.1). Sequence identity is most pronounced in the N-terminal domain, but also includes a conserved C-terminal Ca^{2+} binding site (Nielsen *et al.*, 2001). α- and β-synuclein can be phosphorylated on a conserved serine residue S129 and S118, respectively (Nakajo *et al.*, 1993; Okochi *et al.*, 2000; Pronin *et al.*, 2000). Both proteins are located in presynaptic nerve terminals (Maroteaux *et al.*, 1988; Nakajo *et al.*, 1990) and show extensive colocalisation (Kahle *et al.*, 2000). Also, α-synuclein and β-synuclein can form heterodimers and coimmunoprecipitate (Jensen *et al.*, 1997; Hashimoto *et al.*, 2001). Furthermore, functional similarities have also been reported. α- and β-synuclein are potent selective inhibitors of phospholipase D2 (PLD2) (Jenco *et al.*, 1998). The phosphorylation of α-synuclein interferes with the inhibition of PLD2 (Pronin *et al.*, 2000).

However, there was no indication of an altered β-synuclein expression in the BL6JHUK strain compared to the wildtype strains 129/Ola and ICR, as judged by Western blotting. The expression of the protein increased during postnatal development to reach a plateau in adult animals, in agreement with previous studies on the temporal expression of rat β-synuclein protein (Shibayama-Imazu *et al.*, 1993). The antibody PER4 crossreacts with α- and β-synuclein (Spillantini *et al.*, 1998b). When used for Western blotting, the expected result was obtained, representing an overlaid picture of the individual α-synuclein and β-synuclein probing.

The expression profile of γ-synuclein mRNA in the BL6JHUK strain was also investigated. However, no significant changes were detected between different strains throughout postnatal development. This result was also confirmed by the cDNA array experiment performed at developmental time point E18.5, on which the γ-synuclein EST clone GenBank AA272342 (NCBI) had been present.

Taken together, the results suggest that the absence of α-synuclein does not influence the expression levels of the other members of the protein family, β- and γ-synuclein, as judged by Western and Northern blotting. However, a functional compensation of the proteins can not be excluded, since this would not necessarily have to be reflected by changes in the protein or mRNA expression levels. Furthermore, even dramatic changes in specific localised brain areas may not be detected by the chosen approach, in which whole brain material was used. Thus, functional compensation between the synucleins would have to be addressed by the generation of mice with deletions of different synuclein gene loci (*Snca*, *Sncb*, *Sncg*).

4.1.7 Potential downstream effects in animals with the *Snca* deletion

The deletion of α-synuclein can be expected to have an impact on its downstream interaction partners. This again may be reflected by changes in expression levels of interacting proteins. To evaluate such a possibility, the expression levels of synphilin-1 were analysed in the absence of α-synuclein. Synphilin-1 had been identified to specifically interact with α-synuclein via the C-termini of both proteins (Engelender *et al.*, 1999; Kawamata *et al.*, 2001). Also, synphilin-1 is present in LB in PD, suggesting an involvement in the pathophysiology of the disease (Wakabayashi *et al.*, 2000).

However, it was shown that the absence of α-synuclein did not influence the expression levels of synphilin-1. The mRNA and protein expression was not significantly altered in the BL6JHUK strain compared to the wildtype strains 129/Ola and ICR at any time point in postnatal development. Due to the low specificity of the antibody (ab6179; Abcam) a number of proteins were detected in mouse brain. This could be explained by the small size of the epitope against which the antibody had

been raised. The strongest signals resulted from an 85 kDa protein that was expressed increasingly throughout development and that is most likely to be mouse synphilin-1. A different antibody (ab6178; Abcam) failed to recognise the respective protein band in mouse brain tissue. This was probably caused by a number of mismatches between the mouse synphilin-1 protein sequence and the human epitope against which it had been raised. Since antibodies against different epitopes of synphilin-1 are currently not available, the result can not be independently validated. However, the obtained data consistently show that the expression of synphilin-1 is not affected by the deletion of α-synuclein.

Furthermore, it can be inferred from the initial cDNA array experiment that the deletion of *Snca* does not result in significant changes in the expression levels of the other genes represented on the array. These include ubiquitin C-terminal hydrolase L1 (UCH-L1 or PGP 9.5; EST clone GenBank AA285969, NCBI) that has also been found in LB (Lowe *et al.*, 1990). This transcript was highly expressed in the wildtype and the $NR1^{R/+}$ RNA sample with the *Snca* deletion (16699 vs. 14393 arbitrary units, respectively). However, the cDNA array experiment only analysed 9000 EST clones, with some degree of redundancy concerning the gene loci. Thus, only a fraction of the entire mouse genome, currently estimated to be in the range of 50000 to 85000 genes was analysed (December 2001; MGSC Ensembl database and *Mus musculus* statistics, UniGene database, NCBI). Therefore, differentially expressed genes under the control of α-synuclein might have escaped detection. Likewise, the cDNA array experiment performed on adult hippocampus $polyA^+$-RNA preparations did not produce differentially expressed candidate genes. This could be expected, since both samples were pooled from three hippocampi according to their NMDA receptor genotype and not to the *Snca* deletion. It resulted that within the wildtype group only one animal expressed α-synuclein, whereas the mutant $NR1^{Rneo/+}$ group was composed of three α-synuclein-expressing animals. Thus, possible effects of α-synuclein on expression levels would have been diluted out. However, the expression ratio of 1:3 concerning α-synuclein is reflected by the signal ratio on the array of 1.8x (5595 units in $NR1^{Rneo/+}$ vs. 3107 in the wildtype sample), indicating that the cDNA array technique provides a sensitive measurement of mRNA expression.

4.1.8 Future work – deletion of the *Snca* locus in a C57BL/6J substrain

Taken together, the findings identified a C57BL/6J substrain that carries a deletion of the *Snca* locus. Although the deletion is relatively small in size covering an estimated 120-500 kb of chromosomal sequence, further analysis will be needed to establish if other, possibly unknown genes are also affected. This may be approached by the study of YAC clones containing the *Snca* locus.

The absence of α-synuclein in the C57BL/6J substrain makes it a promising tool to address the physiological function of the protein. This is particularly interesting in relation to its involvement in the pathophysiology of PD. So far, no downstream effects caused by the absence of α-synuclein were identified. To further examine consequences of the lack of α-synuclein, cDNA array experiments could screen a larger number of genes. Alternatively, proteomic approaches could be used to identify potential effects on the cell function at the protein level, such as protein phosphorylation and protein degradation.

4.2 Screening for downstream effects to the NMDA receptor activation

4.2.1 mRNA profiling in an NR1 mutant mouse model

The original aim of the project was the identification of genes, whose expression is controlled downstream to the NMDA receptor activation. This was approached by cDNA array analysis of a mutant $NR1^{R/+}$ sample compared to a wildtype littermate at E18.5. Coincidence detection of the NMDA receptor is abolished by the mutation N598R in the NR1 subunit. However, differential expression caused by the mutation in the NR1 subunit was not observed for any gene present on the cDNA array. The lack of α-synuclein expression that was found in the $NR1^{R/+}$ sample was not due to the mutation of the NR1 subunit, but to a deletion of the *Snca* locus. This resulted from backcrossing the $NR1^{Rneo/+}$ colony into the α-synuclein-deficient strain BL6JHUK. However, the mouse colony had remained heterogeneous concerning this deletion. The expression of the remaining genes on the cDNA array (approximately 9000 immobilised EST sequences) was not significantly altered between the two samples, thus the attempt of identifying downstream effects to the NMDA receptor had failed in this approach.

At a later stage of the project, a second cDNA array experiment was performed on adult $NR1^{Rneo/+}$ mutant mice, addressing the original aim of the project. In this model, the insertion of the neo cassette led to the expression of small amounts of NR1 N598R mutant receptor subunits in the range of 5% of the wildtype expression levels (Chen, b in preparation). A similar hypomorphic expression of NR1 subunits had also been observed in a previous study (Mohn *et al.*, 1999). As a result of the hypomorphic expression of NR1 N598R subunits, adult $NR1^{Rneo/+}$ mutant mice display behavioural impairments in the water maze paradigm. Also, an electrophysiological phenotype in the DG area of the hippocampus had been found (Chen, b in preparation). For these reasons, expression profiling was performed exclusively on hippocampal material. Again, the expression of all genes represented on the cDNA array was not significantly altered between the mutant $NR1^{Rneo/+}$ and the wildtype samples. Although some data points suggested minor changes of gene expression in the range of twofold, such potential expression changes are difficult to be validated using methodological approaches such as Northern or Western blotting.

4.2.2 Survival of $NR1^{Rneo/+}$ animals

The analysis of the life expectancy of the $NR1^{Rneo/+}$ colony produced a number of interesting observations. Survival was drastically decreased by the presence of the mutant allele in $NR1^{Rneo/+}$ animals. This finding can be correlated to the electrophysiological and behavioural phenotypes observed in these animals (Chen, b in preparation).

However, a further decrease in the life expectancy was noticed in $NR1^{Rneo/+}$ animals that were also affected by the *Snca* deletion. In contrast, the *Snca* deletion had no effect on animals expressing wildtype NR1 subunits. This is the first description of an observation that suggests a beneficial effect related to the expression of α-synuclein *in vivo*. Furthermore, the finding may partially explain why the wildtype α-synuclein allele had still been present in the mouse colony after a number of backcrosses into the α-synuclein-deficient strain BL6JHUK. It was speculated that the decreased life expectancy was one of several factors that might select for the presence of the *Snca* gene in the mouse population. $NR1^{Rneo/+}$ males that are not affected by the *Snca* deletion could be used for a longer period for breeding, due to their increased life expectancy. Thus, a higher number of offspring would be generated from these animals compared to the α-synuclein-deficient $NR1^{Rneo/+}$ males. However, it can not be ruled out, that the BL6JHUK strain itself remained heterogeneous for the deletion of *Snca*. In this case, the described effect may only play a minor role in determining the genotypes present in the mouse colony.

4.2.3 Future work – NR1 mutant mouse model

Although the mutant NR1 mouse model is partially understood, it is not yet clear what causes the death of $NR1^{R/+}$ animals shortly after birth (Rudhard *et al.*, in preparation). Similarly, it remains to be determined why animals expressing as little as 5% of the mutant N598R allele ($NR1^{Rneo/+}$) display such severe phenotypes concerning survival, learning, and signal processing (Chen, b in preparation). To address these questions genome-wide expression profiling of the mutant mouse model could be performed on the mRNA or on the protein levels.

Furthermore, it remains to be established what the exact nature of the interaction between the NMDA receptor mutation and the α-synuclein deletion is. It appears that the deletion of *Snca* reduces the learning performance and the survival in adult $NR1^{Rneo/+}$ animals, but does not cause a noticeable phenotype by itself (P.Chen, personal communication, data not shown; Chen *et al.*, a in preparation). Thus, the identification of the mechanism that underlies the $NR1^{Rneo/+}$ phenotype is likely to lead to an explanation concerning the role of α-synuclein within this context. However, the possible deletion of further genes in the strain BL6JHUK has to be taken into account.

4.3 Sindbis viral expression of α-synuclein fusion proteins

4.3.1 Preparation and analysis of recombinant Sindbis virions

Sindbis viral (SV) constructs for the expression of α-synuclein fusion proteins with eGFP and RFP were based on the pSinRep5 plasmid (Fig.15; Invitrogen; Bredenbeek *et al.*, 1993). *In vitro* transcribed cRNA from these constructs was used to transfect BHK cells that produced recombinant Sindbis virions. The helper pDH26S used in this approach contains the PE2 and E1 structural protein sequences that were derived from a neurovirulent SV strain (Lustig *et al.*, 1988; Bredenbeek *et al.*, 1993). Virus particles were collected at 24 and 48 hours post-transfection and were used in the following studies for the expression of the recombinant proteins eGFP-α-synuclein (GS), α-synuclein-eGFP (SG), or α-synuclein-RFP (SR).

The expression of green fluorescent signals was observed on BHK cell monolayers as early as 6 hours post-infection with the virion preparations vSG and vGS. However, the appearance of red fluorescence was delayed to approximately 12 hours in cells infected with vSR. This is consistent with a slow process of maturation of the RFP molecule. Another disadvantage of this expression construct is the potential oligomerisation of the RFP domain (Baird *et al.*, 2000).

The quality of the virion preparations was established with plaque assays on BHK cell monolayers. At 48 hours post-infection plaques were 200-400 μm in diameter and titers of plaque-forming units (PFU) and infectious units (IU) were counted. In the virion harvests vGS(24) and vSG(24), IU titers were in the range of 2-5 x 10^5/ml. These values were increased by two orders of magnitude in the 48 hour harvests. However, the IU titers were below the reported yields for pSinRep5-based replicons in combination with the helper construct pDH26S of ~0.5-5 x 10^8 IU/ml (Bredenbeek *et al.*, 1993; Ehrengruber *et al.*, 1999). The harvest vSG(24) contained 10^3 PFU/ml, comparable to the reported value of $<10^4$ PFU/ml (Bredenbeek *et al.*, 1993). However, vGS(24) and vSR(24) had significantly higher titers of 1-2 x 10^4 PFU/ml. All virion preparations harvested at 48 hours post-transfection had very high counts of PFU titers.

The presence of plaque-forming activity suggested the formation of replication-competent virions that contained genomic information for both structural and

nonstructural viral proteins. The expression of structural proteins in infected BHK cells could be shown by immunohistochemistry. Replication competence has been reported to be either caused by copackaging or by recombination events (Weiss and Schlesinger, 1991; Bredenbeek *et al.*, 1993). The latter is likely to occur at least in some cases, since plaques did not generally exhibit green fluorescence. However, cells in many plaques also expressed eGFP-containing proteins, although at lower levels compared to the isolated bright fluorescent cells. This indicated that some recombinant sequence information was retained in these virions.

Taken together, the results indicate the presence of replication-competent virions in the preparations. It is likely that by optimising the transfection protocol, culturing conditions, and time points of virion harvest higher IU/PFU ratios could be obtained. However, the preparation vSG(24) contained sufficient IU with a low titer of PFU (500:1). Therefore, this product appeared suitable to be used for the expression of the SG fusion protein.

4.3.2 Biochemical analysis of expressed α-synuclein fusion proteins

The expression of viral and recombinant proteins was studied in BHK cells that were infected with the virion harvests vGS(24), vSG(24), and vSR(24). Metabolic labelling of cells infected with vGS(24) and vSR(24) suggested that high virus titers could lead to the shutdown of host cell protein synthesis and to the overexpression of viral proteins. The expression of the viral structural proteins capsid, E2, and E1 was confirmed by Western blotting with anti-SV antibody. Consistent with the plaque assays, this effect was less pronounced with vSG(24), which contains a low ratio of PFU/IU.

The expression of recombinant proteins in BHK cells was detected with antibodies raised against α-synuclein, GFP, and RFP. Upon infection with vSG(24), the 45 kDa protein SG was expressed at high levels, with minimal proteolytic degradation. Similarly, vSR(24) yielded a 45 kDa product, however, a larger degree of proteolysis occurred. In contrast, infection with vGS(24) led to the expression of two products of 35 kDa and 40 kDa, rather than the expected 45 kDa GS fusion protein. Both bands included α-synuclein and eGFP epitopes as judged by Western blotting. The presence of the two specific bands could be caused by recombination events

during the preparation of the virions, consistent with the high PFU/IU ratio in this preparation. Alternatively, the result could be caused by an efficient, specific proteolytic cleavage of the expressed fusion protein within the BHK cells, but this is less likely since not even traces of a 45 kDa band were detected. Truncations of overexpressed α-synuclein-eGFP fusion protein in transfected H4 human neuroglioma cells had been previously observed following proteasome inhibition. However, this study failed to analyse the expressed fusion proteins in neurons (McLean *et al.*, 2001). This control experiment is critical to the study of the physiological role of a neuronal protein overexpressed in neurons, since protein processing could differ in distinct cell lines.

To exclude differences in the processing of overexpressed proteins in different cell types, the expression of SG fusion protein was assessed in rat organotypic hippocampal slices. The viral harvest vSG(48) was chosen to obtain high infection rates, although this could increase the problems associated with PFU titers. Since the experiment was specifically aimed at analysing the expression of SG fusion protein, the result could be extrapolated on the vSG(24) preparation. Also, slices were harvested after 24 hours post-infection to limit the degree of reinfection with replication-competent virions. Slices were then subjected to immunoprecipitation with anti-GFP antibody. Silver staining indicated that predominantly one protein of the expected size of 45 kDa was purified from the homogenate. Western blotting identified the purified antigen as SG fusion protein. However, two main degradation products of the 45 kDa protein were recognised with GFP antibodies, suggesting that these truncated proteins retained the eGFP domain, but underwent degradation within the α-synuclein sequence. Degradation within the eGFP domain could also occur, although these truncated products would not be purified by immunoprecipitation using a GFP antibody. Interestingly, polyclonal GFP antibody recognised a band of approximately 65 kDa in the homogenate. It is likely that this band represents an SDS-insoluble aggregated form of the fusion protein SG, similar to previously described α-synuclein aggregates (Narayanan and Scarlata, 2001). It can not be established if this aggregation occurred during the expression of the SG fusion protein within the cells, or after the homogenisation, caused by long incubations of the sample on ice or by repeated freeze-thaw cycles.

The results consistently show that infection with vSG leads to the expression of the α-synuclein-eGFP fusion protein and that proteolytic degradation of the expressed 45 kDa protein is limited.

4.3.3 Expression of α-synuclein-eGFP fusion protein in hippocampal cultures

Endogenous α-synuclein is highly expressed in the hippocampus (Hong *et al.*, 1998; Petersen *et al.*, 1999). Previously, organotypic slice cultures have been successfully combined with the Sindbis viral expression system for the heterologous expression of eGFP in hippocampal pyramidal and granular neurons, and in interneurons, with little infection of glial cells (Ehrengruber *et al.*, 1999). Therefore, organotypic slice cultures were chosen for the expression of recombinant α-synuclein-eGFP (SG) fusion protein.

The morphology of rat hippocampal slice cultures was studied using Nissl and OsO_4 staining. These methods did not reveal a detailed morphology, since the thickness and the profile of the slice prevented imaging at high magnification on a non-confocal system, but were aimed at monitoring the overall organotypic organisation. The distribution of cell nuclei in the cell body layers of the DG and CA fields and of membrane-dense regions in the adjacent neuropil showed that the cultures retained their organotypic organisation throughout one week *in vitro*. This is comparable to previous morphological analysis of organotypic slices under these culture conditions (Stoppini *et al.*, 1991). The preparation vSG(24) was chosen for infection, since the plaque assays and biochemical analysis indicated a low ratio of PFU/IU and the expression of a single fusion protein with little proteolytic degradation. The expression of mouse α-synuclein in rat organotypic slices was not expected to pose a problem, since the mouse and rat α-synuclein sequences differ by a single amino acid residue in position 121 of the protein (Fig.1).

As previously reported (Ehrengruber *et al.*, 1999), infection occurred predominantly in hippocampal interneurons and pyramidal neurons as judged by their morphology, but also in some glial cells. However, infection of interneurons was more frequent compared to pyramidal neurons. This could be caused by the bulk application of virions onto the slice in contrast to the application of virions by microinjection that

has been described (Ehrengruber *et al.*, 1999). Subcellularly, the overexpression of SG fusion protein led to a fluorescent signal in all cellular compartments (i.e. soma, dendrites, and axon). This was expected for a vastly overexpressed fusion protein that is composed of the two cytoplasmic domains α-synuclein and eGFP. Within the soma bright fluorescent signals were present in the cell nucleus as well as in emerging axons and dendrites. The dendrites often showed spines along their axes. However, very strong fluorescent signals were particularly detected in isolated beaded structures in close proximity to the cell that were likely to originate from the axonal compartment of the infected cell itself. This was not observed in cells expressing recombinant eGFP alone (C.Tigaret, personal communication; data not shown). These signals were therefore interpreted as presynaptic boutons, in which some accumulation of the expression product SG had occurred. This would be in agreement with the described presynaptic localisation of α-synuclein (Maroteaux *et al.*, 1988). A presynapic localisation has not been previously reported for recombinant eGFP (Ehrengruber *et al.*, 1999), but was observed for expressed yellow fluorescent protein YFP (Hasbani *et al.*, 2001). However, this result can be expected for a highly expressed cytosolic protein and does not necessarily represent an accumulation of the protein in a specific compartment.

Ultimately, the observed fluorescent signals would have to be quantified in comparison to an internal control to establish a potentially targeted localisation of SG fusion protein to the presynaptic terminal. Previously, no specific accumulation of α-synuclein-eGFP in presynaptic locations was observed in primary neurons (McLean *et al.*, 2001). However, this study failed to analyse the nature of the expressed proteins in neurons. Thus, the signal necessary for a presynaptic localisation could have been lost following protein degradation, or could have been masked by adjacent protein sequences in the respective expression constructs. Consistent with this, the authors observed cellular inclusions containing α-synuclein that were not immunoreactive for GFP and did not display green fluorescence (McLean *et al.*, 2001). Although initial immunocytochemical experiments suggest that such inclusions are not found in primary neurons at 6 hours post-infection with vSG(48), further studies will be needed to clarify the described findings (data not shown).

4.3.4 Future work – viral expression of α-synuclein

Future work involves a more detailed study of the subcellular localisation of recombinant α-synuclein in hippocampal neurons. The accumulation of α-synuclein fusion proteins in presynaptic terminals could be validated using an immunohistochemical approach, to show the colocalisation of presynaptic markers such as synaptophysin with the observed green fluorescence. Alternatively, the coexpression of RFP in bicistronic replicons or under the control of a second P_{SG} could serve as internal control for the localisation of the α-synuclein-eGFP protein. Based on these results, further studies will address the nature of the presynaptic localisation signal in α-synuclein. This could be achieved by generating truncated α-synuclein-eGFP expression constructs and testing the propensity of the expressed proteins to accumulate in presynaptic locations in neurons. Further studies could involve the expression of α-synuclein fusion proteins in mouse organotypic hippocampal slices from the α-synuclein-deficient C57BL/6J substrain. The reintroduction of α-synuclein into neurons may serve as a tool to address the physiological function of the protein in living cells. This could involve morphological, pharmacological, and electrophysiological techniques on living slices.

Conclusions

The present thesis describes the discovery of a chromosomal deletion in a subpopulation of the widely used inbred mouse strain C57BL/6J. Such cryptic genetic alterations in a model that is thought to be well defined may underlie confusing results of well-executed experiments. The described substrain C57BL/6JOlaHsd-Del(6)*Snca*1Slab has a deletion of the α-synuclein locus and may be a valuable tool to obtain a better insight into the physiological function of α-synuclein and its role in synucleinopathies. So far, no downstream effects of the α-synuclein deletion were identified.

In the second part of the project, a viral expression system was established for heterologous expression of α-synuclein fusion proteins. This system is useful in the study of the subcellular localisation and of protein interactions of α-synuclein.

References

Abeliovich, A., Schmitz, Y., Farinas, I., Choi-Lundberg, D., Ho, W. H., Castillo, P. E., Shinsky, N., Verdugo, J. M., Armanini, M., Ryan, A., Hynes, M., Phillips, H., Sulzer, D., and Rosenthal, A. (2000). Mice lacking alpha-synuclein display functional deficits in the nigrostriatal dopamine system. Neuron *25*, 239-252.

Agapov, E. V., Frolov, I., Lindenbach, B. D., Pragai, B. M., Schlesinger, S., and Rice, C. M. (1998). Noncytopathic Sindbis virus RNA vectors for heterologous gene expression. Proc Natl Acad Sci U S A *95*, 12989-12994.

Akopian, A. N., and Wood, J. N. (1995). Peripheral nervous system-specific genes identified by subtractive cDNA cloning. J Biol Chem *270*, 21264-21270.

Alimova-Kost, M. V., Ninkina, N. N., Imreh, S., Gnuchev, N. V., Adu, J., Davies, A. M., and Buchman, V. L. (1999). Genomic structure and chromosomal localization of the mouse persyn gene. Genomics *56*, 224-227.

Ancolio, K., Alves da Costa, C., Ueda, K., and Checler, F. (2000). Alpha-synuclein and the Parkinson's disease-related mutant Ala53Thr-alpha-synuclein do not undergo proteasomal degradation in HEK293 and neuronal cells. Neurosci Lett *285*, 79-82.

Arima, K., Ueda, K., Sunohara, N., Arakawa, K., Hirai, S., Nakamura, M., Tonozuka-Uehara, H., and Kawai, M. (1998). NACP/alpha-synuclein immunoreactivity in fibrillary components of neuronal and oligodendroglial cytoplasmic inclusions in the pontine nuclei in multiple system atrophy. Acta Neuropathol (Berl) *96*, 439-444.

Atrazhev, A. M., and Elliott, J. F. (1996). Simplified desalting of ligation reactions immediately prior to electroporation into E. coli. Biotechniques *21*, 1024.

Baird, G. S., Zacharias, D. A., and Tsien, R. Y. (2000). Biochemistry, mutagenesis, and oligomerization of DsRed, a red fluorescent protein from coral. Proc Natl Acad Sci U S A *97*, 11984-11989.

Bandopadhyay, R., de Silva, R., Khan, N., Graham, E., Vaughan, J., Engelender, S., Ross, C., Morris, H., Morris, C., Wood, N. W., Daniel, S., and Lees, A. (2001). No pathogenic mutations in the synphilin-1 gene in Parkinson's disease. Neurosci Lett *307*, 125-127.

Barbieri, S., Hofele, K., Wiederhold, K. H., Probst, A., Mistl, C., Danner, S., Kauffmann, S., Sommer, B., Spooren, W., Tolnay, M., Bilbe, G., and van der Putten, H. (2001). Mouse models of alpha-synucleinopathy and Lewy pathology. Alpha-synuclein expression in transgenic mice. Adv Exp Med Biol *487*, 147-167.

Bayer, T. A., Jakala, P., Hartmann, T., Egensperger, R., Buslei, R., Falkai, P., and Beyreuther, K. (1999a). Neural expression profile of alpha-synuclein in developing human cortex. Neuroreport *10*, 2799-2803.

Bayer, T. A., Jakala, P., Hartmann, T., Havas, L., McLean, C., Culvenor, J. G., Li, Q. X., Masters, C. L., Falkai, P., and Beyreuther, K. (1999b). Alpha-synuclein accumulates in Lewy bodies in Parkinson's disease and dementia with Lewy bodies but not in Alzheimer's disease beta-amyloid plaque cores. Neurosci Lett *266*, 213-216.

Behe, P., Stern, P., Wyllie, D. J., Nassar, M., Schoepfer, R., and Colquhoun, D. (1995). Determination of NMDA NR1 subunit copy number in recombinant NMDA receptors. Proc R Soc Lond B Biol Sci *262*, 205-213.

Bennett, M. C., Bishop, J. F., Leng, Y., Chock, P. B., Chase, T. N., and Mouradian, M. M. (1999). Degradation of alpha-synuclein by proteasome. J Biol Chem *274*, 33855-33858.

Birnboim, H. C., and Doly, J. (1979). A rapid alkaline procedure for screening recombinant plasmid DNA. Nucleic Acids Res *7*, 1513.

Bliss, T. V., and Collingridge, G. L. (1993). A synaptic model of memory: long-term potentiation in the hippocampus. Nature *361*, 31-39.

Bliss, T. V., and Lomo, T. (1973). Long-lasting potentiation of synaptic transmission in the dentate area of the anaesthetized rabbit following stimulation of the perforant path. J Physiol (Lond) *232*, 331-356.

Bourne, H. R., and Nicoll, R. (1993). Molecular machines integrate coincident synaptic signals. Cell *72 Suppl*, 65-75.

Bredenbeek, P. J., Frolov, I., Rice, C. M., and Schlesinger, S. (1993). Sindbis virus expression vectors: packaging of RNA replicons by using defective helper RNAs. J Virol *67*, 6439-6446.

Bruening, W., Giasson, B. I., Klein-Szanto, A. J., Lee, V. M., Trojanowski, J. Q., and Godwin, A. K. (2000). Synucleins are expressed in the majority of breast and ovarian carcinomas and in preneoplastic lesions of the ovary. Cancer *88*, 2154-2163.

Buchman, V. L., Adu, J., Pinon, L. G., Ninkina, N. N., and Davies, A. M. (1998a). Persyn, a member of the synuclein family, influences neurofilament network integrity. Nat Neurosci *1*, 101-103.

Buchman, V. L., Hunter, H. J., Pinon, L. G., Thompson, J., Privalova, E. M., Ninkina, N. N., and Davies, A. M. (1998b). Persyn, a member of the synuclein family, has a distinct pattern of expression in the developing nervous system. J Neurosci *18*, 9335-9341.

Burnashev, N., Schoepfer, R., Monyer, H., Ruppersberg, J. P., Gunther, W., Seeburg, P. H., and Sakmann, B. (1992). Control by asparagine residues of calcium permeability and magnesium blockade in the NMDA receptor. Science *257*, 1415-1419.

Campion, D., Martin, C., Heilig, R., Charbonnier, F., Moreau, V., Flaman, J. M., Petit, J. L., Hannequin, D., Brice, A., and Frebourg, T. (1995). The NACP/synuclein gene: chromosomal assignment and screening for alterations in Alzheimer disease. Genomics *26*, 254-257.

Chen, X., de Silva, H. A., Pettenati, M. J., Rao, P. N., St George-Hyslop, P., Roses, A. D., Xia, Y., Horsburgh, K., Ueda, K., and Saitoh, T. (1995). The human NACP/alpha-synuclein gene: chromosome assignment to 4q21.3-q22 and TaqI RFLP analysis. Genomics *26*, 425-427.

Chen, P. E., Specht, C. G., Morris, R. G. M., and Schoepfer, R. (a in preparation). Spatial learning is unimpaired in mice containing a deletion of the alpha-synuclein locus.

Chen, P. E., Errington, M. L., Kneussel, M., Annala, A. J., Rast, G. F., Specht, C. G., Rudhard, Y., Tigaret, C. M., Nassar, M. A., Morris, R. G. M., Bliss, T. V. P., and Schoepfer, R. (b in preparation). Mice with reduced levels of NR1 N598R NMDA receptors show deficits in spatial learning.

Choi, D. W. (1988). Calcium-mediated neurotoxicity: relationship to specific channel types and role in ischemic damage. Trends-Neurosci *11*, 465-469.

Choi, D. W. (1992). Excitotoxic cell death. J-Neurobiol *23*, 1261-1276.

Chomczynski, P., and Sacchi, N. (1987). Single-step method of RNA isolation by acid guanidinium thiocyanate-phenol-chloroform extraction. Anal Biochem *162*, 156-159.

Chung, K. K., Zhang, Y., Lim, K. L., Tanaka, Y., Huang, H., Gao, J., Ross, C. A., Dawson, V. L., and Dawson, T. M. (2001). Parkin ubiquitinates the alpha-synuclein-interacting protein, synphilin-1: implications for Lewy-body formation in Parkinson disease. Nat Med *7*, 1144-1150.

Ciabarra, A. M., Sullivan, J. M., Gahn, L. G., Pecht, G., Heinemann, S., and Sevarino, K. A. (1995). Cloning and characterization of chi-1: a developmentally regulated member of a novel class of the ionotropic glutamate receptor family. J Neurosci *15*, 6498-6508.

Clayton, D. F., and George, J. M. (1999). Synucleins in synaptic plasticity and neurodegenerative disorders. J Neurosci Res *58*, 120-129.

Colantuoni, C., Purcell, A. E., Bouton, C. M., and Pevsner, J. (2000). High throughput analysis of gene expression in the human brain. J Neurosci Res *59*, 1-10.

Cole, R. N., and Hart, G. W. (2001). Cytosolic O-glycosylation is abundant in nerve terminals. J Neurochem *79*, 1080-1089.

Cole, A. J., Saffen, D. W., Baraban, J. M., and Worley, P. F. (1989). Rapid increase of an immediate early gene messenger RNA in hippocampal neurons by synaptic NMDA receptor activation. Nature *340*, 474-476.

Colley, W. C., Sung, T. C., Roll, R., Jenco, J., Hammond, S. M., Altshuller, Y., Bar-Sagi, D., Morris, A. J., and Frohman, M. A. (1997). Phospholipase D2, a distinct phospholipase D isoform with novel regulatory properties that provokes cytoskeletal reorganization. Curr Biol *7*, 191-201.

Conway, K. A., Harper, J. D., and Lansbury, P. T. (1998). Accelerated in vitro fibril formation by a mutant alpha-synuclein linked to early-onset Parkinson disease. Nat Med *4*, 1318-1320.

Conway, K. A., Lee, S. J., Rochet, J. C., Ding, T. T., Williamson, R. E., and Lansbury, P. T., Jr. (2000). Acceleration of oligomerization, not fibrillization, is a shared property of both alpha-synuclein mutations linked to early-onset Parkinson's disease: implications for pathogenesis and therapy. Proc Natl Acad Sci U S A *97*, 571-576.

Conway, K. A., Rochet, J. C., Bieganski, R. M., and Lansbury Jr, P. T. (2001). Kinetic stabilization of the alpha-synuclein protofibril by a dopamine-alpha-synuclein adduct. Science *294*, 1346-1349.

Culvenor, J. G., McLean, C. A., Cutt, S., Campbell, B. C., Maher, F., Jakala, P., Hartmann, T., Beyreuther, K., Masters, C. L., and Li, Q. X. (1999). Non-Abeta component of Alzheimer's disease amyloid (NAC) revisited. NAC and alpha-synuclein are not associated with Abeta amyloid. Am J Pathol *155*, 1173-1181.

Curras, M. C., and Pallotta, B. S. (1996). Single-channel evidence for glycine and NMDA requirement in NMDA receptor activation. Brain Res *740*, 27-40.

Davidson, W. S., Jonas, A., Clayton, D. F., and George, J. M. (1998). Stabilization of alpha-synuclein secondary structure upon binding to synthetic membranes. J Biol Chem *273*, 9443-9449.

Davis, S., and Laroche, S. (1998). A molecular biological approach to synaptic plasticity and learning. C R Acad Sci III *321*, 97-107.

Dingledine, R., Borges, K., Bowie, D., and Traynelis, S. F. (1999). The glutamate receptor ion channels. Pharmacol Rev *51*, 7-61.

Dower, W. J., Miller, J. F., and Ragsdale, C. W. (1988). High efficiency transformation of E.coli by high voltage electroporation. Nucleic Acids Res *16*, 6127-6145.

Duda, J. E., Lee, V. M., and Trojanowski, J. Q. (2000). Neuropathology of synuclein aggregates: new insights into mechanisms of neurodegenerative diseases. J Neurosci Res *61*, 121-127.

Ehlers, M. D., Zhang, S., Bernhadt, J. P., and Huganir, R. L. (1996). Inactivation of NMDA receptors by direct interaction of calmodulin with the NR1 subunit. Cell *84*, 745-755.

Ehrengruber, M. U., Lundstrom, K., Schweitzer, C., Heuss, C., Schlesinger, S., and Gahwiler, B. H. (1999). Recombinant Semliki Forest virus and Sindbis virus efficiently infect neurons in hippocampal slice cultures. Proc Natl Acad Sci U S A *96*, 7041-7046.

Ellis, C. E., Schwartzberg, P. L., Grider, T. L., Fink, D. W., and Nussbaum, R. L. (2001). Alpha-synuclein is phosphorylated by members of the Src family of protein-tyrosine kinases. J Biol Chem *276*, 3879-3884.

Engelender, S., Kaminsky, Z., Guo, X., Sharp, A. H., Amaravi, R. K., Kleiderlein, J. J., Margolis, R. L., Troncoso, J. C., Lanahan, A. A., Worley, P. F., Dawson, V. L., Dawson, T. M., and Ross, C. A. (1999). Synphilin-1 associates with alpha-synuclein and promotes the formation of cytosolic inclusions. Nat Genet *22*, 110-114.

Engelender, S., Wanner, T., Kleiderlein, J. J., Wakabayashi, K., Tsuji, S., Takahashi, H., Ashworth, R., Margolis, R. L., and Ross, C. A. (2000). Organization of the human synphilin-1 gene, a candidate for Parkinson's disease. Mamm Genome *11*, 763-766.

Engert, F., and Bonhoeffer, T. (1999). Dendritic spine changes associated with hippocampal long-term synaptic plasticity. Nature *399*, 66-70.

Farrer, M., Destee, A., Levecque, C., Singleton, A., Engelender, S., Becquet, E., Mouroux, V., Richard, F., Defebvre, L., Crook, R., Hernandez, D., Ross, C. A., Hardy, J., Amouyel, P., and Chartier-Harlin, M. C. (2001). Genetic analysis of synphilin-1 in familial Parkinson's disease. Neurobiol Dis *8*, 317-323.

Feany, M. B., and Bender, W. W. (2000). A Drosophila model of Parkinson's disease. Nature *404*, 394-398.

Flint, S. J., Enquist, L. W., Krug, R. M., Racaniello, V. R., and Skalka, A. M. (2000). Principles of virology : molecular biology, pathogenesis, and control (Washington, D.C.: ASM Press).

Forrest, D., Yuzaki, M., Soares, H. D., Ng, L., Luk, D. C., Sheng, M., Stewart, C. L., Morgan, J. I., Connor, J. A., and Curran, T. (1994). Targetted disruption of NMDA receptor 1 gene abolishes NMDA response and results in neonatal death. Neuron *13*, 325-338.

Frolov, I., Hoffman, T. A., Pragai, B. M., Dryga, S. A., Huang, H. V., Schlesinger, S., and Rice, C. M. (1996). Alphavirus-based expression vectors: strategies and applications. Proc Natl Acad Sci U S A *93*, 11371-11377.

Galvin, J. E., Uryu, K., Lee, V. M., and Trojanowski, J. Q. (1999). Axon pathology in Parkinson's disease and Lewy body dementia hippocampus contains alpha-, beta-, and gamma-synuclein. Proc Natl Acad Sci U S A *96*, 13450-13455.

Galvin, J. E., Schuck, T. M., Lee, V. M., and Trojanowski, J. Q. (2001). Differential expression and distribution of alpha-, beta-, and gamma-synuclein in the developing human substantia nigra. Exp Neurol *168*, 347-355.

Geigenmuller-Gnirke, U., Weiss, B., Wright, R., and Schlesinger, S. (1991). Complementation between Sindbis viral RNAs produces infectious particles with a bipartite genome. Proc Natl Acad Sci U S A *88*, 3253-3257.

George, J. M., Jin, H., Woods, W. S., and Clayton, D. F. (1995). Characterization of a novel protein regulated during the critical period for song learning in the zebra finch. Neuron *15*, 361-372.

Ghee, M., Fournier, A., and Mallet, J. (2000). Rat alpha-synuclein interacts with Tat binding protein 1, a component of the 26S proteasomal complex. J Neurochem *75*, 2221-2224.

Giasson, B. I., Uryu, K., Trojanowski, J. Q., and Lee, V. M. (1999). Mutant and wild type human alpha-synucleins assemble into elongated filaments with distinct morphologies in vitro. J Biol Chem *274*, 7619-7622.

Giasson, B. I., Duda, J. E., Forman, M. S., Lee, V. M., and Trojanowski, J. Q. (2001a). Prominent perikaryal expression of alpha- and beta-synuclein in neurons of dorsal root ganglion and in medullary neurons. Exp Neurol *172*, 354-362.

Giasson, B. I., Murray, I. V., Trojanowski, J. Q., and Lee, V. M. (2001b). A hydrophobic stretch of 12 amino acid residues in the middle of alpha-synuclein is essential for filament assembly. J Biol Chem *276*, 2380-2386.

Goedert, M. (2001). Alpha-synuclein and neurodegenerative diseases. Nat Rev Neurosci *2*, 492-501.

Grant, S. G., O'Dell, T. J., Karl, K. A., Stein, P. L., Soriano, P., and Kandel, E. R. (1992). Impaired long-term potentiation, spatial learning, and hippocampal development in fyn mutant mice. Science *258*, 1903-1910.

Griffin, D. E. (1998). A review of alphavirus replication in neurons. Neurosci Biobehav Rev *22*, 721-723.

Haldi, M. L., Strickland, C., Lim, P., VanBerkel, V., Chen, X., Noya, D., Korenberg, J. R., Husain, Z., Miller, J., and Lander, E. S. (1996). A comprehensive large-insert yeast artificial chromosome library for physical mapping of the mouse genome. Mamm Genome *7*, 767-769.

Han, H., Weinreb, P. H., and Lansbury, P. T., Jr. (1995). The core Alzheimer's peptide NAC forms amyloid fibrils which seed and are seeded by beta-amyloid: is NAC a common trigger or target in neurodegenerative disease? Chem Biol *2*, 163-169.

Hasbani, M. J., Schlief, M. L., Fisher, D. A., and Goldberg, M. P. (2001). Dendritic spines lost during glutamate receptor activation reemerge at original sites of synaptic contact. J Neurosci *21*, 2393-2403.

Hashimoto, M., Rockenstein, E., Mante, M., Mallory, M., and Masliah, E. (2001). Beta-synuclein inhibits alpha-synuclein aggregation. A possible role as an anti-Parkinsonian factor. Neuron *32*, 213-223.

Hebb, D. O. (1949). The organization of behavior; a neuropsychological theory (New York, Wiley).

Hicks, A., Davis, S., Rodger, J., Helme-Guizon, A., Laroche, S., and Mallet, J. (1997). Synapsin I and syntaxin 1B: key elements in the control of neurotransmitter release are regulated by neuronal activation and long-term potentiation in vivo. Neuroscience *79*, 329-340.

Hollmann, M., Boulter, J., Maron, C., Beasley, L., Sullivan, J., Pecht, G., and Heinemann, S. (1993). Zinc potentiates agonist-induced currents at certain splice variants of the NMDA receptor. Neuron *10*, 943-954.

Hong, L., Ko, H. W., Gwag, B. J., Joe, E., Lee, S., Kim, Y. T., and Suh, Y. H. (1998). The cDNA cloning and ontogeny of mouse alpha-synuclein. Neuroreport *9*, 1239-1243.

Hsu, L. J., Mallory, M., Xia, Y., Veinbergs, I., Hashimoto, M., Yoshimoto, M., Thal, L. J., Saitoh, T., and Masliah, E. (1998). Expression pattern of synucleins (non-Abeta component of Alzheimer's disease amyloid precursor protein/alpha-synuclein) during murine brain development. J Neurochem *71*, 338-344.

Huerta, P. T., Scearce, K. A., Farris, S. M., Empson, R. M., and Prusky, G. T. (1996). Preservation of spatial learning in fyn tyrosine kinase knockout mice. Neuroreport *7*, 1685-1689.

Husi, H., Ward, M. A., Choudhary, J. S., Blackstock, W. P., and Grant, S. G. (2000). Proteomic analysis of NMDA receptor-adhesion protein signaling complexes. Nat Neurosci *3*, 661-669.

Ii, K., Ito, H., Tanaka, K., and Hirano, A. (1997). Immunocytochemical co-localization of the proteasome in ubiquitinated structures in neurodegenerative diseases and the elderly. J Neuropathol Exp Neurol *56*, 125-131.

Ish-Horowitz, D., and Burke, J. F. (1981). Rapid and efficient cosmid cloning. Nucleic Acids Res *9*, 2989.

Ishii, T., Moriyoshi, K., Sugihara, H., Sakurada, K., Kadotani, H., Yokoi, M., Akazawa, C., Shigemoto, R., Mizuno, N., Masu, M., and *et al.* (1993). Molecular characterization of the family of the N-methyl-D-aspartate receptor subunits. J Biol Chem *268*, 2836-2843.

Iwai, A., Masliah, E., Yoshimoto, M., Ge, N., Flanagan, L., de Silva, H. A., Kittel, A., and Saitoh, T. (1995). The precursor protein of non-Abeta component of Alzheimer's disease amyloid is a presynaptic protein of the central nervous system. Neuron *14*, 467-475.

Iwata, A., Miura, S., Kanazawa, I., Sawada, M., and Nukina, N. (2001). Alpha-synuclein forms a complex with transcription factor Elk-1. J Neurochem *77*, 239-252.

Jackson, A. C., Moench, T. R., Griffin, D. E., and Johnson, R. T. (1987). The pathogenesis of spinal cord involvement in the encephalomyelitis of mice caused by neuroadapted Sindbis virus infection. Lab Invest *56*, 418-423.

Jakes, R., Spillantini, M. G., and Goedert, M. (1994). Identification of two distinct synucleins from human brain. FEBS Lett *345*, 27-32.

Jenco, J. M., Rawlingson, A., Daniels, B., and Morris, A. J. (1998). Regulation of phospholipase D2: selective inhibition of mammalian phospholipase D isoenzymes by alpha- and beta-synucleins. Biochemistry *37*, 4901-4909.

Jensen, P. H., Hojrup, P., Hager, H., Nielsen, M. S., Jacobsen, L., Olesen, O. F., Gliemann, J., and Jakes, R. (1997). Binding of Abeta to alpha- and beta-synucleins: identification of segments in alpha-synuclein/NAC precursor that bind Abeta and NAC. Biochem J *323*, 539-546.

Jensen, P. H., Nielsen, M. S., Jakes, R., Dotti, C. G., and Goedert, M. (1998). Binding of alpha-synuclein to brain vesicles is abolished by familial Parkinson's disease mutation. J Biol Chem *273*, 26292-26294.

Ji, H., Liu, Y. E., Jia, T., Wang, M., Liu, J., Xiao, G., Joseph, B. K., Rosen, C., and Shi, Y. E. (1997). Identification of a breast cancer-specific gene, BCSG1, by direct differential cDNA sequencing. Cancer Res *57*, 759-764.

Johnston, J. R. (1994). Molecular genetics of yeast: a practical approach (Oxford; New York: IRL Press at Oxford University Press).

Kahle, P. J., Neumann, M., Ozmen, L., Muller, V., Jacobsen, H., Schindzielorz, A., Okochi, M., Leimer, U., van Der Putten, H., Probst, A., Kremmer, E., Kretzschmar, H. A., and Haass, C. (2000). Subcellular localization of wild-type and Parkinson's disease-associated mutant alpha-synuclein in human and transgenic mouse brain. J Neurosci *20*, 6365-6373.

Kawamata, H., McLean, P. J., Sharma, N., and Hyman, B. T. (2001). Interaction of alpha-synuclein and synphilin-1: effect of Parkinson's disease-associated mutations. J Neurochem *77*, 929-934.

Kneussel, M. (1997). Ein transgenes Mausmodell mit der N598R-Mutation in der NMDAR1-Rezeptor-Untereinheit mittels "Gene Targeting". Thesis. In Fachbereich Biologie (Darmstadt: Technische Hochschule Darmstadt).

Kornau, H. C., Schenker, L. T., Kennedy, M. B., and Seeburg, P. H. (1995). Domain interaction between NMDA receptor subunits and the postsynaptic density protein PSD-95. Science *269*, 1737-1740.

Kornitzer, D., and Ciechanover, A. (2000). Modes of regulation of ubiquitin-mediated protein degradation. J Cell Physiol *182*, 1-11.

Kruger, R., Kuhn, W., Muller, T., Woitalla, D., Graeber, M., Kosel, S., Przuntek, H., Epplen, J. T., Schols, L., and Riess, O. (1998). Ala30Pro mutation in the gene encoding alpha-synuclein in Parkinson's disease. Nat Genet *18*, 106-108.

Kuzuhara, S., Mori, H., Izumiyama, N., Yoshimura, M., and Ihara, Y. (1988). Lewy bodies are ubiquitinated. A light and electron microscopic immunocytochemical study. Acta Neuropathol *75*, 345-353.

Laemmli, U. K. (1970). Cleavage of structural proteins during the assembly of the head of bacteriophage T4. Nature *227*, 680-685.

Laird, P. W., Zijderveld, A., Linders, K., Rudnicki, M. A., Jaenisch, R., and Berns, A. (1991). Simplified mammalian DNA isolation procedure. Nucleic Acids Res *19*, 4293.

Lane, D., and Harlow, E. (1988). Antibodies: a laboratory manual (Cold Spring Harbor, NY: Cold Spring Harbor Laboratory).

Lavedan, C. (1998). The synuclein family. Genome Res *8*, 871-880.

Lavedan, C., Leroy, E., Dehejia, A., Buchholtz, S., Dutra, A., Nussbaum, R. L., and Polymeropoulos, M. H. (1998a). Identification, localization and characterization of the human gamma-synuclein gene. Hum Genet *103*, 106-112.

Lavedan, C., Leroy, E., Torres, R., Dehejia, A., Dutra, A., Buchholtz, S., Nussbaum, R. L., and Polymeropoulos, M. H. (1998b). Genomic organization and expression of the human beta-synuclein gene (SNCB). Genomics *54*, 173-175.

Lee, F. J., Liu, F., Pristupa, Z. B., and Niznik, H. B. (2001). Direct binding and functional coupling of alpha-synuclein to the dopamine transporters accelerate dopamine-induced apoptosis. Faseb J *15*, 916-926.

Lennon, G., Auffray, C., Polymeropoulos, M., and Soares, M. B. (1996). The I.M.A.G.E. Consortium: an integrated molecular analysis of genomes and their expression. Genomics *33*, 151-152.

Liscovitch, M., Czarny, M., Fiucci, G., and Tang, X. (2000). Phospholipase D: molecular and cell biology of a novel gene family. Biochem J *345 Pt 3*, 401-415.

Lowe, J., McDermott, H., Landon, M., Mayer, R. J., and Wilkinson, K. D. (1990). Ubiquitin carboxyl-terminal hydrolase (PGP 9.5) is selectively present in ubiquitinated inclusion bodies characteristic of human neurodegenerative diseases. J Pathol *161*, 153-160.

Lu, X., and Silver, J. (2001). Transmission of replication-defective Sindbis helper vectors encoding capsid and envelope proteins. J Virol Methods *91*, 59-65.

Lustig, S., Jackson, A. C., Hahn, C. S., Griffin, D. E., Strauss, E. G., and Strauss, J. H. (1988). Molecular basis of Sindbis virus neurovirulence in mice. J Virol *62*, 2329-2336.

Lynch, G., Larson, J., Kelso, S., Barrionuevo, G., and Schottler, F. (1983). Intracellular injections of EGTA block induction of hippocampal long-term potentiation. Nature *305*, 719-721.

MacDermott, A. B., Mayer, M. L., Westbrook, G. L., Smith, S. J., and Barker, J. L. (1986). NMDA-receptor activation increases cytoplasmic calcium concentration in cultured spinal cord neurones. Nature *321*, 519-522.

Maroteaux, L., Campanelli, J. T., and Scheller, R. H. (1988). Synuclein: a neuron-specific protein localized to the nucleus and presynaptic nerve terminal. J Neurosci *8*, 2804-2815.

Masliah, E., Rockenstein, E., Veinbergs, I., Mallory, M., Hashimoto, M., Takeda, A., Sagara, Y., Sisk, A., and Mucke, L. (2000). Dopaminergic loss and inclusion body formation in alpha-synuclein mice: implications for neurodegenerative disorders. Science *287*, 1265-1269.

Masliah, E., Rockenstein, E., Veinbergs, I., Sagara, Y., Mallory, M., Hashimoto, M., and Mucke, L. (2001). Beta-amyloid peptides enhance alpha-synuclein accumulation and neuronal deficits in a transgenic mouse model linking Alzheimer's disease and Parkinson's disease. Proc Natl Acad Sci U S A *98*, 12245-12250.

Mayer, M. L., Westbrook, G. L., and Guthrie, P. B. (1984). Voltage-dependent block by Mg2+ of NMDA responses in spinal cord neurones. Nature *309*, 261-263.

McLean, P. J., Kawamata, H., and Hyman, B. T. (2001). Alpha-synuclein-enhanced green fluorescent protein fusion proteins form proteasome sensitive inclusions in primary neurons. Neuroscience *104*, 901-912.

McNaught, K. S., and Jenner, P. (2001). Proteasomal function is impaired in substantia nigra in Parkinson's disease. Neurosci Lett *297*, 191-194.

Mohn, A. R., Gainetdinov, R. R., Caron, M. G., and Koller, B. H. (1999). Mice with reduced NMDA receptor expression display behaviors related to schizophrenia. Cell *98*, 427-436.

Monyer, H., Sprengel, R., Schoepfer, R., Herb, A., Higuchi, M., Lomeli, H., Burnashev, N., Sakmann, B., and Seeburg, P. H. (1992). Heteromeric NMDA receptors: molecular and functional distinction of subtypes. Science *256*, 1217-1221.

Monyer, H., Burnashev, N., Laurie, D. J., Sakmann, B., and Seeburg, P. H. (1994). Developmental and regional expression in the rat brain and functional properties of four NMDA receptors. Neuron *12*, 529-540.

Moriyoshi, K., Masu, M., Ishii, T., Shigemoto, R., Mizuno, N., and Nakanishi, S. (1991). Molecular cloning and characterization of the rat NMDA receptor. Nature *354*, 31-37.

Morris, R. (1984). Developments of a water-maze procedure for studying spatial learning in the rat. J Neurosci Methods *11*, 47-60.

Morris, R. G., Anderson, E., Lynch, G. S., and Baudry, M. (1986). Selective impairment of learning and blockade of long-term potentiation by an N-methyl-D-aspartate receptor antagonist, AP5. Nature *319*, 774-776.

Murphy, D. D., Rueter, S. M., Trojanowski, J. Q., and Lee, V. M. (2000). Synucleins are developmentally expressed, and alpha-synuclein regulates the size of the presynaptic vesicular pool in primary hippocampal neurons. J Neurosci *20*, 3214-3220.

Nagano, Y., Yamashita, H., Nakamura, T., Takahashi, T., Kondo, E., and Nakamura, S. (2001). Lack of binding observed between human alpha-synuclein and Bcl-2 protein family. Neurosci Lett *316*, 103-107.

Nakajo, S., Omata, K., Aiuchi, T., Shibayama, T., Okahashi, I., Ochiai, H., Nakai, Y., Nakaya, K., and Nakamura, Y. (1990). Purification and characterization of a novel brain-specific 14-kDa protein. J Neurochem *55*, 2031-2038.

Nakajo, S., Tsukada, K., Omata, K., Nakamura, Y., and Nakaya, K. (1993). A new brain-specific 14-kDa protein is a phosphoprotein. Its complete amino acid sequence and evidence for phosphorylation. Eur J Biochem *217*, 1057-1063.

Nakamura, T., Yamashita, H., Takahashi, T., and Nakamura, S. (2001). Activated Fyn phosphorylates alpha-synuclein at tyrosine residue 125. Biochem Biophys Res Commun *280*, 1085-1092.

Narayanan, V., and Scarlata, S. (2001). Membrane binding and self-association of alpha-synucleins. Biochemistry *40*, 9927-9934.

Narhi, L., Wood, S. J., Steavenson, S., Jiang, Y., Wu, G. M., Anafi, D., Kaufman, S. A., Martin, F., Sitney, K., Denis, P., Louis, J. C., Wypych, J., Biere, A. L., and Citron, M. (1999). Both familial Parkinson's disease mutations accelerate alpha-synuclein aggregation. J Biol Chem *274*, 9843-9846.

Nayak, A., Zastrow, D. J., Lickteig, R., Zahniser, N. R., and Browning, M. D. (1998). Maintenance of late-phase LTP is accompanied by PKA-dependent increase in AMPA receptor synthesis. Nature *394*, 680-683.

Nielsen, M. S., Vorum, H., Lindersson, E., and Jensen, P. H. (2001). Ca2+ binding to alpha-synuclein regulates ligand binding and oligomerization. J Biol Chem *276*, 22680-22684.

Ninkina, N. N., Alimova-Kost, M. V., Paterson, J. W., Delaney, L., Cohen, B. B., Imreh, S., Gnuchev, N. V., Davies, A. M., and Buchman, V. L. (1998). Organization, expression and polymorphism of the human persyn gene. Hum Mol Genet *7*, 1417-1424.

Nishi, M., Hinds, H., Lu, H. P., Kawata, M., and Hayashi, Y. (2001). Motoneuron-specific expression of NR3B, a novel NMDA-type glutamate receptor subunit that works in a dominant-negative manner. J Neurosci *21*, RC185.

Nowak, L., Bregestovski, P., Ascher, P., Herbet, A., and Prochiantz, A. (1984). Magnesium gates glutamate-activated channels in mouse central neurones. Nature *307*, 462-465.

Okochi, M., Walter, J., Koyama, A., Nakajo, S., Baba, M., Iwatsubo, T., Meijer, L., Kahle, P. J., and Haass, C. (2000). Constitutive phosphorylation of the Parkinson's disease associated alpha-synuclein. J Biol Chem *275*, 390-397.

Ostrerova, N., Petrucelli, L., Farrer, M., Mehta, N., Choi, P., Hardy, J., and Wolozin, B. (1999). Alpha-synuclein shares physical and functional homology with 14-3-3 proteins. J Neurosci *19*, 5782-5791.

Paik, S. R., Lee, J. H., Kim, D. H., Chang, C. S., and Kim, J. (1997). Aluminum-induced structural alterations of the precursor of the non-Abeta component of Alzheimer's disease amyloid. Arch Biochem Biophys *344*, 325-334.

Paupard, M. C., Friedman, L. K., and Zukin, R. S. (1997). Developmental regulation and cell-specific expression of N-methyl-D-aspartate receptor splice variants in rat hippocampus. Neuroscience *79*, 399-409.

Pendleton, R. G., Parvez, F., Sayed, M., and Hillman, R. (2002). Effects of pharmacological agents upon a transgenic model of Parkinson's disease in Drosophila melanogaster. J Pharmacol Exp Ther *300*, 91-96.

Perrin, R. J., Woods, W. S., Clayton, D. F., and George, J. M. (2000). Interaction of human alpha-synuclein and Parkinson's disease variants with phospholipids. Structural analysis using site-directed mutagenesis. J Biol Chem *275*, 34393-34398.

Petersen, K., Olesen, O. F., and Mikkelsen, J. D. (1999). Developmental expression of alpha-synuclein in rat hippocampus and cerebral cortex. Neuroscience *91*, 651-659.

Polo, J. M., Belli, B. A., Driver, D. A., Frolov, I., Sherrill, S., Hariharan, M. J., Townsend, K., Perri, S., Mento, S. J., Jolly, D. J., Chang, S. M., Schlesinger, S., and Dubensky, T. W., Jr. (1999). Stable alphavirus packaging cell lines for Sindbis virus and Semliki Forest virus-derived vectors. Proc Natl Acad Sci U S A *96*, 4598-4603.

Polymeropoulos, M. H., Lavedan, C., Leroy, E., Ide, S. E., Dehejia, A., Dutra, A., Pike, B., Root, H., Rubenstein, J., Boyer, R., Stenroos, E. S., Chandrasekharappa, S., Athanassiadou, A., Papapetropoulos, T., Johnson, W. G., Lazzarini, A. M., Duvoisin, R. C., Di Iorio, G., Golbe, L. I., and Nussbaum, R. L. (1997). Mutation in the alpha-synuclein gene identified in families with Parkinson's disease. Science *276*, 2045-2047.

Pronin, A. N., Morris, A. J., Surguchov, A., and Benovic, J. L. (2000). Synucleins are a novel class of substrates for G protein-coupled receptor kinases. J Biol Chem *275*, 26515-26522.

Rathke-Hartlieb, S., Kahle, P. J., Neumann, M., Ozmen, L., Haid, S., Okochi, M., Haass, C., and Schulz, J. B. (2001). Sensitivity to MPTP is not increased in Parkinson's disease-associated mutant alpha-synuclein transgenic mice. J Neurochem *77*, 1181-1184.

Rideout, H. J., Larsen, K. E., Sulzer, D., and Stefanis, L. (2001). Proteasomal inhibition leads to formation of ubiquitin/alpha-synuclein-immunoreactive inclusions in PC12 cells. J Neurochem *78*, 899-908.

Rochet, J. C., Conway, K. A., and Lansbury, P. T., Jr. (2000). Inhibition of fibrillization and accumulation of prefibrillar oligomers in mixtures of human and mouse alpha-synuclein. Biochemistry *39*, 10619-10626.

Rudhard, Y., Kneussel, M., Nassar, M. A., Rast, G. F., Annala, A. J., Chen, P. E., Tigaret, C. M., Dean, I., Roes, J., Gibb, A. J., Hunt, S. P., and Schoepfer, R. (in preparation). Coincidence detection by NMDA-receptors is required for whisker-related pattern formation in brainstem of newborn mice.

Sambrook, J., Fritsch, E. F., and Maniatis, T. (1989). Molecular Cloning: A laboratory manual, 2nd Edition (Cold Spring Harbor, NY: Cold Spring Harbor Laboratory Press).

Sandberg, R., Yasuda, R., Pankratz, D. G., Carter, T. A., Del Rio, J. A., Wodicka, L., Mayford, M., Lockhart, D. J., and Barlow, C. (2000). Regional and strain-specific gene expression mapping in the adult mouse brain. Proc Natl Acad Sci U S A *97*, 11038-11043.

Sanes, J. R., and Lichtman, J. W. (1999). Can molecules explain long-term potentiation? Nat Neurosci *2*, 597-604.

Sastry, B. R., Goh, J. W., and Auyeung, A. (1986). Associative induction of posttetanic and long-term potentiation in CA1 neurons of rat hippocampus. Science *232*, 988-990.

Schwenk, F., Baron, U., and Rajewsky, K. (1995). A cre-transgenic mouse strain for the ubiquitous deletion of loxP-flanked gene segments including deletion in germ cells. Nucleic Acids Res *23*, 5080-5081.

Segrest, J. P., Jones, M. K., De Loof, H., Brouillette, C. G., Venkatachalapathi, Y. V., and Anantharamaiah, G. M. (1992). The amphipathic helix in the exchangeable apolipoproteins: a review of secondary structure and function. J Lipid Res *33*, 141-166.

Serpell, L. C., Berriman, J., Jakes, R., Goedert, M., and Crowther, R. A. (2000). Fiber diffraction of synthetic alpha-synuclein filaments shows amyloid-like cross-beta conformation. Proc Natl Acad Sci U S A *97*, 4897-4902.

Sheng, M., Cummings, J., Roldan, L. A., Jan, Y. N., and Jan, L. Y. (1994). Changing subunit composition of heteromeric NMDA receptors during development of rat cortex. Nature *368*, 144-147.

Shibasaki, Y., Baillie, D. A., St Clair, D., and Brookes, A. J. (1995). High-resolution mapping of SNCA encoding alpha-synuclein, the non-Abeta component of Alzheimer's disease amyloid precursor, to human chromosome 4q21.3-->q22 by fluorescence in situ hybridization. Cytogenet Cell Genet *71*, 54-55.

Shibayama-Imazu, T., Okahashi, I., Omata, K., Nakajo, S., Ochiai, H., Nakai, Y., Hama, T., Nakamura, Y., and Nakaya, K. (1993). Cell and tissue distribution and developmental change of neuron specific 14 kDa protein (phosphoneuroprotein 14). Brain Res *622*, 17-25.

Shimura, H., Hattori, N., Kubo, S., Yoshikawa, M., Kitada, T., Matsumine, H., Asakawa, S., Minoshima, S., Yamamura, Y., Shimizu, N., and Mizuno, Y. (1999). Immunohistochemical and subcellular localization of Parkin protein: absence of protein in autosomal recessive juvenile parkinsonism patients. Ann Neurol *45*, 668-672.

Single, F. N., Rozov, A., Burnashev, N., Zimmermann, F., Hanley, D. F., Forrest, D., Curran, T., Jensen, V., Hvalby, O., Sprengel, R., and Seeburg, P. H. (2000). Dysfunctions in mice by NMDA receptor point mutations NR1(N598Q) and NR1(N598R). J Neurosci *20*, 2558-2566.

Smerdou, C., and Liljestrom, P. (1999). Two-helper RNA system for production of recombinant Semliki forest virus particles. J Virol *73*, 1092-1098.

Sopher, B. L., Koszdin, K. L., McClain, M. E., Myrick, S. B., Martinez, R. A., Smith, A. C., and La Spada, A. R. (2001). Genomic organization, chromosome location, and expression analysis of mouse beta-synuclein, a candidate for involvement in neurodegeneration. Cytogenet Cell Genet *93*, 117-123.

Souza, J. M., Giasson, B. I., Lee, V. M., and Ischiropoulos, H. (2000). Chaperone-like activity of synucleins. FEBS Lett *474*, 116-119.

Specht, C. G., and Schoepfer, R. (2001). Deletion of the alpha-synuclein locus in a subpopulation of C57BL/6J inbred mice. BMC Neurosci *2*, 11.

Spencer, F., Ketner, G., Connelly, C., and Hieter, P. (1993). Targeted recombination-based cloning and manipulation of large DNA segments in yeast. Methods: A companion to Methods in Enzymology *5*, 161-175.

Spillantini, M. G., Divane, A., and Goedert, M. (1995). Assignment of human alpha-synuclein (SNCA) and beta-synuclein (SNCB) genes to chromosomes 4q21 and 5q35. Genomics *27*, 379-381.

Spillantini, M. G., Schmidt, M. L., Lee, V. M., Trojanowski, J. Q., Jakes, R., and Goedert, M. (1997). Alpha-synuclein in Lewy bodies. Nature *388*, 839-840.

Spillantini, M. G., Crowther, R. A., Jakes, R., Cairns, N. J., Lantos, P. L., and Goedert, M. (1998a). Filamentous alpha-synuclein inclusions link multiple system atrophy with Parkinson's disease and dementia with Lewy bodies. Neurosci Lett *251*, 205-208.

Spillantini, M. G., Crowther, R. A., Jakes, R., Hasegawa, M., and Goedert, M. (1998b). Alpha-synuclein in filamentous inclusions of Lewy bodies from Parkinson's disease and dementia with lewy bodies. Proc Natl Acad Sci U S A *95*, 6469-6473.

Stoppini, L., Buchs, P. A., and Muller, D. (1991). A simple method for organotypic cultures of nervous tissue. J Neurosci Methods *37*, 173-182.

Sucher, N. J., Akbarian, S., Chi, C. L., Leclerc, C. L., Awobuluyi, M., Deitcher, D. L., Wu, M. K., Yuan, J. P., Jones, E. G., and Lipton, S. A. (1995). Developmental and regional expression pattern of a novel NMDA receptor-like subunit (NMDAR-L) in the rodent brain. J Neurosci *15*, 6509-6520.

Suzuki, T., and Okumura-Noji, K. (1995). NMDA receptor subunits epsilon 1 (NR2A) and epsilon 2 (NR2B) are substrates for Fyn in the postsynaptic density fraction isolated from the rat brain. Biochem Biophys Res Commun *216*, 582-588.

Takai, Y., Sasaki, T., and Matozaki, T. (2001). Small GTP-binding proteins. Physiol Rev *81*, 153-208.

Thomas, K. L., Davis, S., Laroche, S., and Hunt, S. P. (1994). Regulation of the expression of NR1 NMDA glutamate receptor subunits during hippocampal LTP. Neuroreport *6*, 119-123.

Tobe, T., Nakajo, S., Tanaka, A., Mitoya, A., Omata, K., Nakaya, K., Tomita, M., and Nakamura, Y. (1992). Cloning and characterization of the cDNA encoding a novel brain-specific 14-kDa protein. J Neurochem *59*, 1624-1629.

Tofaris, G. K., Layfield, R., and Spillantini, M. G. (2001). Alpha-synuclein metabolism and aggregation is linked to ubiquitin-independent degradation by the proteasome. FEBS Lett *509*, 22-26.

Touchman, J. W., Dehejia, A., Chiba-Falek, O., Cabin, D. E., Schwartz, J. R., Orrison, B. M., Polymeropoulos, M. H., and Nussbaum, R. L. (2001). Human and mouse alpha-synuclein genes: comparative genomic sequence analysis and identification of a novel gene regulatory element. Genome Res *11*, 78-86.

Tsien, J. Z., Huerta, P. T., and Tonegawa, S. (1996). The essential role of hippocampal CA1 NMDA receptor-dependent synaptic plasticity in spatial memory. Cell *87*, 1327-1338.

Ueda, K., Fukushima, H., Masliah, E., Xia, Y., Iwai, A., Yoshimoto, M., Otero, D. A., Kondo, J., Ihara, Y., and Saitoh, T. (1993). Molecular cloning of cDNA encoding an unrecognized component of amyloid in Alzheimer disease. Proc Natl Acad Sci U S A *90*, 11282-11286.

Ueda, K., Saitoh, T., and Mori, H. (1994). Tissue-dependent alternative splicing of mRNA for NACP, the precursor of non-Abeta component of Alzheimer's disease amyloid. Biochem Biophys Res Commun *205*, 1366-1372.

van der Putten, H., Wiederhold, K. H., Probst, A., Barbieri, S., Mistl, C., Danner, S., Kauffmann, S., Hofele, K., Spooren, W. P., Ruegg, M. A., Lin, S., Caroni, P., Sommer, B., Tolnay, M., and Bilbe, G. (2000). Neuropathology in mice expressing human alpha-synuclein. J Neurosci *20*, 6021-6029.

Volles, M. J., Lee, S. J., Rochet, J. C., Shtilerman, M. D., Ding, T. T., Kessler, J. C., and Lansbury, P. T., Jr. (2001). Vesicle permeabilization by protofibrillar alpha-synuclein: implications for the pathogenesis and treatment of Parkinson's disease. Biochemistry *40*, 7812-7819.

Wakabayashi, K., Matsumoto, K., Takayama, K., Yoshimoto, M., and Takahashi, H. (1997). NACP, a presynaptic protein, immunoreactivity in Lewy bodies in Parkinson's disease. Neurosci Lett *239*, 45-48.

Wakabayashi, K., Hayashi, S., Kakita, A., Yamada, M., Toyoshima, Y., Yoshimoto, M., and Takahashi, H. (1998). Accumulation of alpha-synuclein/NACP is a cytopathological feature common to Lewy body disease and multiple system atrophy. Acta Neuropathol (Berl) *96*, 445-452.

Wakabayashi, K., Engelender, S., Yoshimoto, M., Tsuji, S., Ross, C. A., and Takahashi, H. (2000). Synphilin-1 is present in Lewy bodies in Parkinson's disease. Ann Neurol *47*, 521-523.

Weinreb, P. H., Zhen, W., Poon, A. W., Conway, K. A., and Lansbury, P. T., Jr. (1996). NACP, a protein implicated in Alzheimer's disease and learning, is natively unfolded. Biochemistry *35*, 13709-13715.

Weiss, B. G., and Schlesinger, S. (1991). Recombination between Sindbis virus RNAs. J Virol *65*, 4017-4025.

Williams, J. H., Errington, M. L., Lynch, M. A., and Bliss, T. V. (1989). Arachidonic acid induces a long-term activity-dependent enhancement of synaptic transmission in the hippocampus. Nature *341*, 739-742.

Wirths, O., Weickert, S., Majtenyi, K., Havas, L., Kahle, P. J., Okochi, M., Haass, C., Multhaup, G., Beyreuther, K., and Bayer, T. A. (2000). Lewy body variant of Alzheimer's disease: alpha-synuclein in dystrophic neurites of Abeta plaques. Neuroreport *11*, 3737-3741.

Withers, G. S., George, J. M., Banker, G. A., and Clayton, D. F. (1997). Delayed localization of synelfin (synuclein, NACP) to presynaptic terminals in cultured rat hippocampal neurons. Brain Res Dev Brain Res *99*, 87-94.

Wo, Z. G., and Oswald, R. E. (1995). Unravelling the modular design of glutamate-gated ion channels. Trends in Neurosciences. *18*, 161-168.

Wyszynski, M., Lin, J., Rao, A., Nigh, E., Beggs, A. H., Craig, A. M., and Sheng, M. (1997). Competitive binding of alpha-actinin and calmodulin to the NMDA receptor. Nature *385*, 439-442.

Yagi, T. (1999). Molecular mechanisms of Fyn-tyrosine kinase for regulating mammalian behaviors and ethanol sensitivity. Biochem Pharmacol *57*, 845-850.

Zhang, S., Ehlers, M. D., Bernhardt, J. P., Su, C. T., and Huganir, R. L. (1998). Calmodulin mediates calcium-dependent inactivation of N-methyl-D-aspartate receptors. Neuron *21*, 443-453.

Zhuo, M., Small, S. A., Kandel, E. R., and Hawkins, R. D. (1993). Nitric oxide and carbon monoxide produce activity-dependent long-term synaptic enhancement in hippocampus. Science *260*, 1946-1950.

Zuo, J., De Jager, P. L., Norman, D. J., and Heintz, N. (1995). Generation of a high-resolution genetic map and a YAC contig of the Lurcher locus on mouse chromosome 6. Genome Res *5*, 381-392.

Zuo, J., De Jager, P. L., Takahashi, K. A., Jiang, W., Linden, D. J., and Heintz, N. (1997). Neurodegeneration in Lurcher mice caused by mutation in delta2 glutamate receptor gene. Nature *388*, 769-773.

Appendix

Oligonucleotide primers

Cre-Seq1s	AGATGTTCGCGATTATCTTCTA
Cre-Seq2a	AGCTACACCAGAGACGG
Neo-Seq3a	GAAGGCGATAGAAGGCGATGCGC
Neo-Seq4s	GCTGCATACGCTTGATCCGGCTACC
GluN-Seq3a	GGCGTTGAGCTGTATCTTCC
mNR1-Seq10a	CAGGGGCATTGCTGCGGGAGTC
mNR1-Seq38s	ACCAGTCGCACAGTCCAGGCAGCT
mNR1-Seq103s	GTCCATACTCAAGTGAGTCTGCCC
mSynA-PCR1s	AACTGCAGTTCTTCAGAAGCCTAGGGAGC
mSynA-PCR2a	GCTCTAGACTGGGCACATTGGAACTGAG
mSynA-PCR7s	GAAGATCTATGGATGTGTTCATGAAAGGAC
mSynA-PCR8a	GCTCTAGATTGGGTGCAATGACATTCTTAG
mSynA-PCR9a	GGAAGATCTGCTCCGGCTTCAGGCTCATAGTCTTG
mSynA-Seq2s	AAGACTATGAGCCTGAAGCCTAAG
mSynA-Seq5a	AGTGTGAAGCCACAACAATATCC
mSynA-Seq9s	AGAAGACCAAAGAGCAAGTGACA
mSynA-Seq10a	ATCTGGTCCTTCTTGACAAAGC
mSynG-PCR4a	GGAAGATCTGCTCCGTCTTCTCCACTCTTGGCCTC
mSynG-Seq1s	GCAAACACCATGGACGTCTTC
hSynph-Seq1s	CAGTTGGAGTGCGTACGCTGGATGGT
hSynph-Seq2s	CTTCTGTGGCTTCTTCAGTTTATGC
hSynph-Seq3a	GGCTTTTCCCCAGCGTGGTTCTGCAT
hSynph-Seq10a	GCTGCCTTATTCTTTCCTTTGCTAGC
mTubA1-Seq1s	ACACCTTCTTCAGTGAGACAGG
mTubA1-Seq2a	CTCATTGTCTACCATGAAGGCAC

Genomic markers (PCR primer pairs)

Abcg2	CAGGTAGGCAATTGTGAGGA; TGATAAATCAGGGCATCGAA
Atoh1	CTGCAGGCGAGAGACCTTC; TCAGCTTGCACAGCTGTTC
Atoh2	TACTGCAGTGCATATGAATC; TCGTAAGGGAAGTGGCTGTC
Grid2	GGCACAGGGCTCCTAATGGG; CCAGATTGAGCCCCAGAGTGG
Snca (PCR a)	TCAGACAGCTGACAGAAAGTCC; AATGTCTTCTAGTCAGGGTCC
Snca (PCR b)	TGCAGCCTCTATGTCTACTTC; GAGTAATCTGAATGCGTTATATTC
Snca (PCR c)	AGCCCTTGAGAAGTGCAGTC; AAGTATACTTGCATCTTACAATC
Snca (PCR d)	ACAAGGATGGCAGTAGATATC; TGAAGACCCTCAAGTAATACTC
D6Mit120	ATCAGTCATTTCTACTTTCAATCCTAA; CATGATTAAGTTCACTCCTATGTGTG
D6Mit122	GACACCCAGCATCCATCTTT; TTGTAATTTTTAAAAGATAGGTGTGTG
D6Mit299	TCATGAATATCAAAGACACACATCC; AAGCACATGCATTAGTATTTCCC
D6Mit357	TACAATGGCTCTCCTCCCTG; CCTCAGGATTTAAATAAATTCAAGC
32.MMHAP36PLC5.seq	TGGTCATTGATGAAAACACATTT; TTGACCTAATAGCTGGCATGTG

Expression constructs and recombinant protein sequences

Recombinant expression contructs are based on the pSinRep5 plasmid (Invitrogen; Bredenbeek *et al.*, 1993). The sequences are shown between the two cloning sites *Xba* I and *Not* I (in bold; TCTAGA and GCGGCCGC, respectively). Coding sequences are shown in upper case and cDNA sequences corresponding to the linking peptides are underlined. The respective sequences of expressed fusion proteins are indicated below the cDNA sequences. Linking peptide sequences are underlined.

pSinR5-EG-aSyn construct, *Xba* I/*Not* I fragment (1638 bp)

1 75

tctagacgcgtaagcttgcttgttctttttgcagaagctcagaataaacgctcaactttgaccATGGTGAGCAAG
GGCGAGGAGCTGTTCACCGGGGTGGTGCCCATCCTGGTCGAGCTGGACGGCGACGTAAACGGCCACAAGTTCAGC
GTGTCCGGCGAGGGCGAGGGCGATGCCACCTACGGCAAGCTGACCCTGAAGTTCATCTGCACCACCGGCAAGCTG
CCCGTGCCCTGGCCCACCCTCGTGACCACCCTGACCTACGGCGTGCAGTGCTTCAGCCGCTACCCCGACCACATG
AAGCAGCACGACTTCTTCAAGTCCGCCATGCCCGAAGGCTACGTCCAGGAGCGCACCATCTTCTTCAAGGACGAC
GGCAACTACAAGACCCGCGCCGAGGTGAAGTTCGAGGGCGACACCCTGGTGAACCGCATCGAGCTGAAGGGCATC
GACTTCAAGGAGGACGGCAACATCCTGGGGCACAAGCTGGAGTACAACTACAACAGCCACAACGTCTATATCATG
GCCGACAAGCAGAAGAACGGCATCAAGGTGAACTTCAAGATCCGCCACAACATCGAGGACGGCAGCGTGCAGCTC
GCCGACCACTACCAGCAGAACACCCCCATCGGCGACGGCCCCGTGCTGCTGCCCGACAACCACTACCTGAGCACC
CAGTCCGCCCTGAGCAAAGACCCCAACGAGAAGCGCGATCACATGGTCCTGCTGGAGTTCGTGACCGCCGCCGGG
ATCACTCTCGGCATGGACGAGCTGTACAAGTCCGGACTCAGATCTATGGATGTGTTCATGAAAGGACTTTCAAAG
GCCAAGGAGGGAGTTGTGGCTGCTGCTGAGAAAACCAAGCAGGGTGTGGCAGAGGCAGCTGGAAAGACAAAAGAG
GGAGTCCTCTATGTAGGTTCCAAAACTAAGGAAGGAGTGGTTCATGGAGTGACAACAGTGGCTGAGAAGACCAAA
GAGCAAGTGACAAATGTTGGAGGAGCAGTGGTGACTGGTGTGACAGCAGTCGCTCAGAAGACAGTGGAGGGAGCT
GGGAATATAGCTGCTGCCACTGGCTTTGTCAAGAAGGACCAGATGGGCAAGGGTGAGGAGGGGTACCCACAGGAA
GGAATCCTGGAAGACATGCCTGTGGATCCTGGCAGTGAGGCTTATGAAATGCCTTCAGAGGAAGGCTACCAAGAC
TATGAGCCTGAAGCCTAAgaatgtcattgcacccaatctaggtaccatgcatgatatcctcgaggttaccgggcc
caatgatccgaccagcaaaactcgatgtacttccgaggaactgatgtgcataatgcatcaggctggtacattaga
tccccgcttaccgcgggcaatatagcaacactaaaaactcgatgtacttccgaggaagcgcagtgcataatgctg
cgcagtgttgccacataaccactatattaaccatttatctagcggacgccaaaaactcaatgtatttctgaggaa
gcgtggtgcataatgccacgcagcgtctgcataacttttattatttcttttattaatcaacaaaattttgttttt
aacatttcaaaaaaaaaaaaaaaaaaaaaaaaaaaaaaaaaaaggggaattcctcgataattaa**gcggccgc**

pSinR5-aSyn-EG construct, *Xba* I/*Not* I fragment (1622 bp)

1 75

tctagacgcgtaagcttgcttgttctttttgcagaagctcagaataaacgctcaactttgaccATGGATGTGTTC
ATGAAAGGACTTTCAAAGGCCAAGGAGGGAGTTGTGGCTGCTGCTGAGAAAACCAAGCAGGGTGTGGCAGAGGCA
GCTGGAAAGACAAAAGAGGGAGTCCTCTATGTAGGTTCCAAAACTAAGGAAGGAGTGGTTCATGGAGTGACAACA
GTGGCTGAGAAGACCAAAGAGCAAGTGACAAATGTTGGAGGAGCAGTGGTGACTGGTGTGACAGCAGTCGCTCAG
AAGACAGTGGAGGGAGCTGGGAATATAGCTGCTGCCACTGGCTTTGTCAAGAAGGACCAGATGGGCAAGGGTGAG
GAGGGGTACCCACAGGAAGGAATCCTGGAAGACATGCCTGTGGATCCTGGCAGTGAGGCTTATGAAATGCCTTCA
GAGGAAGGCTACCAAGACTATGAGCCTGAAGCCGGAGCAGATCTGCACATGGTGAGCAAGGGCGAGGAGCTGTTC
ACCGGGGTGGTGCCCATCCTGGTCGAGCTGGACGGCGACGTAAACGGCCACAAGTTCAGCGTGTCCGGCGAGGGC
GAGGGCGATGCCACCTACGGCAAGCTGACCCTGAAGTTCATCTGCACCACCGGCAAGCTGCCCGTGCCCTGGCCC
ACCCTCGTGACCACCCTGACCTACGGCGTGCAGTGCTTCAGCCGCTACCCCGACCACATGAAGCAGCACGACTTC
TTCAAGTCCGCCATGCCCGAAGGCTACGTCCAGGAGCGCACCATCTTCTTCAAGGACGACGGCAACTACAAGACC
CGCGCCGAGGTGAAGTTCGAGGGCGACACCCTGGTGAACCGCATCGAGCTGAAGGGCATCGACTTCAAGGAGGAC
GGCAACATCCTGGGGCACAAGCTGGAGTACAACTACAACAGCCACAACGTCTATATCATGGCCGACAAGCAGAAG
AACGGCATCAAGGTGAACTTCAAGATCCGCCACAACATCGAGGACGGCAGCGTGCAGCTCGCCGACCACTACCAG
CAGAACACCCCCATCGGCGACGGCCCCGTGCTGCTGCCCGACAACCACTACCTGAGCACCCAGTCCGCCCTGAGC
AAAGACCCCAACGAGAAGCGCGATCACATGGTCCTGCTGGAGTTCGTGACCGCCGCCGGGATCACTCTCGGCATG
GACGAGCTGTACAAGTAAagcggccgtaccatgcatgatatcctcgaggttaccgggcccaatgatccgaccagc

aaaactcgatgtacttccgaggaactgatgtgcataatgcatcaggctggtacattagatccccgcttaccgcgg
gcaatatagcaacactaaaaactcgatgtacttccgaggaagcgcagtgcataatgctgcgcagtgttgccacat
aaccactatattaaccatttatctagcggacgccaaaaactcaatgtatttctgaggaagcgtggtgcataatgc
cacgcagcgtctgcataacttttattatttcttttattaatcaacaaaattttgtttttaacatttcaaaaaaaa
aaaaaaaaaaaaaaaaaaaaaaaaaggggaattcctcgataattaa**gcggccgc**

pSinR5-aSyn-RFP construct, *Xba* I/*Not* I fragment (1590 bp)

1 75
tctagacgcgtaagcttgcttgttctttttgcagaagctcagaataaacgctcaactttgaccATGGATGTGTTC
ATGAAAGGACTTTCAAAGGCCAAGGAGGGAGTTGTGGCTGCTGCTGAGAAAACCAAGCAGGGTGTGGCAGAGGCA
GCTGGAAAGACAAAAGAGGGAGTCCTCTATGTAGGTTCCAAAACTAAGGAAGGAGTGGTTCATGGAGTGACAACA
GTGGCTGAGAAGACCAAAGAGCAAGTGACAAATGTTGGAGGAGCAGTGGTGACTGGTGTGACAGCAGTCGCTCAG
AAGACAGTGGAGGGAGCTGGGAATATAGCTGCTGCCACTGGCTTTGTCAAGAAGGACCAGATGGGCAAGGGTGAG
GAGGGGTACCCACAGGAAGGAATCCTGGAAGACATGCCTGTGGATCCTGGCAGTGAGGCTTATGAAATGCCTTCA
GAGGAAGGCTACCAAGACTATGAGCCTGAAGCCGGAGCAGATCCACCGGTCGCCACCATGGTGCGCTCCTCCAAG
AACGTCATCAAGGAGTTCATGCGCTTCAAGGTGCGCATGGAGGGCACCGTGAACGGCCACGAGTTCGAGATCGAG
GGCGAGGGCGAGGGCCGCCCCTACGAGGGCCACAACACCGTGAAGCTGAAGGTGACCAAGGGCGGCCCCCTGCCC
TTCGCCTGGGACATCCTGTCCCCCCAGTTCCAGTACGGCTCCAAGGTGTACGTGAAGCACCCCGCCGACATCCCC
GACTACAAGAAGCTGTCCTTCCCCGAGGGCTTCAAGTGGGAGCGCGTGATGAACTTCGAGGACGGCGGCGTGGTG
ACCGTGACCCAAGACTCCTCCCTGCAGGACGGCTGCTTCATCTACAAGGTGAAGTTCATCGGCGTGAACTTCCCC
TCCGACGGCCCCGTAATGCAGAAGAAGACCATGGGCTGGGAGGCCTCCACCGAGCGCCTGTACCCCCGCGACGGC
GTGCTGAAGGGCGAGATCCACAAGGCCCTGAAGCTGAAGGACGGCGGCCACTACCTGGTGGAGTTCAAGTCCATC
TACATGGCCAAGAAGCCCGTGCAGCTGCCCGGCTACTACTACGTGGACTCCAAGCTGGACATCACCTCCCACAAC
GAGGACTACACCATCGTGGAGCAGTACGAGCGCACCGAGGGCCGCCACCACCTGTTCCTGTAGcggccgtaccat
gcatgatatcctcgaggttaccgggcccaatgatccgaccagcaaaactcgatgtacttccgaggaactgatgtg
cataatgcatcaggctggtacattagatccccgcttaccgcgggcaatatagcaacactaaaaactcgatgtact
tccgaggaagcgcagtgcataatgctgcgcagtgttgccacataaccactatattaaccatttatctagcggacg
ccaaaaactcaatgtatttctgaggaagcgtggtgcataatgccacgcagcgtctgcataacttttattatttct
tttattaatcaacaaaattttgtttttaacatttcaaaaaaaaaaaaaaaaaaaaaaaaaaaaaaaaaaggggaa
ttcctcgataattaa**gcggccgc**

eGFP-α-synuclein fusion protein (GS; 384 residues)

1 75
MVSKGEELFTGVVPILVELDGDVNGHKFSVSGEGEGDATYGKLTLKFICTTGKLPVPWPTLVTTLTYGVQCFSRY
PDHMKQHDFFKSAMPEGYVQERTIFFKDDGNYKTRAEVKFEGDTLVNRIELKGIDFKEDGNILGHKLEYNYNSHN
VYIMADKQKNGIKVNFKIRHNIEDGSVQLADHYQQNTPIGDGPVLLPDNHYLSTQSALSKDPNEKRDHMVLLEFV
TAAGITLGMDELYKSGLRSMDVFMKGLSKAKEGVVAAAEKTKQGVAEAAGKTKEGVLYVGSKTKEGVVHGVTTVA
EKTKEQVTNVGGAVVTGVTAVAQKTVEGAGNIAAATGFVKKDQMGKGEEGYPQEGILEDMPVDPGSEAYEMPSEE
GYQDYEPEA*

α-synuclein-eGFP fusion protein (SG; 384 residues)

1 75
MDVFMKGLSKAKEGVVAAAEKTKQGVAEAAGKTKEGVLYVGSKTKEGVVHGVTTVAEKTKEQVTNVGGAVVTGVT
AVAQKTVEGAGNIAAATGFVKKDQMGKGEEGYPQEGILEDMPVDPGSEAYEMPSEEGYQDYEPEAGADLHMVSKG
EELFTGVVPILVELDGDVNGHKFSVSGEGEGDATYGKLTLKFICTTGKLPVPWPTLVTTLTYGVQCFSRYPDHMK
QHDFFKSAMPEGYVQERTIFFKDDGNYKTRAEVKFEGDTLVNRIELKGIDFKEDGNILGHKLEYNYNSHNVYIMA
DKQKNGIKVNFKIRHNIEDGSVQLADHYQQNTPIGDGPVLLPDNHYLSTQSALSKDPNEKRDHMVLLEFVTAAGI
TLGMDELYK*

α-synuclein-RFP fusion protein (SR; 374 residues)

1 75
MDVFMKGLSKAKEGVVAAAEKTKQGVAEAAGKTKEGVLYVGSKTKEGVVHGVTTVAEKTKEQVTNVGGAVVTGVT
AVAQKTVEGAGNIAAATGFVKKDQMGKGEEGYPQEGILEDMPVDPGSEAYEMPSEEGYQDYEPEAGADPPVATMV
RSSKNVIKEFMRFKVRMEGTVNGHEFEIEGEGEGRPYEGHNTVKLKVTKGGPLPFAWDILSPQFQYGSKVYVKHP
ADIPDYKKLSFPEGFKWERVMNFEDGGVVTVTQDSSLQDGCFIYKVKFIGVNFPSDGPVMQKKTMGWEASTERLY
PRDGVLKGEIHKALKLKDGGHYLVEFKSIYMAKKPVQLPGYYYVDSKLDITSHNEDYTIVEQYERTEGRHHLFL*

BMC Neuroscience

BioMed Central

Research article

Deletion of the alpha-synuclein locus in a subpopulation of C57BL/6J inbred mice

Christian G Specht and Ralf Schoepfer*

Address: Laboratory for Molecular Pharmacology, UCL, Gower Street, London WC1E 6BT, UK

E-mail: Christian G Specht - c.specht@ucl.ac.uk; Ralf Schoepfer* - r.schoepfer@ucl.ac.uk

*Corresponding author

Published: 24 August 2001

BMC Neuroscience 2001, 2:11

Received: 25 May 2001

Accepted: 24 August 2001

This article is available from: http://www.biomedcentral.com/1471-2202/2/11

Abstract

Background: The presynaptic protein α-synuclein is involved in a range of neurodegenerative diseases. Here we analyze potential compensatory mechanisms in α-synuclein null mutant mice. Furthermore, the findings reveal problems that may be associated with inbred mouse strains.

Results: Expression profiling by cDNA array technology in a transgenic mouse model revealed striking differences only in the expression level of α-synuclein. This was caused by a chromosomal deletion of the α-synuclein locus in the C57BL/6J inbred strain used for backcrossing. However, the deletion is only present in a subpopulation of C57BL/6J mice, namely animals from Harlan. No other genes are known to be affected by the deletion, which is estimated to be smaller than 2 cM. We propose to name this strain C57BL/6S. C57BL/6S animals appear phenotypically normal. They show no upregulation of β-synuclein or γ-synuclein, excluding a compensatory mechanism. Also, the expression of synphilin-1 was unaffected.

Conclusions: The C57BL/6S strain should help in the understanding of the physiological function of α-synuclein and its involvement in synucleinopathies. Also, the findings exemplify unexpected complications that may arise during the study of transgenic models or inbred strains, in particular when combined with genome wide screening techniques.

Background

The linkage of two missense mutations in the human α-synuclein gene to rare inherited forms of Parkinson's disease (PD) [1,2] has implied that the protein plays a part in neurodegenerative diseases. Subsequently, α-synuclein was shown to be the major component of Lewy bodies (LB) in PD [3,4] as well as in a range of other neurodegenerative diseases, classified as synucleinopathies [for review see [5]].

During development, mice express increasing levels of α-synuclein mRNA, peaking at postnatal day seven (P7) [6,7]. The α-synuclein protein is mainly expressed in neurons and located in the presynaptic termini [8,9]. So far, a number of animal models have been developed for the study of α-synuclein. Overexpression of wildtype or mutant α-synucleins in mice [10,11] or *Drosophila*[12] resulted in pathological and behavioral phenotypes similar to those found in PD. Homozygous α-synuclein knockout mice are viable, fertile, and have apparently normal brain morphology. Hippocampal synaptic plasticity in these mice was identical to wildtype animals as judged by LTP measurements. However, an alteration of

dopamine release in the nigrostriatal system was observed [13].

The primary protein sequence of β-synuclein [14,15] shows a high degree of identity to α-synuclein (particularly in the N-terminal region), with both sharing similar expression patterns and subcellular localization [15,16]. Thus, it can be speculated that the two proteins may have similar physiological functions. γ-synuclein [17], the third member of the synuclein family is mainly expressed in the peripheral nervous system throughout development and, at lower levels, in brain [18]. β- and γ-synuclein have also been implicated in axonal pathological processes [19].

Yeast-two-hybrid analysis with human DNA fragments has identified synphilin-1 as a specific interaction partner of α-synuclein [20]. Little is known about its function, however, it was shown to be present in most Lewy bodies in PD (but absent from α-synuclein positive Lewy neurites) [21].

Wide scale mRNA expression profiling by cDNA array technology on a transgenic mouse model led us to the discovery of a C57BL/6J substrain with a chromosomal deletion spanning the α-synuclein gene locus (*Snca*). Subsequently, we analyzed the consequences of the absence of α-synuclein on the expression levels of β- and γ-synuclein and synphilin-1.

Results

The analysis of brain mRNA expression profiles by cDNA array technology demonstrated striking differences in the expression levels of α-synuclein in an engineered mouse model (Kneussel, Annala, Schoepfer; in preparation), with arbitrary expression units of 3495 (wildtype) and 457 (transgenic). All other analyzed genes were not significantly altered in their expression (less than factor 2x; Fig. 1A). The transgenic animals used in this study had been backcrossed into the BL6JHUK strain (see methods). Since further investigation on the transgenic model led to contradictory results (data not shown), mRNA expression levels were compared between different wildtype strains used in the generation of the transgenic mice.

α-synuclein is not expressed in the BL6JHUK strain at any developmental stage

Expression of α-synuclein in brains of 129/Ola, ICR, and BL6JHUK mice was compared by Northern blot analysis. A clear difference between the strains was observed at any considered developmental time point. No signal could be detected in BL6JHUK mice, whereas the other strains expressed equal amounts of the α-synuclein transcript (Fig. 1B). Between P0 and P15 mRNA expression increased in 129/Ola and ICR mice as previously described [6,7]. Expression of α-synuclein mRNA was observed as early as on embryonic day 14 (E14; on total embryo RNA) and E17 (brain RNA) in ICR but not in BL6JHUK mice (data not shown).

Consistent with this result, no detectable expression of α-synuclein protein was observed in BL6JHUK in contrast to the 129/Ola and ICR strains (Fig. 1C). In agreement with previous studies protein levels increased during postnatal development [7], but were consistently absent from the BL6JHUK strain. At prenatal stages (using homogenates from embryo at E14 and brain at E17), α-synuclein expression was below detection levels in ICR and BL6JHUK animals (data not shown).

The BL6JHUK strain is a knockout model for α-synuclein

Although α-synuclein expression was not observed in the BL6JHUK strain the detection of low expression levels could require methods of greater sensitivity. Therefore, mRNA expression of α-synuclein was determined by semi-quantitative RT-PCR analysis (Fig. 2A). Amplification on brain total RNA of an ICR mouse at P15 with specific α-synuclein primers resulted in a detectable cDNA fragment after as few as 20 PCR cycles. However no product was detected using BL6JHUK RNA, even after 35 cycles of amplification. When BL6JHUK RNA was contaminated with low levels of ICR RNA the appearance of the α-synuclein PCR product could be observed even at a dilution factor of 10^4 after 35 cycles. This indicates that expression of α-synuclein mRNA in BL6JHUK is decreased by at least this factor compared to the ICR strain. Identical results were obtained with P8 and E14 samples (data not shown). Therefore, the α-synuclein gene locus (*Snca*) in the BL6JHUK strain must be considered a null allele.

To further elucidate the mechanism underlying this phenomenon, the presence of the *Snca* locus was analyzed. Genomic PCR experiments revealed the absence of the α-synuclein locus in BL6JHUK mice (Fig. 2B). In contrast to the ICR and 129/Ola strains, amplification of genomic DNA fragments corresponding to exon 4 and exon 6 of the α-synuclein gene yielded no PCR product in the BL6JHUK sample. PCR amplification spanning intronic α-synuclein sequences (exons 1 to 2, exons 5 to 6) yielded identical results (data not shown). Reproducibility was confirmed on a number of BL6JHUK mice (n = 8) from four batches of animals. Sequence alignment with the mouse α-synuclein chromosomal sequence (GenBank AF163865; [22]) locates the chromosome 6 genomic marker D6Mit357 to the sequence between exons 4 and 5 (data not shown). Again, this primer pair did not yield an amplification product on BL6JHUK DNA, whereas loci in close proximity to *Snca* were not deleted (Fig. 2C).

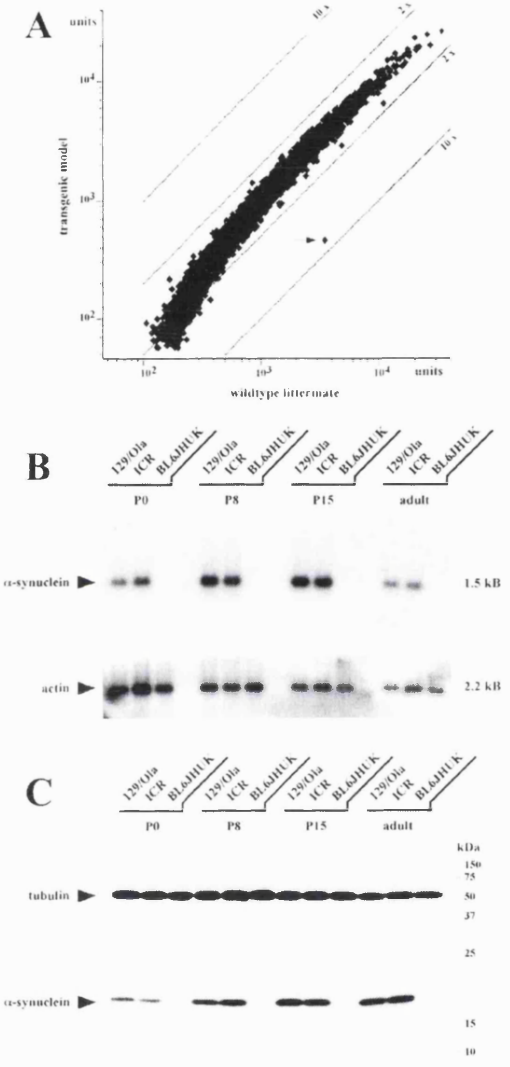

Figure 1
α-synuclein expression levels. A. cDNA array experiment using brain polyA$^+$-RNA from a transgenic mouse and a wildtype littermate at the developmental time point E18.5. From all analyzed genes (approximately 9000 ESTs), only the expression of α-synuclein (GenBank W41663) was significantly altered (indicated by an arrow; differential expression factor 7.6x). The data are represented without background substraction. Expression is quantified as units of fluorescence intensity. Diagonals indicate differential expression by 2x and 10x, respectively.**B.** Northern blot of brain polyA$^+$-RNA (500 ng per lane) from 129/Ola, ICR, and BL6JHUK mice at the developmental time points P0, P8, P15, and adult, probed with an α-synuclein 3'UTR probe. The α-synuclein transcript size is approximately 1.5 kB. RNA samples were pooled from 4 animals (at P0), or from 2 animals (at P8 and P15) from the same litter. After stripping the membrane was re-probed with an actin probe. **C.** Brain homogenate from 129/Ola, ICR, and BL6JHUK mice at P0, P8, P15, and adult age was separated by 15% SDS-PAGE (20 μg protein per lane). The Western blot membrane was simultaneously probed with the monoclonal anti α-synuclein and anti α-tubulin antibodies. Recognized protein bands have apparent molecular weights of approximately 19 kDa and 55 kDa, respectively.

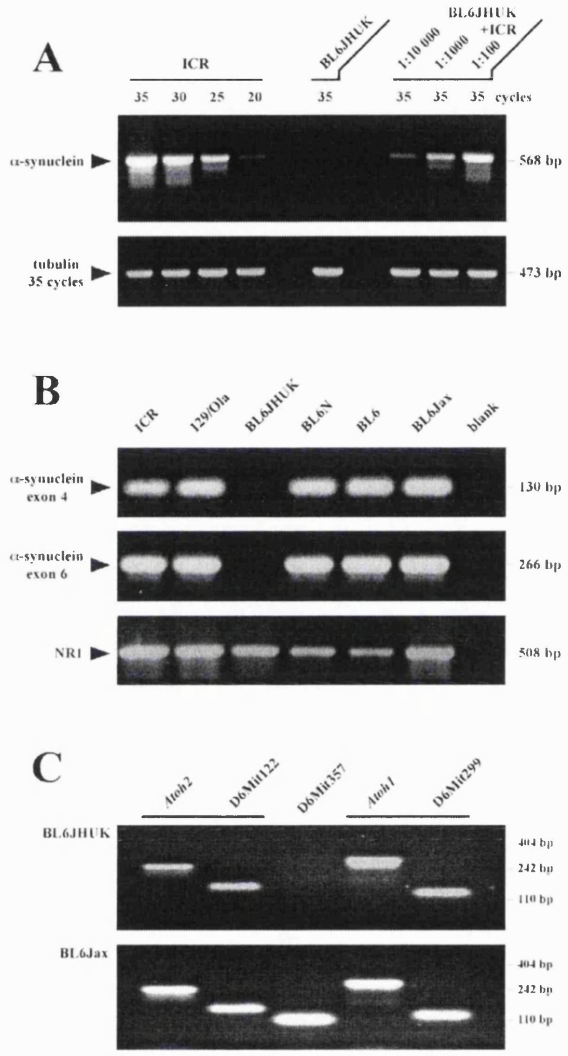

Figure 2
Deletion of the α-synuclein gene locus in the BL6JHUK strain. A. Semi-quantitative analysis of α-synuclein expression in BL6JHUK mice by RT-PCR, sized on a 1.5% agarose gel. A 568 bp α-synuclein band is detected after as few as 20 PCR cycles on brain total RNA of an ICR mouse at P15. No signal was detected in the BL6JHUK sample even after 35 cycles. However, when the BL6JHUK sample was contaminated with as little as 0.01% ICR RNA, the α-synuclein band could still be detected after 35 PCR cycles. The control shows amplification of a 473 bp tubulin fragment with constant 35 cycles. **B.** Probing for the presence of the α-synuclein gene in the ICR, 129/Ola, BL6JHUK, BL6N, BL6, and BL6Jax strains. Genomic α-synuclein DNA fragments of exon 4 and of exon 6 were amplified by PCR and the products separated on a 2% agarose gel. In a control experiment, a fragment of the NR1 gene was amplified. Fragment sizes are 130 bp, 266 bp, and 508 bp, respectively. **C.** Genomic PCR on BL6JHUK and BL6Jax DNA with the markers *Atoh2*, D6Mit122, D6Mit357, *Atoh1*, and D6Mit299. The D6Mit357 signal was absent from the BL6JHUK strain, whereas all other markers amplified on the two DNA samples. *Atoh2* and D6Mit122 are both currently mapped to about 1 cM upstream of *Snca* (marker D6Mit357), *Atoh1* and D6Mit299 both to about 1 cM downstream of this locus [[22]; and databases cited there]. PCR products were separated on a 2% agarose gel.

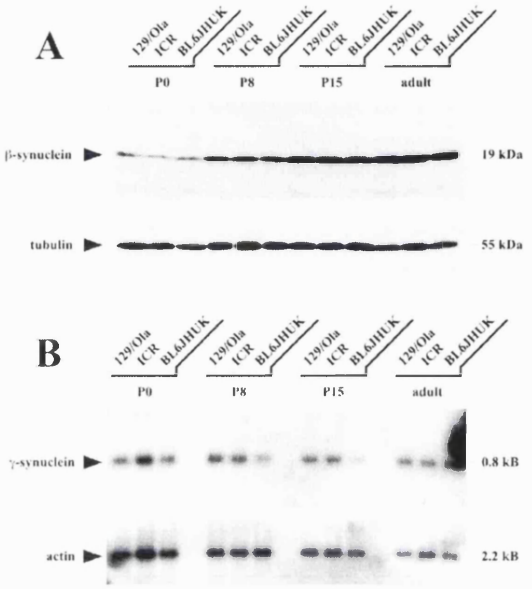

Figure 3
Developmental expression of β- and γ-synuclein in different mouse strains. A. 15% SDS-PAGE was performed on brain homogenate from the 129/Ola, ICR, and the BL6JHUK strain at time points P0, P8, P15, and adult (20 μg protein per lane). The Western blot membrane was probed with polyclonal anti β-synuclein IgG, detecting the 19 kDa protein. The lower part shows the anti α-tubulin control. **B.** Northern blot of brain polyA$^+$-RNA (500 ng per lane) from 129/Ola, ICR, and BL6JHUK mice at different developmental stages (P0, P8, P15, and adult). Probing with a 3'UTR γ-synuclein probe detects a transcript of approximately 0.8 kB. RNA samples were pooled from 4 animals (at P0), or from 2 animals (at P8 and P15) from one litter (same membrane as in Fig. 1B, actin control identical to Fig. 1B).

Further analysis of mouse strains related to BL6JHUK (BL6N and BL6) revealed that both did not contain the deletion (Fig. 2B). Western blotting confirmed α-synuclein protein expression in adult BL6N and BL6 animals (data not shown). To establish whether the entire C57BL/6J strain was affected by the deletion, C57BL/6J DNA samples from two different sources were compared. It appeared that BL6Jax DNA (C57BL/6J provided by Jackson Laboratory, Bar Harbor, ME) was not affected by the deletion. This is in contrast to BL6JHUK DNA (C57BL/6J from Harlan, Bicester, UK) (Figs. 2B and 2C). Therefore only a subpopulation of the C57BL/6J mice carries the deletion of the *Snca* locus and thus we suggest that this new strain should be called 'C57BL/6S'.

Lack of Compensatory upregulation of β or γ-synuclein in α-synuclein null mice BL6JHUK

Since α-synuclein null mice do not display any striking phenotype (our observation; [13]) expression of β-synuclein was analyzed for possible compensatory mechanisms. Western blot analysis revealed that protein levels of β-synuclein remain unaffected by the α-synuclein deletion at any stage of postnatal development (Fig. 3A). Expression of the 19 kDa protein was uniform in the 129/Ola, ICR, and the BL6JHUK strain and increased noticeably during postnatal development.

Furthermore, Northern blot analysis indicated that the expression of γ-synuclein was not significantly altered by the absence of α-synuclein in BL6JHUK mice during postnatal development (Fig. 3B). This had been already indicated by the array analysis (Fig. 1A). The γ-synuclein signal (arbitrary expression units) was 2325 (wildtype) vs. 2492 (transgenic animal with *Snca* deletion).

Lack of alteration of synphilin-1 expression in α-synuclein null mice BL6JHUK

Human α-synuclein had been shown to specifically interact with human synphilin-1 protein [20]. Therefore, the influence of the α-synuclein deletion on expression levels of synphilin-1 in mice was tested. Synphilin-1 expression was found to be unaffected by the absence of α-synuclein in the knockout strain BL6JHUK. Equal levels of synphilin-1 transcript were detected in the 129/Ola, ICR, and BL6JHUK strains by Northern blotting (Fig. 4A). Likewise, protein expression levels were unaltered between the strains, as judged by Western blot analysis, and showed a slight increase during postnatal development (Fig. 4B).

Discussion

The results unequivocally show that a subpopulation of C57BL/6J mice carry a chromosomal deletion of the α-synuclein gene locus (*Snca*). This deletion is responsible for the absence of α-synuclein mRNA and protein expression in affected animals. Within this paper, the substrain has been referred to as BL6JHUK according to its source (see methods). We now propose to name this new strain C57BL/6S (S for α-synuclein).

The discovery of a chromosomal deletion of α-synuclein in C57BL/6J DNA was unexpected since, for example, the protein had been previously detected in brain from wildtype C57BL/6 mice [16]. Furthermore, α-synuclein cDNA clones have been isolated from C57BL/6J libraries (GenBank W41663 and AA266446), implying the presence of the α-synuclein gene. Indeed, the deletion of α-synuclein was shown to only affect a subpopulation of C57BL/6J animals and did not occur in the related strains C57BL/6N and C57BL/6. It remains to be estab-

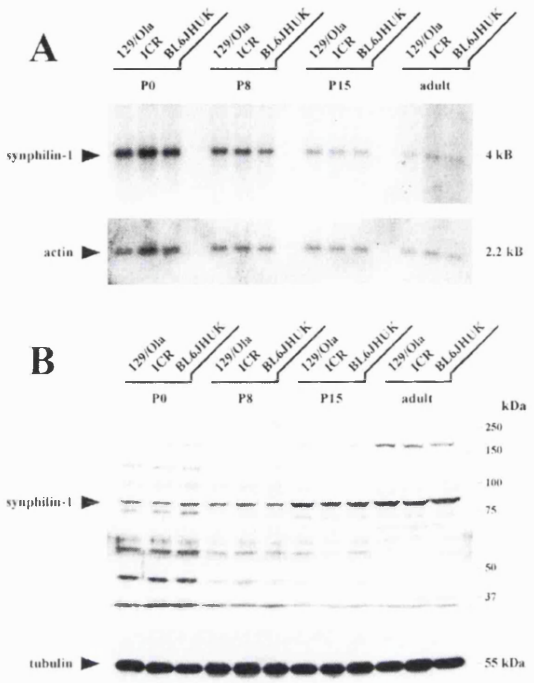

Figure 4
Developmental expression of synphilin-1 in different mouse strains. A. Northern blot of brain polyA$^+$-RNA (500 ng per lane) from 129/Ola, ICR, and BL6JHUK mice at different developmental stages (P0, P8, P15, and adult). Probing with a 1.5 kB synphilin-1 probe detects a transcript of approximately 4 kB. RNA samples were pooled from 4 animals (at P0), or from 2 animals (at P8 and P15) from one litter. After stripping, the membrane was re-probed with an actin probe. **B.** Brain homogenate from 129/Ola, ICR, and BL6JHUK mice at P0, P8, P15, and adult age separated by 7.5% SDS-PAGE (30 µg protein per lane). The Western blot membrane was sequentially probed with polyclonal anti synphilin-1 and monoclonal anti α-tubulin antibodies. The recognized proteins have apparent molecular weights of approximately 85 kDa and 55 kDa, respectively.

lished how widespread this deletion is within different C57BL/6J colonies. The deletion was not present in the C57BL/6J DNA provided by the Jackson Laboratory (Bar Harbor, ME), in contrast to C57BL/6J from Harlan (Bicester, UK). All animals from this source that were analyzed during the year 2000 were shown to carry the mutation (n = 8 from four batches of animals), suggesting that a majority of the colony is affected. However, it cannot be excluded, that the colony is heterogeneous for the deletion. From the information available to us, it seems likely that the mutation has been present in the colony as early as 1998. Further investigation will be needed to determine the prevalence of the deletion within the mouse colony and the time point at which it occurred.

The chromosomal deletion was shown to cover the complete *Snca* locus. Exon 1 and exon 6 of the gene are 97 kB apart (GenBank AF163865; mouse strain 129/SvJ; [22]) and flank the chromosome 6 marker D6Mit357. However, the deletion was shown not to include loci currently mapped at a distance of only 1 cM to each side of *Snca*, namely *Atoh1* and *Atoh2*[22]. At present, no other genes are known to be located between *Atoh1* and *Atoh2*.

In the future, large scale screening of expression profiles [for example [23]] by cDNA array technology or proteomics is likely to identify unexpected genomic variants. It will be interesting to see how frequently such deletions occur and whether they play an important role in evolution. For the moment, the occurrence of such deletions has implications on the number of genetic markers needed to validate mouse strains.

C57BL/6S mice are fertile, appear to be healthy, and have normal life expectancies, in agreement with the data on α-synuclein knockout mice [13]. To explain the lack of a noticeable phenotype in the absence of α-synuclein, potential compensatory mechanisms were tested. However, there was no indication of altered β- or γ-synuclein expression in the C57BL/6S strain. Likewise, the absence of α-synuclein did not alter expression levels of synphilin-1, with which it interacts specifically [20]. Despite the absence of compensatory upregulation it is still possible that α- and β-synuclein have similar functions and this would be addressed by deleting both loci. Furthermore, it can be inferred from the initial cDNA array experiment that the deletion of *Snca* does not result in significant changes in the expression levels of the other genes represented on the array (Fig. 1A). These include ubiquitin C-terminal hydrolase L1 that also has been found in LB [24]. This transcript was highly expressed with 16699 (wildtype) vs. 14393 (transgenic animal with *Snca* deletion) arbitrary expression units.

Conclusions

We have discovered a chromosomal deletion in a subpopulation of the widely used inbred mouse strain C57BL/6J. Such cryptic genetic alterations in a model thought to be well defined may underlie confusing results of well executed experiments. The described strain C57BL/6S has a deletion of the α-synuclein locus and may be a valuable tool to obtain a better insight into the physiological function of α-synuclein and its role in synucleinopathies.

Materials and Methods

Mouse strains and genomic DNA

C57BL/6J mice were obtained from Harlan (Bicester, UK; C57BL/6JOlaHsd). Mice from this source are referred to as BL6JHUK within this publication.

C57BL/6 mice (Harlan, Bicester, UK) are referred to as BL6, and C57BL/6N (Charles River, Margate, UK) as BL6N.

Furthermore, C57BL/6J genomic DNA was obtained from Jackson Laboratory (Bar Harbor, ME; stock JR0664, preparation P34170) and is referred to as BL6Jax.

ICR and 129/Ola mice were obtained from Harlan (Bicester, UK).

Tissue from adult animals (generally three months old) was isolated from mice obtained through their respective suppliers. Samples at developmental stages up to three weeks originate from animals bred at UCL for less than two generations. Unless otherwise stated, material used in the experiments was obtained from individual animals. Generally, male animals were used.

RNA analysis

Total RNA was isolated from brains (including cerebellum) using Trizol reagent (Gibco, Life Technologies, Paisley, UK). PolyA$^+$-RNA was prepared with oligo-dT columns (Oligotex; Qiagen, Crawley, UK). The array experiment was performed by Genome Systems (now Incyte Genomics, St. Louis, MO; mouse GEM 1 microarray, cat. No. GEM-5200) on 600 ng polyA$^+$-RNA (for further information see [http://www.incyte.com/gem]). For Northern blot analysis RNA was size separated by formaldehyde denaturing gel electrophoresis and transferred onto Hybond-N membranes (Amersham Pharmacia, Little Chalfont, UK). After hybridization of the random-primed ^{32}P-probes (Prime-It-Kit; Stratagene, Amsterdam, Holland) the final stringency washes were 0.3x SSPE at 65°C.

Restriction fragments of an α-synuclein cDNA clone (GenBank W41663; I.M.A.G.E. Consortium CloneID 353366; HGMP, Cambridge, UK; [http://image.llnl.gov] ; [25]) were used to generate radiolabelled probes. A probe to the 3'-untranslated region (3'UTR) of α-synuclein was obtained from a 557 bp fragment (BglII/NotI). The 201 bp EcoRI/NcoI (5'UTR) and 469 bp NcoI/NcoI fragments (coding sequence) led to identical results (data not shown).

A 3'UTR probe of γ-synuclein was obtained from a 394 bp restriction fragment (EcoRI/NotI) of a cDNA clone (GenBank BE133521; I.M.A.G.E. Consortium CloneID 1533487; HGMP, Cambridge, UK; [http://image.llnl.gov] ; [25]). Consistent results were obtained using probes for the coding sequence or for full-length cDNA (data not shown).

A probe to the synphilin-1 coding sequence was generated using a 1.5 kB RT-PCR fragment (primers CTTCTGT GGCTTCTTCAGTTTATGC and GCTGCCTTATTCTTTC CTTTGCTAGC). Same results were obtained with a slightly overlapping 290 bp synphilin-1 fragment (primers CAGTTGGAGTGCGTACGCTGGATGGT and GGCTTTTCCCCAGCGTGGTTCTGCAT; data not shown). Primers were designed using the human synphilin-1 sequence (GenBank AF076929). Sequencing revealed a high degree of identity between the human and mouse sequences (approximately 90% and 85% identity within two stretches of about 500 bp each on the cDNA level; data not shown).

A murine 0.9 kB probe to the actin coding sequence served as positive control, revealing a band of about 2.2 kB in brain RNA.

Westerns blot analysis

Total brain tissue was homogenized in boiling lysis buffer (1% SDS, 1 mM Na_3VO_4, 10 mM Tris, pH 7.4), microwaved for 15 seconds, and cleared by centrifugation. Samples were denatured in loading buffer containing SDS and β-mercaptoethanol, followed by SDS-PAGE, using prestained protein markers (Biorad, Hemel Hempstead, UK). Proteins were blotted onto Hybond-P membranes (Amersham Pharmacia).

Membranes were blocked in buffer containing 50 mM Tris pH 8.0, 2 mM $CaCl_2$, 80 mM NaCl, 0.2% (v/v) Igepal CA-630 (Sigma, Poole, UK) and 5% (w/v) dried skimmed milk (Marvel; Premier Brands, Wirral, UK) for one hour to overnight. Primary antibodies were applied for one hour, followed by washes with blocking buffer. Peroxidase-conjugated secondary antibodies (goat anti-rabbit or goat anti-mouse IgG; 111-035-003 and 115-035-003; Jackson ImmunoResearch Laboratories, West Grove, PA) were incubated for one hour at a dilution of 1:10000, followed by washes in blocking buffer and PBS. Membranes were developed with ECL Plus reagent (Amersham Pharmacia) and exposed on film (X-OMAT-AR; Kodak, Hemel Hempstead, UK). Membranes were stripped and re-probed according to the manufacturer's protocol.

Monoclonal mouse anti rat α-synuclein IgG1 (S63320; Transduction Laboratories, Lexington, KY) was used at a concentration of 1:500. Polyclonal rabbit anti human β-synuclein IgG (1:2500; SA3405; Affiniti, Mamhead, UK)

and polyclonal rabbit anti human synphilin-1 IgG (1:1000; ab6179; Abcam, Cambridge, UK) were both used in alternative blocking buffer (PBS containing 0.05% Tween20 and 3% BSA). The synphilin-1 antibody was raised against an N-terminal epitope and recognized several protein bands on Western blots. Since only one of these proteins was of the expected size (approximately 85 kDa) and expressed throughout development this was taken for the genuine target protein synphilin-1.

Monoclonal mouse anti chick α-tubulin IgG1 (1:20000; T9026; Sigma) detected a 55 kDa band, which was used as positive control.

Genomic PCR

Genomic DNA was isolated from tail samples using a proteinase K / SDS protocol [26] with the exception of BL6Jax DNA (C57BL/6J, stock JR0664, preparation P34170; Jackson Laboratory, Bar Harbor, ME).

Touchdown PCR on 1 μg genomic DNA in 25 μl included denaturation at 94°C (30 sec), annealing at 68°C (30 sec with dT = -0.5°C each cycle), and extension at 72°C (45 sec) for 30 cycles, followed by further 10 cycles with constant 52°C annealing temperature. Specific primers amplified mouse α-synuclein exon 4 (AGAAGACCAAAGAGCAAGTGACA and ATCTGGTC CTTCTTGACAAAGC, 130 bp fragment) and α-synuclein exon 6 (AAGACTATGAGCCTGAAGCCTAAG and AGT GTGAAGCCACAACAATATCC, 266 bp), as well as NMDA receptor subunit NR1 (exons 18 to 19, GTCCAT ACTCAAGTGAGTCTGCCC and CAGGGGCATTGCT GCGGGAGTC, 508 bp) as a positive control. This was alternatively performed as an internal control (data not shown).

Amplification of the chromosome 6 genomic marker D6Mit357 (UniSTS database, NCBI, [http://www.ncbi.nlm.nih.gov/genome/sts]) yielded a 100 bp product (primers TACAATGGCTCTCCTCCCTG and CCTCAG GATTTAAATAAATTCAAGC). The size of the deletion was estimated using a range of genetic markers close to the *Snca* locus. Results shown here include the following markers: mouse atonal protein homolog 1 and 2 (*Atoh1*, also known as *MATH-1*, GenBank D43694; primers CT GCAGGCGAGAGACCTTC and TCAGCTTGCACAGCT GTTC, 271 bp product; *Atoh2*, also known as *Nex-1*, GenBank U29086, TACTGCAGTGCATATGAATC and TCG TAAGGGAAGTGGCTGTC, 245 bp), and the markers D6Mit122 (GACACCCAGCATCCATCTTT and TTG TAATTTTTAAAAGATAGGTGTGTG, 139 bp) and D6Mit299 (TCATGAATATCAAAGACACACATCC and AAGCACATGCATTAGTATTTCCC, 119 bp). In these experiments genomic DNA was subjected to 30 PCR cycles (94°C/30 sec, 55°C/30 sec and 72°C/30 sec). Products were sized with MspI digested pBluescript II KS(+) (Stratagene).

RT-PCR

The reverse transcriptase reaction was performed on 50 ng total RNA in 25 μl containing 0.25 μg oligo-dT primer with Ready-To-Go RT-PCR beads (Amersham Pharmacia) at 42°C for 30 minutes, followed by PCR cycling (94°C/30 sec, 55°C/30 sec, 72°C/45 sec) with 5 pmol of each specific primer. The primers AACTGCAGTTCT TCAGAAGCCTAGGGAGC and GCTCTAGACTGGGCA CATTGGAACTGAG were used to amplify a 568 bp mouse α-synuclein fragment (exons 1 to 6 on cDNA). Amplification of a 473 bp mouse tubulin α1 (*Tuba1*) fragment (ACACCTTCTTCAGTGAGACAGG and CTCATT GTCTACCATGAAGGCAC) served as a positive control.

Acknowledgements

This work was funded by a Wellcome Trust Senior Fellowship to RS. We would like to thank Marco Peters for initial characterization of the α-synuclein locus, Steve Davies and Rushee Singh Jolly for helpful discussion and unpublished data, Philip Chen for comments on the manuscript, and Michel Goedert for the supply of antibodies.

References

1. Polymeropoulos MH, Lavedan C, Leroy E, Ide SE, Dehejia A, Dutra A, Pike B, Root H, Rubenstein J, Boyer R, Stenroos ES, Chandrasekharappa S, Athanassiadou A, Papapetropoulos T, Johnson WG, Lazzarini AM, Duvoisin RC, Di Iorio G, Golbe LI, Nussbaum RL: **Mutation in the α-synuclein gene identified in families with Parkinson's disease.** *Science* 1997, **276**:2045-2047
2. Krüger R, Kuhn W, Müller T, Woitalla D, Graeber M, Kösel S, Przuntek H, Epplen JT, Schöls L, Riess O: **Ala30Pro mutation in the gene encoding α-synuclein in Parkinson's disease.** *Nat Genet* 1998, **18**:106-108
3. Spillantini MG, Schmidt ML, Lee VM, Trojanowski JQ, Jakes R, Goedert M: **α-synuclein in Lewy bodies.** *Nature* 1997, **388**:839-840
4. Wakabayashi K, Matsumoto K, Takayama K, Yoshimoto M, Takahashi H: **NACP, a presynaptic protein, immunoreactivity in Lewy bodies in Parkinson's disease.** *Neurosci Lett* 1997, **239**:45-48
5. Duda JE, Lee VM, Trojanowski JQ: **Neuropathology of synuclein aggregates: new insights into mechanisms of neurodegenerative diseases.** *J Neurosci Res* 2000, **61**:121-127
6. Hong L, Ko HW, Gwag BJ, Joe E, Lee S, Kim YT, Suh YH: **The cDNA cloning and ontogeny of mouse D-synuclein.** *Neuroreport* 1998, **9**:1239-1243
7. Hsu LJ, Mallory M, Xia Y, Veinbergs I, Hashimoto M, Yoshimoto M, Thal LJ, Saitoh T, Masliah E: **Expression pattern of synucleins (non-Aβ component of Alzheimer's disease amyloid precursor protein/α-synuclein) during murine brain development.** *J Neurochem* 1998, **71**:338-344
8. Maroteaux L, Campanelli JT, Scheller RH: **Synuclein: a neuron-specific protein localized to the nucleus and presynaptic nerve terminal.** *J Neurosci* 1988, **8**:2804-2815
9. Iwai A, Masliah E, Yoshimoto M, Ge N, Flanagan L, Rohan de Silva HA, Kittel A, Saitoh T: **The precursor protein of non-Aβ component of Alzheimer's disease amyloid is a presynaptic protein of the central nervous system.** *Neuron* 1995, **14**:467-475
10. Masliah E, Rockenstein E, Veinbergs I, Mallory M, Hashimoto M, Takeda A, Sagara Y, Sisk A, Mucke L: **Dopaminergic loss and inclusion body formation in α-synuclein mice: implications for neurodegenerative disorders.** *Science* 2000, **287**:1265-1269
11. van der Putten H, Wiederhold KH, Probst A, Barbieri S, Mistl C, Danner S, Kauffmann S, Hofele K, Spooren WP, Ruegg MA, Lin S, Caroni P, Sommer B, Tolnay M, Bilbe G: **Neuropathology in mice expressing human α-synuclein.** *J Neurosci* 2000, **20**:6021-6029
12. Feany MB, Bender WW: **A Drosophila model of Parkinson's disease.** *Nature* 2000, **404**:394-398

13. Abeliovich A, Schmitz Y, Fariñas I, Choi-Lundberg D, Ho WH, Castillo PE, Shinsky N, Verdugo JM, Armanini M, Ryan A, Hynes M, Phillips H, Sulzer D, Rosenthal A: **Mice lacking α-synuclein display functional deficits in the nigrostriatal dopamine system.** *Neuron* 2000, **25**:239-252
14. Nakajo S, Tsukada K, Omata K, Nakamura Y, Nakaya K: **A new brain-specific 14-kDa protein is a phosphoprotein. Its complete amino acid sequence and evidence for phosphorylation.** *Eur J Biochem* 1993, **217**:1057-1063
15. Jakes R, Spillantini MG, Goedert M: **Identification of two distinct synucleins from human brain.** *FEBS Lett* 1994, **345**:27-32
16. Kahle PJ, Neumann M, Ozmen L, Müller V, Jacobsen H, Schindzielorz A, Okochi M, Leimer U, van der Putten H, Probst A, Kremmer E, Kretzschmar HA, Haass C: **Subcellular localization of wild-type and Parkinson's disease-associated mutant α-synuclein in human and transgenic mouse brain.** *J Neurosci* 2000, **20**:6365-6373
17. Akopian AN, Wood JN: **Peripheral nervous system-specific genes identified by subtractive cDNA cloning.** *J Biol Chem* 1995, **270**:1264-1270
18. Buchman VL, Hunter HJ, Piñón LG, Thompson J, Privalova EM, Ninkina NN, Davies AM: **Persyn, a member of the synuclein family, has a distinct pattern of expression in the developing nervous system.** *J Neurosci* 1998, **18**:9335-9341
19. Galvin JE, Uryu K, Lee VM, Trojanowski JQ: **Axon pathology in Parkinson's disease and Lewy body dementia hippocampus contains α-, β-, and γ-synuclein.** *Proc Natl Acad Sci USA* 1999, **96**:13450-13455
20. Engelender S, Kaminsky Z, Guo X, Sharp AH, Amaravi RK, Kleiderlein JJ, Margolis RL, Troncoso JC, Lanahan AA, Worley PF, Dawson VL, Dawson TM, Ross CA: **Synphilin-1 associates with α-synuclein and promotes the formation of cytosolic inclusions.** *Nat Genet* 1999, **22**:110-114
21. Wakabayashi K, Engelender S, Yoshimoto M, Tsuji S, Ross CA, Takahashi H: **Synphilin-1 ispresent in Lewy bodies in Parkinson's disease.** *Ann Neurol* 2000, **47**:521-523
22. Touchman JW, Dehejia A, Chiba-Falek O, Cabin DE, Schwartz JR, Orrison BM, Polymeropoulos MH, Nussbaum RL: **Human and mouse D-synuclein genes: comparative genomic sequence analysis and identification of a novel gene regulatory element.** *Genome Res* 2001, **11**:78-86
23. Sandberg R, Yasuda R, Pankratz DG, Carter TA, del Rio JA, Wodicka L, Mayford M, Lockhart DJ, Barlow C: **Regional and strain-specific gene expression mapping in the adult mouse brain.** *Proc Natl Acad Sci USA* 2000, **97**:11038-11043
24. Lowe J, McDermott H, Landon M, Mayer RJ, Wilkinson KD: **Ubiquitin carboxyl-terminal hydrolase (PGP 9.5) is selectively present in ubiquitinated inclusion bodies characteristic of human neurodegenerative diseases.** *J Pathol* 1990, **161**:153-160
25. Lennon G, Auffray C, Polymeropoulos M, Soares MB: **The IMAGE consortium: an integrated molecular analysis of genomes and their expression.** *Genomics* 1996, **33**:151-152
26. Laird PW, Zijderveld A, Linders K, Rudnicki MA, Jaenisch R, Berns A: **Simplified mammalian DNA isolation procedure.** *Nucleic Acids Res* 1991, **19**:4293

Notes